

TRANSPORTATION RESEARCH RECORD 1072

Structural Design of Bridges

TRB

TRANSPORTATION RESEARCH BOARD
NATIONAL RESEARCH COUNCIL

WASHINGTON, D.C. 1986

Transportation Research Record 1072

Price \$11.20
Editor: Elizabeth W. Kaplan
Compositor: Joan G. Zubal
Layout: Betty L. Hawkins

mode
1 highway transportation

subject areas
12 planning
25 structures design and performance
40 maintenance

Transportation Research Board publications are available by ordering directly from TRB. They may also be obtained on a regular basis through organizational or individual affiliation with TRB; affiliates or library subscribers are eligible for substantial discounts. For further information, write to the Transportation Research Board, National Research Council, 2101 Constitution Avenue, N.W., Washington, D.C. 20418.

Printed in the United States of America

Library of Congress Cataloging-in-Publication Data
National Research Council. Transportation Research Board.

Structural design of bridges.

(Transportation research record, ISSN 0361-1981 ; 1072)
Reports of the TRB's 65th Annual Meeting held in Washington, D.C., January 13-16, 1986.

1. Bridges—Design—Congresses. 2. Bridges—Live loads—Congresses. I. National Research Council (U.S.). Transportation Research Board. Meeting (65th : 1986 : Washington, D.C.) II. Series.

TE7.H5 no. 1072 380.5 s 86-23512
[TG300] [624'.2]
ISBN 0-309-04066-3

Sponsorship of Transportation Research Record 1072

GROUP 2—DESIGN AND CONSTRUCTION OF TRANSPORTATION FACILITIES

David S. Gedney, Harland Bartholomew & Associates, chairman

Structures Section

John M. Hanson, Wiss, Janney & Elstner & Associates, chairman

Committee on General Structures

Clellon Lewis Loveall, Tennessee Department of Transportation, chairman

John J. Ahlskog, Dan S. Bechly, Neal H. Bettigole, Edwin G. Burdette, Martin P. Burke, Jr., Fernando E. Fagundo, Dah Fwu Fine, Richard S. Fountain, Frederick Gottemoeller, J. Leroy Hulse, Walter J. Jestings, Robert N. Kamp, John M. Kulicki, Andrew Lally, Richard M. McClure, Roy L. Mion, Andrew E. N. Osborn, Kantilal R. Patel, William J. Rogers, David R. Schelling, Arunprakash M. Shirole, Stanley W. Woods

Committee on Concrete Bridges

Robert C. Cassano, California Department of Transportation, chairman

Craig A. Ballinger, John A. Belvedere, Ronald A. Brechler, Stephen L. Bunnell, John H. Clark, W. Gene Corley, C. S. Gloyd, Allan C. Harwood, H. Henrie Henson, James J. Hill, Ti Huang, Roy A. Imbsen, H. Hubert Janssen, Heinz P. Koretzky, John M. Kulicki, R. Shankar Nair, Walter Podolny, Jr., Alex C. Scordelis, Frieder Seible, John F. Stanton, Adrianus Vankampen, Julius F. J. Volgyi, Jr., Donald J. Ward, W. Jack Wilkes

Committee on Dynamics and Field Testing of Bridges

James W. Baldwin, Jr., University of Missouri-Columbia, chairman
Charles F. Galambos, Federal Highway Administration, secretary
Baidar Bakht, Furman W. Barton, David B. Beal, Harold R. Bosch, John L. Burdick, William G. Byers, Gene R. Cudney, Bruce M. Douglas, Ismail A. S. Elkholy, Hota V. S. Gangarao, David William Goodpasture, Roy A. Imbsen, F. Wayne Klaiber, Celal N. Kostem, Robert H. Lee, Fred Moses, M. Noyszewski, Gajanan M. Sabnis, Kwok-Nam Shiu, R. Varadarajan, Ivan M. Viest, Kenneth R. White

George W. Ring III, Transportation Research Board staff

Sponsorship is indicated by a footnote at the end of each paper. The organizational units, officers, and members are as of December 31, 1985.

NOTICE: The Transportation Research Board does not endorse products or manufacturers. Trade and manufacturers' names appear in this Record because they are considered essential to its object.

Contents

BRIDGE FORMULA DEVELOPMENT James S. Noel, Ray W. James, Howard L. Furr, Francisco E. Bonilla, and Lloyd R. Cayes	1
FURTHER STUDIES ON LATERAL LOAD DISTRIBUTION USING A FINITE ELEMENT METHOD Clifford O. Hays, Jr., Larry M. Sessions, and Alan J. Berry	6
APPLICATION OF MICROCOMPUTERS IN BRIDGE DESIGN Ronald A. Love, Furman W. Barton, and Wallace T. McKeel, Jr.	15
SIMPLIFIED METHOD FOR ESTIMATING THERMAL STRESSES IN COMPOSITE BRIDGES M. Soliman and John B. Kennedy	23
MULTI-INCREMENT COST-ALLOCATION METHODOLOGY FOR BRIDGES Ah-Beng Tee, Kumares C. Sinha, and Edward C. Ting	31
TEST-TO-FAILURE OF A JACK-ARCH BRIDGE David B. Beal	40
STRESS STATE IN COUPLING JOINTS OF POSTTENSIONED CONCRETE BRIDGES Frieder Seible, Yury Kropp, and Christopher T. Latham	50
UMBRELLA LOADS FOR BRIDGE DESIGN Heinz P. Koretzky, Kantilal R. Patel, Richard M. McClure, and David A. VanHorn	58
APPLICATION OF EXPERT SYSTEMS IN THE DESIGN OF BRIDGES James G. Welch and Mrinmay Biswas	65
EVALUATION OF STEEL BRIDGES USING IN-SERVICE TESTING Michel Ghosn, Fred Moses, and John Gobieski	71

Bridge Formula Development

JAMES S. NOEL, RAY W. JAMES, HOWARD L. FURR,

FRANCISCO E. BONILLA, and LLOYD R. CAYES

ABSTRACT

The objective of this research was to review the existing bridge formula to determine whether modifications could be suggested to make it more rational. The intent was to more fully use the capacity of existing bridges without significantly shortening the service life of any. A formula, independent of the number of included axles, was developed to accomplish the objective. As is the current formula, it is applicable both to the overall wheelbase and to all included sub-groups of axles. The maximum weights for single and tandem axles were assumed to be unchanged. If enforced, the proposed formula assures that HS 20 bridges will not be loaded to more than 1.05 times the design stress, nor will H 15 bridges be loaded to more than 1.30 times the design stress. The formula reduces the maximum weight allowed on four or more closely spaced axles. However, for most practical lengths, the formula is less restrictive than the current law. A brief study of the influence the proposed formula would have on pavement fatigue was accomplished. For most practical heavy vehicles, the formula would result in a greater number of equivalent axle loads per vehicle. One equivalent axle load causes the same pavement fatigue damage as a single 18,000-lb (80.06-kN) axle. The number of equivalent axle loads is commonly used as a measure of the fatigue damage a heavy vehicle inflicts on the pavement. A detailed study of the effect that the adoption of the proposed formula would have on pavements is recommended. Such a study should consider costs, benefits, and potential formula modifications.

In this paper is described a study of the bridge formula currently prescribed in the Surface Transportation Assistance Act (STAA) of 1982 for regulating truck weights on certain federally funded roadways. This bridge formula, often referred to as Table B (or Formula B), has received criticism from both users and transportation officials for being basically unfair in terms of the stress levels generated in various bridge spans and types by different axle combinations. The most compelling criticism concerns its applicability to long, many-axled vehicles, which are also being studied under the STAA of 1982, for which the formula would allow unreasonably high loads should the current 80,000-lb (355.7-kN) maximum gross weight be increased.

The problem is complicated by the variability in bridge carrying capacities. This is primarily because different bridges were originally designed to different strength levels. Two of the most common of these strength levels are termed H 15 and HS 20 by the AASHTO bridge specifications, in which the HS 20 is significantly stronger than the H 15. This notation for strength levels actually refers to the hypothetical truck loading used for the bridge design. The HS 20 design truck, which has a semitrailer, actually weighs more than twice the weight of the H 15. About 95 percent of the bridges on the Interstate system are rated as HS 20 or better. In general, none are classified as less than H 15. The percentage of HS 20 bridges on the primary and secondary highway systems, however, is significantly lower.

HISTORIC BACKGROUND

The first significant federal legislation concerning truck weights was contained in the Federal Aid Highway Act of 1956, which initially provided for the planning, financing, and construction of the National System of Interstate and Defense Highways. This bill provided that no funds would be used for the Interstate system in any state that allowed vehicles with a single axle weighing more than 18,000 lb (80.06 kN), a tandem axle of 32,000 lb (142.3 kN), and a gross weight of 73,280 lb (325.9 kN). However, a "grandfather clause" provided that any vehicle that operated legally within a state before the passage of the law could continue to operate legally afterwards.

In 1964 the Highway Research Board prepared and submitted to Congress, via the Secretary of Commerce, House Document 354. This document contained a detailed review of the trucking industry and of the regulations governing the operation of heavy vehicles. Further, it recognized the large capital investment the nation had in these heavy vehicles, their importance to the nation's commerce, and their wear and tear on the nation's highway system. Findings of the document were partly based on results of AASHO Road Tests performed in the late 1950s. Probably the most important recommendation made in that document was that Table B, a tabulation of permissible weights of axle groups, depending on the number of axles and the overall length of the group, be adopted for the Interstate system. In addition, it suggested that the single axle limit be increased to 20,000 lb (88.96 kN) and the tandem axle limit to 34,000 lb (151.2 kN).

It is important to note that a footnote to Table B flatly prohibited the operation of certain short-wheelbase, multi-axle trucks over H 15 bridges. The point was clearly made in the document that such

J.S. Noel, R.W. James, H.L. Furr, and F.E. Bonilla, Texas Transportation Institute, The Texas A&M University System, College Station, Tex. 77843-3135. L.R. Cayes, FHWA, U.S. Department of Transportation, Turner Fairbanks Highway Research Center, 6300 Georgetown Pike, McLean, Va. 22101.

vehicles would overstress the H 15 bridges by more than 30 percent, a situation the authors of the document clearly viewed as intolerable.

Little happened in response to these recommendations, however, until 1975, when the U.S. Congress enacted legislation allowing the states to increase the weight limits on the Interstate system to those of Table B. The allowable single axle weight was increased to 20,000 lb (88.96 kN) and the tandem axle weights increased as recommended in the document. Further, the allowable gross vehicle weight was increased to a maximum not to exceed 80,000 lb (355.8 kN) from 73,280 lb (325.9 kN). It is generally believed that this legislation was passed in an attempt to restore to the industry the productivity lost because of the imposition of the 55-mph (88.5-km/hr) speed limit in December 1973.

The most recent legislation is referred to as the Surface Transportation Assistance Act of 1982 (Act of Jan. 6, 1983, Pub. L. No. 97-424, 96 Stat. 2097-2200). The vehicle weight limitations sections (2123-2124) of the act read as follows:

VEHICLE WEIGHT, LENGTH, AND
WIDTH LIMITATIONS

Sec. 133. (a) Section 127 of title 23 of the United States Code is amended to read:

[Section] 172. Vehicle weight limitations--Interstate System

"(a) No funds authorized to be appropriated for any fiscal year under provisions of the Federal-Aid Highway Act of 1956 shall be apportioned to any State which does not permit the use of the National System of Interstate and Defense Highways within its boundaries by vehicles with a weight of twenty thousand pounds carried on any one axle, including enforcement tolerances, or with a tandem axle weight of thirty-four thousand pounds, including enforcement tolerances, or a gross weight of at least eighty thousand pounds for vehicle combinations of five axles or more. However, the maximum gross weight to be allowed by any State for vehicles using the National System of Interstate and Defense Highways shall be twenty thousand pounds carried on one axle, including enforcement tolerances, and a tandem axle weight of thirty-four thousand pounds, including enforcement tolerances and with an overall maximum gross weight, including enforcement tolerances, on a group of two or more consecutive axles produced by application of the following formula:

$$W = 500 \left(\frac{LN}{N-1} + 12N + 36 \right)$$

where W equals overall gross weight on any group of two or more consecutive axles to the nearest five hundred pounds, L equals distance in feet between the extreme of any group of two or more consecutive axles, and N equals number of axles in group under consideration, except that two consecutive sets of tandem axles may carry a gross load of thirty-four thousand pounds each providing the overall distance between the first and last axles of such consecutive sets of tandem axles is thirty-six feet or more: Provided, That

such overall gross weight may not exceed eighty thousand pounds, including all enforcement tolerances, except for those vehicles and loads which cannot be easily dismantled or divided and which have been issued special permits in accordance with applicable State laws, or the corresponding maximum weights permitted for vehicles using the public highways of such State under laws or regulations established by appropriate State authority in effect on July 1, 1956, except in the case of the overall gross weight of any group of two or more consecutive axles, on the date of enactment of the Federal-Aid Highway Amendments of 1974, whichever is the greater. Any amount which is withheld from apportionment to any State pursuant to the foregoing provisions shall lapse. This section shall not be construed to deny apportionment to any State allowing the operation within such State of any vehicles or combinations thereof which the State determines could be lawfully operated within such State on July 1, 1956, except in the case of the overall gross weight of any group of two or more consecutive axles, on the date of enactment of the Federal-Aid Highway Amendments of 1974. With respect to the State of Hawaii, laws or regulations in effect on February 1, 1960, shall be applicable for the purposes of this section in lieu of those in effect on July 1, 1956. With respect to the State of Michigan, laws or regulations in effect on May 1, 1982, shall be applicable for the purposes of this subsection.

"(b) No State may enact or enforce any law denying reasonable access to motor vehicles subject to this title to and from the Interstate Highway System to terminals and facilities for food, fuel, repairs, and rest."

The equation is Formula B from which the weights of Table B are calculated. These limitations are the same as those in Table B, with the 80,000-lb (355.8-kN) gross weight cap. An exception to the bridge Formula B was instituted in the 1974 act and this permitted the maximum weight of tandems spaced 36 ft (10.97 m) to be 68,000 lb (302.5 kN).

FORMULA DEVELOPMENT

An important first step in deriving a new bridge formula to assure specified stress ratios are not exceeded in any H 15 or HS 20 bridge is to identify the lightest and therefore critical bridges. This means finding, for each span, the bridge type that has the least dead load moment and shear. Data were collected from the files of the FHWA and from standard designs of state highway departments to find these minimum weight bridge types. When these lightest weight bridges had been found, it was possible to define the loads that would cause specific stress levels in each span length. This procedure was followed for bridges of both H 15 and HS 20 design.

For example, uniformly distributed loads of every length between 8 and 120 ft (36.58 m) were placed on the lightest weight bridges of every span to evaluate what total load would cause 1.3 times the design stress in H 15 bridges and 1.05 times the design stress in HS 20 bridges. This multitude of calculations was expeditiously completed with a microcom-

puter and resulted in a unique weight for each uniform load length and each bridge design. These maximum loads were then plotted versus length. It was determined that the H 15 bridges with the 1.3 factor dictated the lesser loads up to lengths of about 70 ft (21.34 m). For the longer lengths, the HS 20 bridges with the 1.05 factor controlled.

Two straight lines were drawn near these results and yielded the formula shown in Figure 1. These two straight lines are shown superimposed over a plot of Table B as modified by the STAA of 1982. The equations of the two lines are

$$W = (34 + L) 1,000 \text{ lb} \quad 8 \text{ ft} < L < 56 \text{ ft}$$

$$W = (62 + L/2) 1,000 \text{ lb} \quad 56 \text{ ft} < L$$

Figure 1 shows that the suggested formula would reduce the loads allowed on the shorter axle groupings as was originally recommended by the footnote to Table B in House Document 354.

Application of the proposed formula is to all contiguous subsets of axles in the vehicle. When calculating the allowable weight of such a subset of axles, the wheelbase (L) is the extreme axle spacing in that subset.

In addition, the current limits for single axles [20,000 lb (88.96 kN)] and tandem axles spaced 4 ft (1.219 m) [34,000 lb (151.2 kN)] are retained. Although a rigorous economic study of the costs of pavement damage compared with the increased transportation productivity was beyond the scope of this study, a brief review of the AASHTO Road Test results led to the conclusion that if these limits were retained and the proposed formula were adopted, some additional pavement fatigue damage would result.

ASSUMPTIONS

The assumptions used to make the calculations described previously are, in general, those made by the analyst during the design of a bridge. For example, the impact formula used in the current AASHTO

Standard Specifications for Highway Bridges was assumed to be valid. Similarly, the number and weight of trucks on the bridge in the direction of travel and in adjacent lanes were all as dictated by the design specifications. Finally, the detailed distribution of the load to the several types of members supporting the deck was assumed to follow the design rules.

It is recognized that there is continuing debate about the validity of each of these assumptions, but it is doubtful that the resolution of any one of these debates would alter the results of this study.

One other assumption worth noting is that all bridge design ratings were assumed to be as new. No allowance was made for deterioration due to age or prior service.

STRESS LEVELS CAUSED BY PRACTICAL VEHICLES

The effectiveness of the proposed formula for limiting weights of practical vehicles for specified overstress ratios 1.05 for HS 20 bridges and 1.30 for H 15 bridges is evaluated by comparing the calculated critical weights of selected practical vehicles with the curve defined by the proposed formula. The proposed formula is effective in allowing significantly more weight than does the present formula for many practical vehicles. This is done without exceeding the design total stress, dead load plus live load plus impact (DL + LL + I), by more than a specified percentage: 30 percent in the case of H 15 bridges and 5 percent in the case of HS 20 bridges.

FATIGUE CONSIDERATIONS

The fatigue behavior of highway bridges is influenced primarily by stress range. The stress range is equal to the (LL + I) stresses; therefore any changes in truck weights will result in increased fatigue loading on highway bridges and a corresponding increase

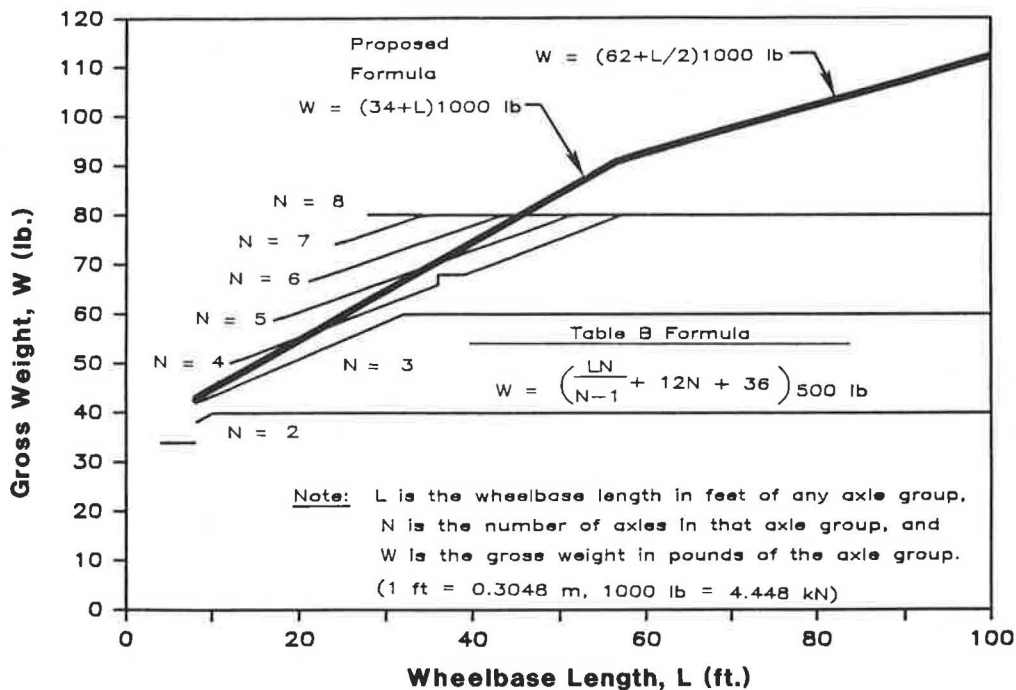


FIGURE 1 Proposed formula shown superimposed on the current Table B formula.

in maintenance costs if the increased fatigue loading causes stresses that are above the fatigue endurance limits. To evaluate the significance of the proposed formula for the fatigue lives of highway bridges, it is necessary to make several simplifying assumptions. It is assumed that existing bridges are loaded in flexure to design allowable stresses by design vehicles. Design allowable stresses are a function of the design lifetime in loading cycles and the weld detail category. It is assumed that flexure governs, and shear is not checked. Because existing single-, tandem-, and triple-axle bogies are not changed, shear stresses are not expected to increase as significantly as flexure stresses. Further, only simple spans were evaluated.

For each span checked, the maximum moment caused by the maximum legal weight vehicles and the maximum moment due to the design live load were calculated. With the assumption that the stress range due to the design loading equals the allowable stress range, the stress range due to the maximum weight vehicles is calculated by multiplying by the appropriate moment ratio.

The calculated stress ranges are compared with the allowable fatigue stress ranges. The ratio of the calculated stress range to the allowable stress range does not exceed 1.05, except for a small range of spans for all the practical vehicles considered for commonly used structural steels. For most spans and details, the increased stress range is still well below the allowable stress range. Span-detail combinations that are most affected by the proposed formula are the more critical details in maximum moment regions of longer, 120- to 160-ft (36.57- to 48.77-m), spans.

PAVEMENT CONSIDERATIONS

In recognition that the passage of heavy vehicles causes fatigue damage to pavements as well as to

bridges and that the country's investment in pavement is several times larger than that in bridges, no change should be made in the bridge formula without considering the consequences of the change for the pavements. The analytical assessment of the impact of such a change on pavement life is not as straightforward as it is for bridges. It is generally accepted that heavy axles, and very short groupings of axles, are more damaging to pavements whereas gross vehicle weights, or longer groupings of axles, are more damaging to bridges.

One measure of the fatigue damage heavy vehicles exert on pavements is termed the "equivalent axle load." The equivalent axle load compares the fatigue damage done by a single axle, or grouping of axles, with the damage done by an 18,000-lb (80.06-kN) axle. So an 18,000-lb (80.06-kN) single axle is arbitrarily assigned an equivalent axle load value of 1.0. A single axle, or grouping of axles, that causes twice as much damage as an 18,000-lb (80.06-kN) axle is given an equivalent axle load value of 2.0. Tables of equivalent axle loads for single and tandem axles, on different types of pavement surfaces, have been tabulated and published. These tables are based primarily on the results of the AASHTO Road Test completed in the late 1950s, during which the deterioration of various pavement surfaces under repeated heavy truck loadings was observed.

These tables make it possible to estimate the number of equivalent axle loads that results from the passage of any given heavy truck. If a truck has two widely spaced axles weighing 18,000 lb (80.06 kN) each, for example, it could be said that the passage of that truck generated 2.0 equivalent axle loads. Another truck with three 18,000-lb (80.06-kN) axles would generate 3.0 equivalent axle loads and would be considered 50 percent more damaging to the pavement. Closely spaced axles have an interactive effect, but equivalent axle loads for tandem axles (groups of two axles jointly suspended) are also tabulated. This makes it possible to calculate the

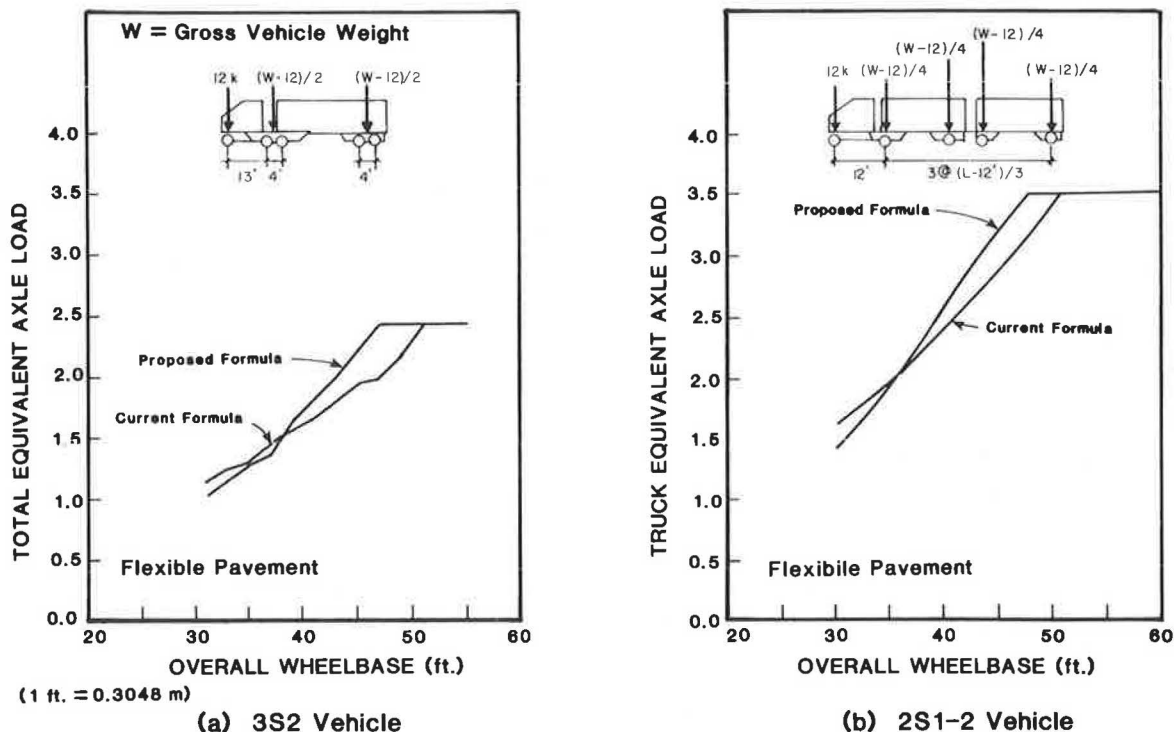


FIGURE 2 Equivalent axle loads per vehicle for proposed and existing formulas.

number of equivalent axle loads generated by most of the heavy truck configurations currently in use.

These calculations were made for trucks that conform to the current bridge formula and for trucks that conform to the proposed bridge formula and the results were compared. These comparisons for two common truck configurations are shown in Figures 2a and 2b. Figure 2a is for the 3S2, a semitrailer truck with a steering axle and two tandems (commonly referred to as the 18-wheeler). Figure 2b is for the 2S1-2, a semitrailer truck with a full trailer on two axles; it has a steering axle with four widely spaced single axles.

For very short and very long vehicles, the equivalent axle loads per truck are about the same. For the short ones, those with wheelbases less than about 36 ft (10.97 m), the proposed formula would lead to smaller equivalent axle loads per truck. If the 80,000-lb (355.8-kN) maximum gross weight per vehicle is maintained, the proposed and current formulas come together at wheelbases just over 50 ft (15.24 m) and are identical for all longer lengths. However, in the intermediate lengths, the equivalent axle loads per truck are significantly greater, in some instances by as much as 20 percent. These in-

termediate truck lengths, 36 to 50 ft (10.97 to 15.24 m), are common, and the increase in equivalent axle loads would certainly have a detrimental effect on the wear-out rate of pavements.

It appears that the average equivalent axle load per vehicle will probably increase if the proposed formula is adopted. Even so, this increase would be more acceptable if it could be shown that the payload per equivalent axle load increased as a result of the change. Figures 3a and 3b show the gross vehicle weights versus wheelbase and plots of the assumed payloads divided by vehicle equivalent axle loads. These payloads were calculated by subtracting an arbitrary vehicle empty weight of 25,000 lb (111.2 kN) from the gross vehicle weights. Disappointingly, the payload per equivalent axle load was found to decrease, if only slightly, for vehicles that comply with the proposed formula.

The calculations and comparisons of the equivalent axle loads per truck are evidence that the new bridge formula, as stated and without further modification, would indeed be detrimental to pavements. Currently, pavement deterioration rates are higher than ever, and a change in the bridge formula should not be allowed to magnify that problem. As a result, it is recommended that a detailed study of the influence of a bridge formula change on pavements be initiated with the goal of suggesting additional modifications that would permit the formula to be used without causing unacceptable pavement deterioration. One alternative such a study could consider would be to reduce the allowed maximum single and tandem axle loads to coincide with the adoption of the new formula.

CONCLUSIONS

The adoption of the proposed bridge formula would bring some changes to the geometry and distribution of truck loads on the axles and bogies. In many cases higher payloads would result without bringing excessively higher stresses to structural bridge members. If overall length limits or maximum gross weights should ever be increased, the formula would continue to be effective for protecting bridges against damaging overstresses, not necessarily a feature of the current formula.

The proposed formula is independent of the number of included axles and as such should be simpler to understand and easier to enforce than is the present formula.

The proposed formula is based on engineering rationale, although several controversial assumptions are used.

If the proposed bridge formula is not enforced, irrespective of what form of the formula is being used, bridges are apt to have foreshortened service lives because of fatigue.

The indiscriminate issuing of overweight truck permits, especially those issued on a periodic or annual basis, is equally apt to result in foreshortened bridge service lives.

Adoption of the proposed bridge formula, without any change in the maximum single and tandem axle loads, will cause an increase in the average equivalent axle load per truck. This is often considered the primary measure of the fatigue damage a vehicle causes to pavement. So, although the proposed formula will satisfactorily protect the bridge structures, there is real concern about its effect on pavements, a consequence that should be carefully evaluated before any changes are made.

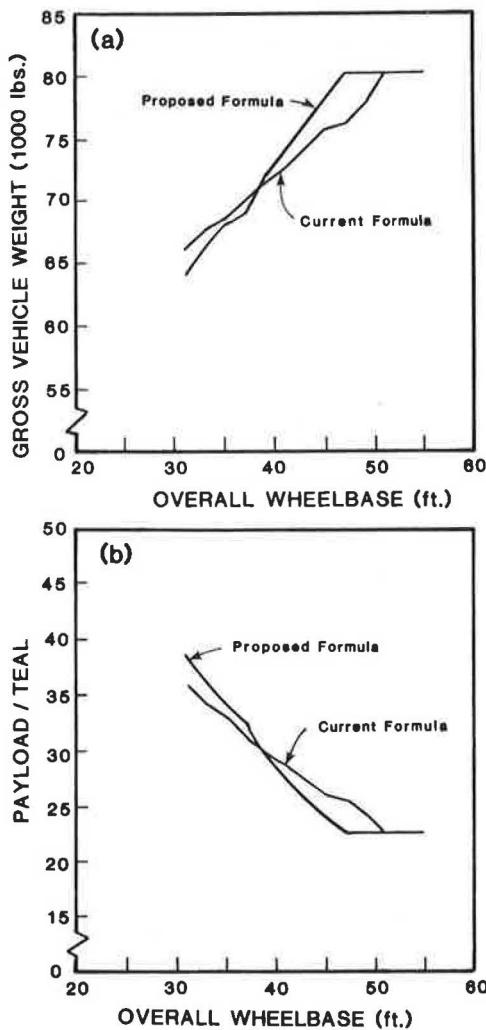


FIGURE 3 Curves illustrating gross vehicle weight and payload per equivalent axle load for 3S2 vehicles complying with proposed and current bridge formulas (1,000 lb = 4.448 kN and 1 ft = 0.3048 m).

Further Studies on Lateral Load Distribution Using a Finite Element Method

CLIFFORD O. HAYS, Jr., LARRY M. SESSIONS, and ALAN J. BERRY

ABSTRACT

A computer program, SALOD, has been written for the Florida Department of Transportation to evaluate the lateral load distribution characteristics of simple-span bridges in flexure. Bridges may be prestressed concrete girder, steel girder, T-beam, or flat slab. The program uses moment influence services generated by the STRUDL finite element system for representative simple-span bridges determined by a statewide survey. Up to three vehicles are placed in critical locations to determine the maximum distribution factors. The effect of span length, which is neglected in AASHTO, was found to be considerable. AASHTO results were found to be slightly unconservative for short spans and quite conservative for longer spans. Field testing, reported elsewhere, has been completed on eight bridges. Comparisons of results from finite element models and measurements of applied truck loading have been generally good. Comparisons of flexural distribution factors from SALOD and the Ontario Highway Bridge Design Code (OHBDC) for prestressed girder bridges showed generally good agreement. However, OHBDC indicates more sensitivity to girder spacing than does SALOD. AASHTO simple-span results compare quite well with SALOD for exterior girders. A limited study of shear distribution factors for girder-slab bridges showed that shear distribution factors do not vary significantly with span length and that AASHTO factors appeared adequate for design.

Lateral load distribution based on flexure in highway bridges has been the subject of previous research at the University of Florida (1). The AASHTO procedure for computing flexural distribution factors is generally used for bridge design by the Florida Department of Transportation (FDOT) and tends to be overly conservative for analyzing infrequent bridge overloads, which causes unnecessary rerouting of vehicles in some circumstances.

A computer program, Structural Analysis for Load Distribution (SALOD), was developed in prior research to compute accurate flexural distribution factors for a variety of girder-slab bridges under specific vehicular loading. The SALOD program uses a data base of influence surfaces that were generated using the finite element method of analysis with the STRUDL software package available on the FDOT computer system. The program has proven useful to the FDOT not only for large overload vehicles but also in evaluating bridges for legally permitted standard vehicles that may cause larger moments than AASHTO design vehicles because of close axle spacings.

A brief summary of the SALOD program, comparisons of the flexural distribution factors obtained using SALOD and the recommendations of the Ontario Highway Bridge Design Code (OHBDC) for a wide range of prestressed concrete girder bridges, and a brief study of shear distribution in prestressed concrete girders are presented. In addition, field studies were made to verify the finite element technique used in developing the SALOD program. These studies, reported elsewhere (2), demonstrated that the SALOD program

could be used to obtain accurate predictions of flexural lateral load distribution.

SALOD COMPUTER PROGRAM

The SALOD program computes flexural distribution factors (or effective widths) for the following simple-span bridge systems: (a) prestressed concrete girders, (b) cast-in-place T-beams, (c) steel girders, and (d) flat slabs. A bridge can be loaded with as many as three standard (vehicle data stored in the program) or nonstandard vehicles. The program arranges the vehicles and locates them on the bridge in such a manner as to produce the maximum midspan girder moment. The distribution factor is computed as the ratio of this moment to half the simple beam moment due to one of the vehicles.

The midspan girder moment is obtained through the use of midspan moment influence surfaces. A permanently stored data base of influence surfaces has been generated for the four bridge types previously listed using the finite element method of analysis in conjunction with the McAuto STRUDL software package (3), which is available on the FDOT computer system. The selection of important bridge parameters, their range, and specific values within that range to be included in the data base was based on a statewide bridge parameter survey, practicality, and preliminary studies.

The SALOD program uses interpolation and a limited amount of extrapolation between the combinations of specific bridge parameter values represented in the data base to obtain an influence surface for the actual bridge data input for analysis. The SALOD program generates a mesh for the bridge being analyzed. This mesh is similar to the mesh used in the finite element model that was used to develop the set of influence surfaces for that particular bridge type.

C.O. Hays, Jr., Department of Civil Engineering, University of Florida, Gainesville, Fla. 32601. L.M. Sessions, Florida Department of Transportation, Tallahassee, Fla. 32310. A.J. Berry, Post, Buckley, Schuh & Jernigan, Inc., 3715 Northside Parkway, N.W., Atlanta, Ga. 30327.

The moment at midspan is computed by (a) distributing each wheel load to the finite element nodes, (b) multiplying each nodal load by the corresponding interpolated influence value at that node, and (c) summing the values obtained for all the wheel loads on the bridge. The maximum moment and critical locations of the vehicles are found by performing this operation with the vehicles systematically positioned at various longitudinal and lateral locations; vehicle spacing and clearance requirements are taken into consideration. For the girder bridges, this is done separately for each girder.

SALOD Finite Element Modeling

The following list gives the major assumptions and decisions made while developing the finite element models (Figure 1).

1. Linearly elastic behavior was assumed. This follows common practice (4) and results in a safe distribution of girder moments due to the ductile behavior of girder-slab bridges (5).
2. All girders, including the exterior girder, were assumed to have the same moment of inertia.
3. Plate bending elements were used for the finite element model of the bridge deck. Standard frame elements were used to model the girders and diaphragms.
4. The deck elements over the girders were artificially thickened to increase the transverse plate bending stiffness of the slab due to the girders for prestressed girder and T-beam bridges.
5. On the basis of the statewide survey, slab thickness was taken as 7.0 in. for prestressed girder and steel girder bridges and 7.5 in. for T-beam bridges. A study (1) showed that slab thickness has a minor effect on influence surface values.
6. Ten elements per half-span were used in the longitudinal (Y) direction for all the finite element models except that for flat slabs.
7. Two elements over the girders and four elements between adjacent girders were used in the lateral (X) direction for prestressed girder and T-beam bridges. Steel girder bridges had six equally spaced elements between girder centerlines.

8. For T-beam models, the ratio of girder spacing to girder width was held constant at five. Natesaiyer (6) showed that this gave generally good results for a wide range of actual T-beam dimensions.

9. Composite action between girders and deck slab was assumed for T-beams and prestressed girders; steel girders may be composite or noncomposite. Effective slab width was calculated on the basis of standard AASHTO recommendations, which are acceptable because minor variations in moment of inertia have little effect on influence surface values (1).

10. A torsional moment of inertia (J) of 20 in.⁴ was used for steel girder bridges. Small J-values have little effect on load distribution (7). For all T-beam bridges, a torsional moment of inertia of 10,000 in.⁴ was used. For prestressed girders, the torsional moment of inertia was obtained from a previous finite element solution (8).

11. Diaphragms with an 8- x 54-in. cross section were used only at the span ends for prestressed girder and steel girder bridges. Variation in the moment of inertia of end diaphragms had a negligible effect on influence values (1). End diaphragms were omitted from the T-beam model. Intermediate diaphragms were omitted from all models for simplicity because it has been shown that they often have a negligible effect on load distribution (9,10).

12. Half-span bridge models were used because of their structural symmetry about midspan (critical moment location).

13. The boundary conditions at midspan were set such that the midspan moments would be taken only by the girders and the slab moments at midspan would be neglected (prestressed girder and steel girder bridges). This simplification is acceptable because a study showed that the moment taken by the slab is negligible except for short spans (1). However, slab centerline moments were included for T-beam bridges, which generally have short spans.

General Assumptions and Procedures

The following list gives some general assumptions and procedures used in developing SALOD.

1. The maximum moment was assumed to occur at midspan. This is not true for a series of concen-

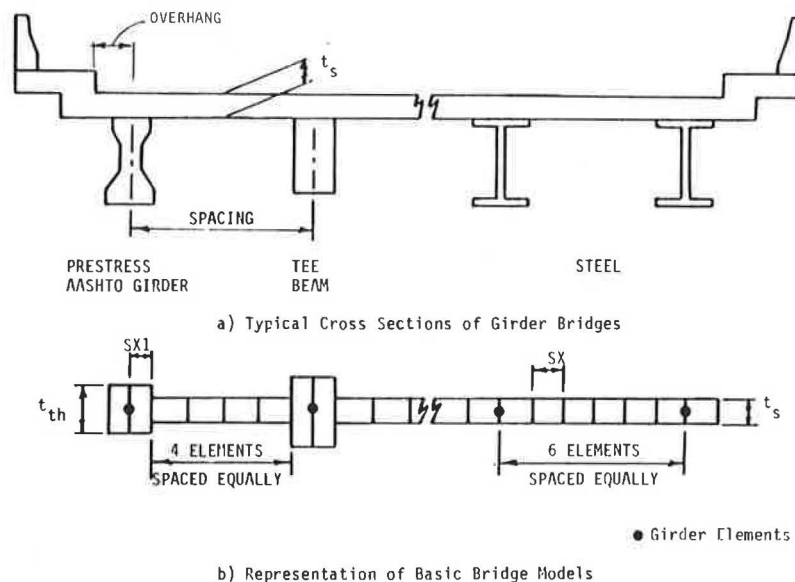


FIGURE 1 Typical section view of slab and girders.

trated loads; however, a study showed that the distribution factor is not significantly affected (1).

2. The modulus of elasticity was computed using the American Concrete Institute (4) recommendations for normal weight concrete.

3. Concrete 28-day compressive stress (f'_c) of 3,400 psi was used for the deck slab as required by FDOT specifications.

4. Standard AASHTO prestressed concrete girder Types II, III, and IV were used with a 28-day f'_c of 5,000 psi.

5. Only four-, five-, and six-girder bridges were considered. Studies (1,11) showed that a six-girder SALOD solution may be used to obtain generally conservative results for bridges with more than six girders.

6. The moment of inertia for steel girder bridges was calculated at the midspan cross section. A study showed that variation in moment of inertia along the span due to cover plate cutoff had little effect on influence surface values at the centerline of bridges (1).

7. Bridge skew was neglected. This will generally give conservative results for girder-slab bridges (12).

8. Standard FDOT vehicles stored by the SALOD program were SU 2, SU 3, SU 4, C 3, C 4, and C 5. Also, H 20 and HS 20 standard AASHTO vehicles were stored in the program. Nonstandard vehicles can be input by the user.

9. For vehicle clearance limitations used by the SALOD program, the vehicles' wheels are assumed to be 9 in. wide. As applied loads, they are assumed to act as concentrated point loads.

10. Wheel loads are distributed to adjacent nodes assuming a series of simple stringers is acting.

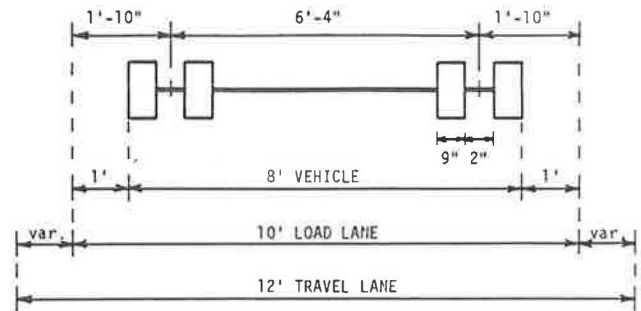
11. A travel lane of 12 ft with a 10-ft load lane, which can be shifted to any position in the travel lane, is used to determine spacing limitations between vehicles for multiple vehicle loading (Figure 2). These spacing limits were developed using standard AASHTO vehicles; however, for nonstandard vehicles with different widths, the same spacing limitations are followed.

FORCE COMPUTER PROGRAM

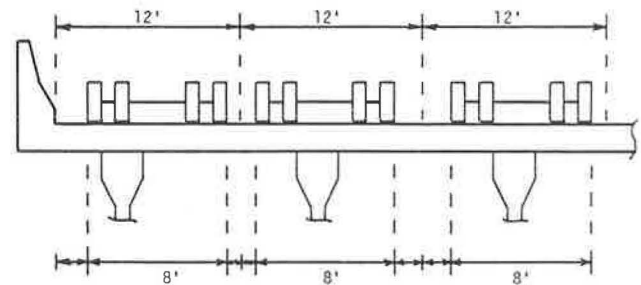
The FORCE program was developed as a labor-saving aid in the analysis of bridges by the finite element procedure using the STRUDL software package. The program sets up a full-span finite element model for simply supported prestressed concrete girder, T-beam, steel girder, and flat slab bridges; computes the nodal loads for as many as three simultaneously acting vehicles placed at any location on the bridge; and generates a STRUDL program that can subsequently be executed. Many of the assumptions used in the finite element models that are generated by FORCE are similar to those previously described for the SALOD program. However, FORCE has more generality than SALOD and thus can be used for a wider range of bridges than permitted by SALOD. FORCE was used extensively in the shear studies and field studies (2). Details on the FORCE program are available elsewhere (11).

DETAILED COMPARISON OF SALOD AND OHBDC FLEXURAL DISTRIBUTION FACTORS

The OHBDC (13,14) method for computing flexural distribution factors takes span length, girder spacing, and stiffness properties into consideration. A comparison of SALOD and OHBDC distribution factors may help mutually reinforce their validity.



a. Standard width vehicle in travel lane



SPACING CASE

1:	1'	3'+1'=4'	3'+1'=4'
2:	3'	1'+1'=2'	3'+1'=4'
3:	2'	2'+1'=3'	3'+1'=4'
4:	3'	1'+2'=3'	2'+1'=3'

b. Spacing cases for multiple travel lanes

FIGURE 2 Lane loading by standard vehicles.

OHBDC Method

The method used by OHBDC for computing flexural distribution factors was developed using orthotropic plate theory and checked by the grillage analogy method (15-17). Various bridge parameters such as slab stiffness (longitudinal and transverse), girder moment of inertia and torsional inertia, bridge width, span length, and girder spacing are combined to obtain two dimensionless parameters (α and θ) that characterize the orthotropic plate. Graphs, which are plots of α versus θ at various D-values (ratio of total longitudinal moment to the maximum intensity of longitudinal moment per unit length), are presented in the code. Depending on the number of lanes, separate graphs are included for interior and exterior girders along with a graph for determining a lane-width correction factor. To analyze a bridge, first α and θ are computed, then the proper graph is chosen to obtain a D-value. The D-value is then corrected to account for bridge width. The final corrected value (D_q) is used to compute the distribution factor, equal to S/D_q , where S is the girder spacing.

OHBDC Modification Factors and Critical Loading

In the development of the OHBDC graphs, modification factors were used to account for the probability of the presence of multiple vehicles on a bridge. The modification factors used were 1.0, 0.9, and 0.8 for one, two, and three vehicles, respectively. Also, the graphs were developed on the basis of the criti-

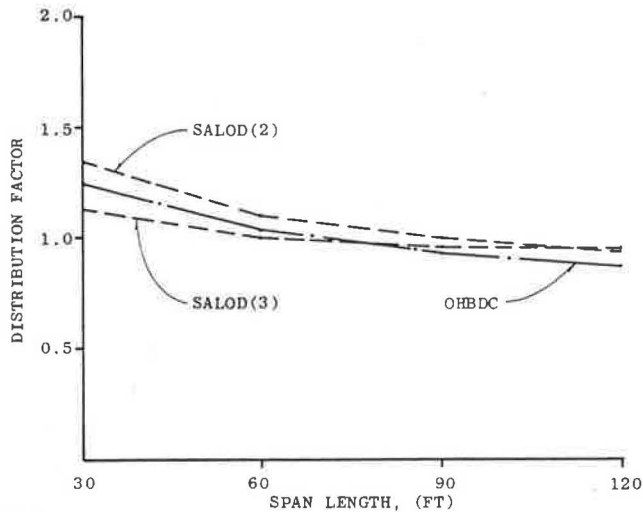
cal loading case. For example, a three-lane bridge could be loaded with one, two, or three vehicles simultaneously. The theoretical D-values were divided by the appropriate probability modification factor. To make a direct comparison with SALOD, the same modification factors were applied to the SALOD results.

Bridge and Loading Parameters Studied

The bridges used in this study were analyzed by SALOD and OHBDC and the results are presented in the form of a parametric study. There are two separate sets of graphs--one set for interior girders and one for exterior girders. Additional curves are included elsewhere (11).

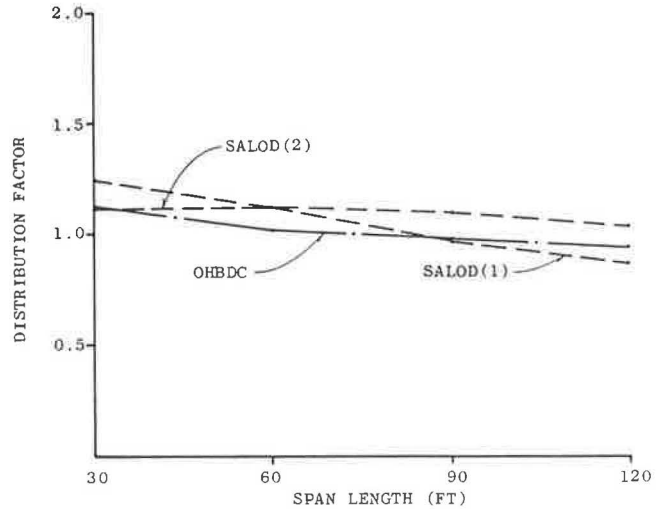
The graphs showing the effect of span length are shown in Figure 3 for interior girders and in Figure 4 for exterior girders. The bridges used in this study had five Type III prestressed concrete girders spaced at 7.0 ft with span lengths of 30, 60, 90, and 120 ft. The overhang was selected as 3.0 ft to conform closely with OHBDC maximum overhang requirements. In the analyses, three design lanes with a width of 12.0 ft were used. This was slightly conservative because the bridge was only 34 ft wide. The bridge was loaded with one, two, and three standard H 20 vehicles. The SALOD solution for one H 20 vehicle was never critical for interior girders and the modified three-H 20 solution was never critical for exterior girders. Therefore, these two curves were omitted from the corresponding graphs.

The sets of graphs showing the effect of girder spacing are shown in Figure 5 (a and b) for interior girders and in Figure 6 (a and b) for exterior girders. The bridges used in this study had a constant distance of 28 ft between centerlines of exterior girders with an overhang of 3.0 ft on each side. Bridges with span lengths of 30, 60, 90, and 120 ft were used. However, results are shown herein for only the 30- and 120-ft spans. Each bridge had four, five, or six Type III prestressed concrete girders with corresponding 9.33-, 7.0-, or 5.6-ft spacings, respectively. All other conditions were the same as previously described for the span length study.



- Notes:
 1) SALOD distribution factors are modified using OHBDC probability factors.
 2) SALOD(N) = SALOD solution for N vehicles.
 3) Girder spacing = 7.0 feet.

FIGURE 3 Variation of SALOD and OHBDC flexural distribution factors with span length for interior girders.

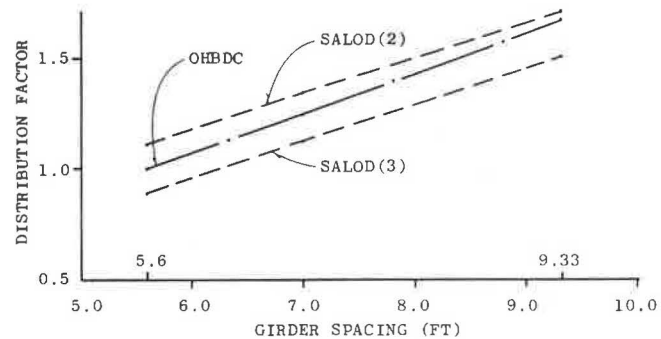


- Notes:
 1) SALOD distribution factors are modified using OHBDC probability factors.
 2) SALOD(N) = SALOD solution for N vehicles.
 3) Girder spacing = 7.0 feet.

FIGURE 4 Variation of SALOD and OHBDC flexural distribution factors with span length for exterior girders.

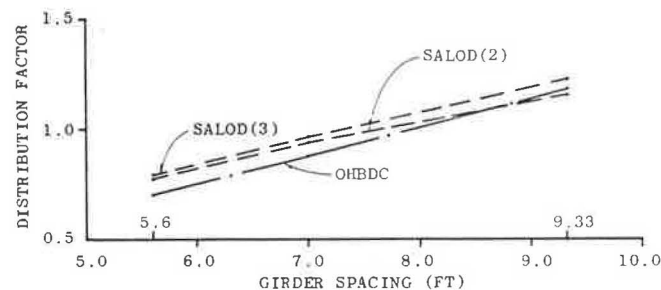
Discussion of Results

Figure 3 shows that the distribution factor varies significantly with span length for both SALOD and OHBDC solutions. Both show about the same percentage change in the distribution factors with changing



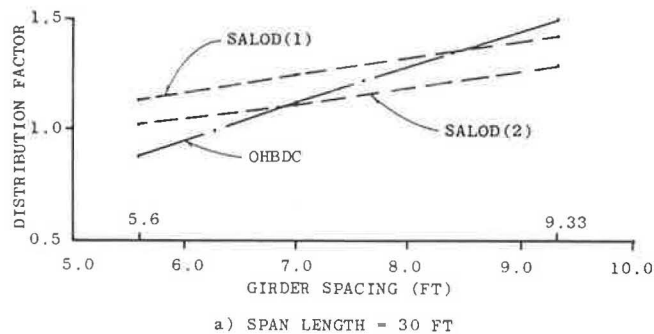
a) SPAN LENGTH = 30 FT

- Notes:
 1) SALOD distribution factors are modified using OHBDC probability factors.
 2) SALOD(N) = SALOD solution for N vehicles.



b) SPAN LENGTH = 120 FT

FIGURE 5 Variation of SALOD and OHBDC flexural distribution factors with girder spacing for interior girders.



Notes:

- 1) SALOD distribution factors are modified using OHBDC probability factors.
- 2) SALOD(N) = SALOD solution for N vehicles.

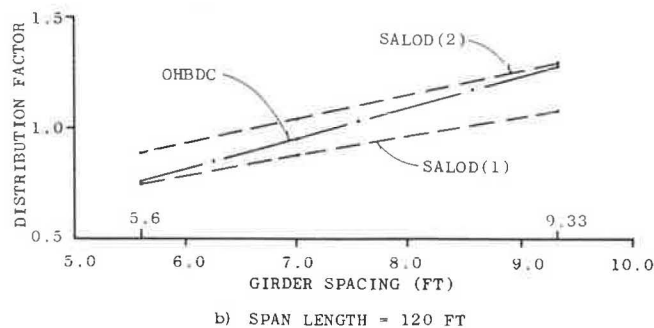


FIGURE 6 Variation of SALOD and OHBDC flexural distribution factors with girder spacing for exterior girders.

span; however, the critical SALOD curve is generally conservative, compared with that of OHBDC, by about 8 percent. This can be attributed mainly to two averaging processes used by OHBDC when idealizing the bridge as an orthotropic plate. First, this method uses a smeared, or average, stiffness across the width of the bridge, whereas SALOD accounts for the exact position of increased stiffness due to the girders. Second, OHBDC graphs are based on moments that are averaged over a certain transverse width of plate to eliminate highly localized intensities of longitudinal moments resulting under concentrated loads as predicted by orthotropic plate analysis (15).

Figure 5 (a and b) compares the distribution factor variation with girder spacing at different span lengths. The critical SALOD distribution factors are always slightly conservative compared with those from OHBDC. The difference changes slightly depending on span length and girder spacing; however, both methods show essentially the same variation in the distribution factor with girder spacing.

Figure 4 shows the variation of SALOD and OHBDC distribution factors with span length for exterior girders. Both methods exhibit the same trends with span length variation. The critical SALOD values are about 10 percent higher than those of OHBDC. However, Figure 6 (a and b) illustrates that the OHBDC distribution factors show a much more pronounced effect with changing girder spacing than SALOD. The method used by OHBDC for averaging the peak moments may be less accurate for exterior girders than for interior ones because of eccentric loading. Also, the exterior girder distribution factor is quite sensitive to vehicle positioning relative to the position of the exterior girder.

DESIGN COMPARISONS OF SALOD, AASHTO, AND OHBDC FLEXURAL DISTRIBUTION FACTORS

The previous comparison was used to help validate the SALOD and OHBDC procedures. It is also interesting to compare the results that would be used for design by AASHTO, OHBDC, and SALOD. The bridge data used for the following comparison are the same data used in developing Figures 3 and 4 for the previous SALOD and OHBDC comparison. Figure 7a shows the variation of critical interior girder distribution factors with span length for SALOD, AASHTO, and OHBDC. Figure 7b shows the same variation for exterior girders. The OHBDC curves are based on those in Figures 3 and 4 except that the SALOD distribution factors are now modified according to the AASHTO probability factors of 1.0, 1.0, and 0.9 for one, two, and three vehicles, respectively. The AASHTO distribution factors are computed as $S/5.5$ for interior girders, and the simple-beam criterion recommended by AASHTO is used for exterior girders.

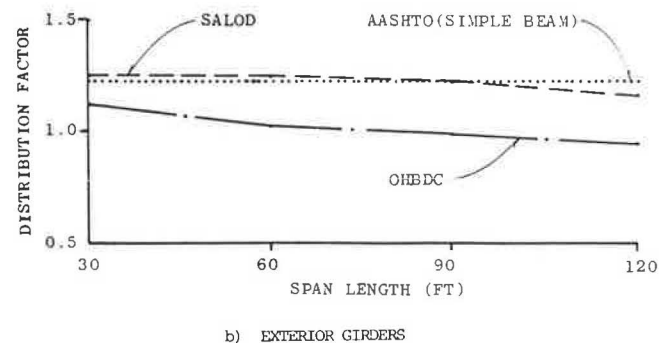
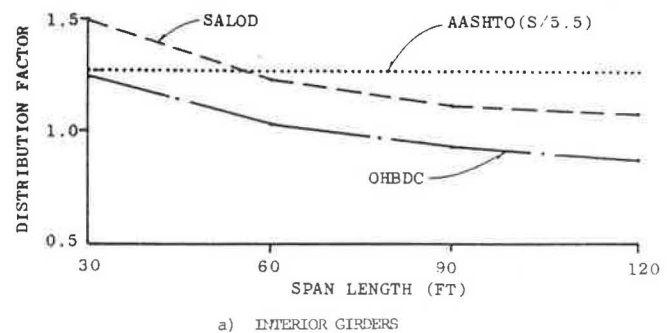


FIGURE 7 Variation of SALOD, AASHTO, and OHBDC flexural distribution factors with span length.

In Figure 7a for interior girders, it can be seen that AASHTO, which neglects the span length effect, matches OHBDC for the 30-ft span length and agrees with the SALOD results for the 60-ft span length. SALOD and OHBDC both become less conservative with increasing span length and differ by about 17 percent. This large difference is the result of OHBDC's having more liberal modification factors than AASHTO and other reasons discussed previously. Also, it should be noted that the basic design vehicles specified by the Ontario code (13) are heavier than those recommended by AASHTO (18). Both SALOD and OHBDC show a definite span length effect--about a 22 percent change in the distribution factor between the 30- and 120-ft span lengths--whereas AASHTO shows no span effect.

Figure 7b for exterior girders shows that SALOD agrees well with the AASHTO simple-beam results. The OHBDC distribution factors are again lower than those computed by SALOD. The effect of span-length on the distribution factors for exterior girders is quite small.

SHEAR STUDIES

The distribution of shear in girder-slab bridges has received little attention in previous literature. The OHBDC gives recommendations for design based on studies using the grillage analogy method for developing shear distribution factors (13).

Shear Distribution Study for Prestressed Concrete Girder Bridges

Variations of shear and moment distribution factors along the span lengths for exterior girders and critical interior girders were determined using STRUDL finite element models generated by the FORCE program. These variations were plotted along with the results obtained using the SALOD program and OHBDC. Both shear and moment distribution factor variations were plotted because AASHTO recommendations for computing the shear capacity of prestressed concrete girders include an equation for the combined effect of shear and moment. The STRUDL and SALOD distribution factors were modified using OHBDC probability factors for a direct comparison of methods.

Bridge and Loading Parameters

The bridges used in the following studies are the same as those used in the flexural distribution factor study presented in this paper, except the 120-ft span bridges are not included in the shear study.

Vehicle loading for all bridges consisted of one H 20 and then two-H 20 standard AASHTO vehicles. All vehicles were facing in the forward (positive Y) direction. The critical lateral positioning of the vehicles to create the maximum girder shear was obtained by using the vehicle and bridge clearance limitations used by the SALOD program (Figure 2).

In the longitudinal direction, seven loading positions were used for Load Position 1, and the vehicles were positioned with their rear axle at the span end (Y = 0). For Load Positions 2 through 7, the vehicles were positioned with their rear axle at Y/L equal to 0.05, 0.1, 0.2, 0.3, 0.4, and 0.5, respectively (where Y is the distance from the span end and L is the span length).

STRUDL Distribution Factors

Finite element solutions were obtained with the vehicles at each of these load positions. The distribution factors were computed by dividing the output shears and moments by one-half of the corresponding simple-beam shears and moments at the same locations.

OHBDC Shear Distribution Factors

Shear distribution factors used for design by the OHBDC (13,14) are based on bridge type, number of lanes, and a correction factor that is used when the girder spacing is less than 2.0 m (6.56 ft). Also, OHBDC does not distinguish between exterior and interior girders for shear.

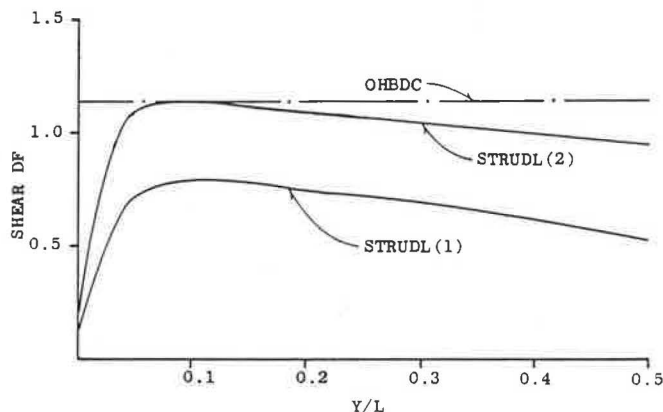
Variation of Distribution Factors Along Span

Complete results of this shear study are presented elsewhere (11) in graphs similar to those shown in Figures 8 and 9. The figures show the variation of shear and moment distribution factors along the span computed using STRUDL. Also the results from SALOD and OHBDC are included. The SALOD distribution factors are based on and shown only for flexure.

As can be seen in these graphs, for interior girders, the two-H 20 solution is always critical for both shear and flexure. The shear distribution factors (STRUDL) vary significantly along the span, especially close to the span end. The sharp decrease in the distribution factor near the end is due to the end diaphragm. The end diaphragm was assumed to be in contact with the slab and thus was connected at all the nodes between the exterior girders. If the slab is not in contact with the diaphragm, the model will overestimate the diaphragm's effect at the end of the span.

The maximum shear distribution factor appears to occur at Y/L of about 0.05 and the distribution factor begins to decrease at positions farther from the span end. The short-span bridges show a continued decrease in the shear distribution factor to span centerline. For longer spans (not shown here), the curves decrease to a minimum at about quarter-span and then rise slightly at positions close to the span centerline.

The flexural distribution factors also vary along the span. However, this variation is much less than for shear distribution, except for positions of Y less than about 0.2 L where moments are small. The SALOD distribution factors agree well with the STRUDL



- Notes:
 1) SALOD and STRUDL distribution factors are modified using OHBDC probability factors.
 2) (N) = solution for N vehicles.

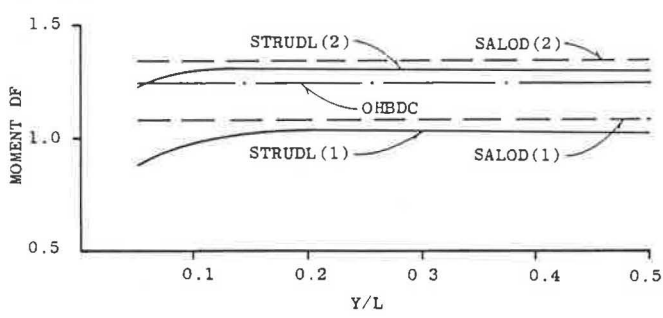
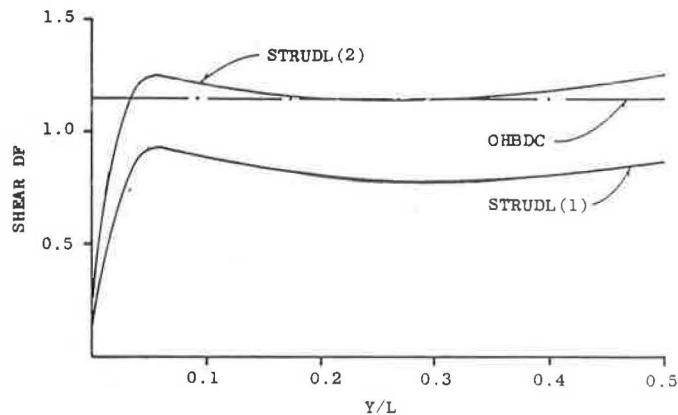


FIGURE 8 Variation of shear and moment distribution factors along the span for the critical interior girder with 30-ft span.



Notes:

- 1) SALOD and STRUDL distribution factors are modified using OHBDC probability factors.
- 2) (N) = solution for N vehicles.

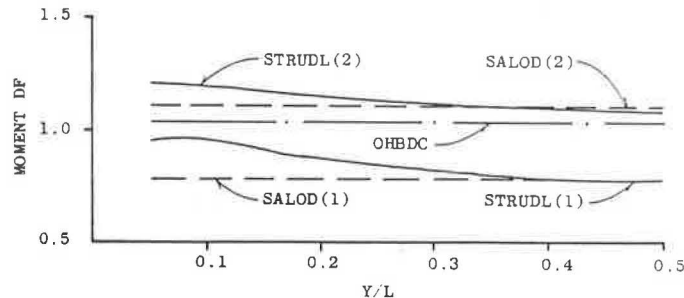


FIGURE 9 Variation of shear and moment distribution factors along the span for the critical interior girder with 60-ft span.

flexural distribution factors at midspan as expected. Thus SALOD flexural distribution factors are sufficiently close to the STRUDL factors for flexure at Y/L greater than about 0.2.

Because the AASHTO specifications for the design of prestressed concrete girders include an equation that considers the ratio of girder shear to moment, it is interesting to study the ratio of STRUDL shear distribution factors to STRUDL flexural distribution factors. This ratio was computed at Y/L in the region of 0.2 to 0.3 for all the bridges (11) and was found to vary widely from bridge to bridge, ranging from about 0.8 to about 1.2 for interior girders. This ratio increased with increasing span length and decreased with increasing girder spacing. However, the ratio for short spans showed little change with girder spacing.

The STRUDL and OHBDC shear distribution factors were found to match best at Y/L between 0.2 and 0.3, except at the wider girder spacings. However, the OHBDC procedure was apparently developed for maximum shear near the span end (3).

Shear Distribution Factor Parameter Study

The shear distribution factor parameter study shown in Figures 10 (a and b) for interior girders and 11 (a and b) for exterior girders contains results for AASHTO, OHBDC, and STRUDL. Additional graphs are included elsewhere (11). The STRUDL distribution factors were determined using the critical loading condition without modifying the results for probability of loading for a more direct comparison with AASHTO.

The STRUDL analysis for the shear study (11)

developed shear distribution factors at several positions along the span. However, shear in prestressed girders may be more critical at quarter-span (19). Thus the shear distribution factors plotted in Figures 10 and 11 were determined from the largest value in the region of Y/L between 0.2 and 0.3 for the critical loading.

AASHTO Shear Distribution Factors

For loads at the support, AASHTO recommends computing the shear distribution factors assuming simple-beam action between girders in the transverse direction. For loads away from the support, AASHTO recommends using the flexural criteria for computing shear distribution factors. This requires using the formula $S/5.5$ for interior girders and the simple-beam approach for exterior girders.

In the figures, graph (a) shows the variation in the shear distribution factors with changing span length for the bridges with girder spacing of 7.0 ft. As seen in this figure, there is no significant variation in the shear distribution factors with changing span. STRUDL varies only 3 percent, and AASHTO and OHBDC do not consider span length.

Figure 10b shows the variation in the shear distribution factor with changing girder spacing for interior girders with a 60-ft span. The STRUDL curves are generally slightly less sloped than are those of the other two methods. That is, STRUDL shear distribution factors show less sensitivity to changing girder spacing. OHBDC is generally unconservative compared with STRUDL. This is primarily due to the probability factors that are implicit in the OHBDC

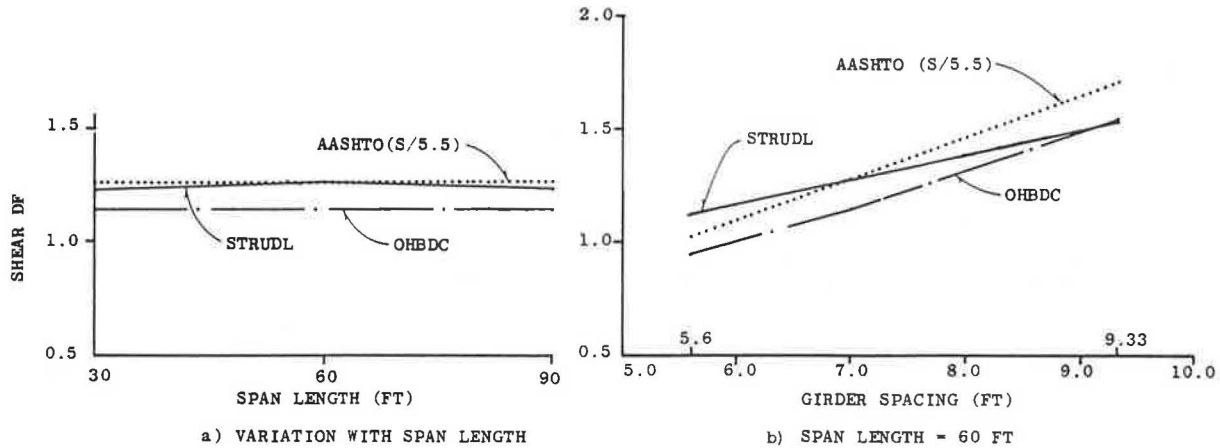


FIGURE 10 Shear distribution factors for interior girders.

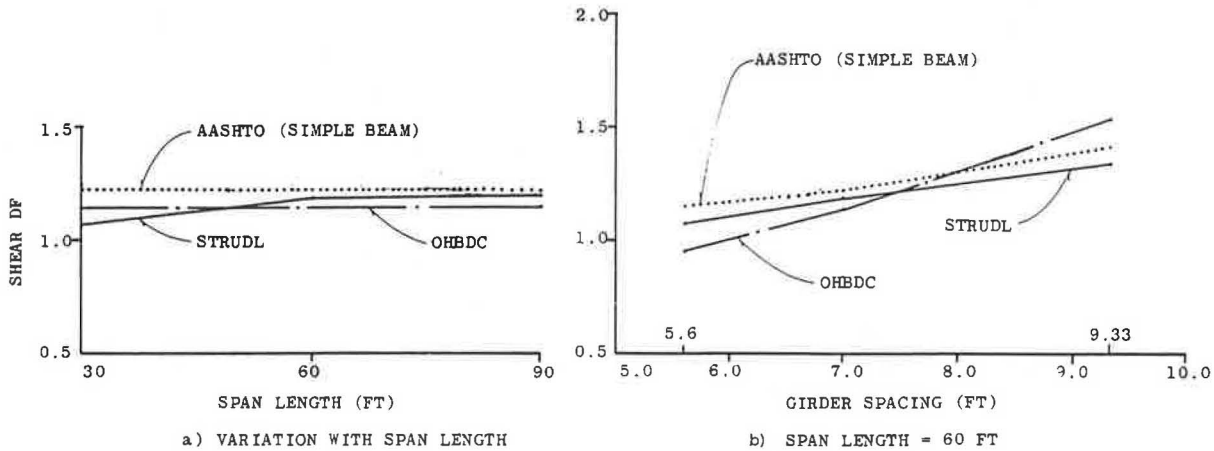


FIGURE 11 Shear distribution factors for exterior girders.

solution. However, at wider girder spacings, OHBDC tends to become conservative. The AASHTO curves are consistently close to the STRUDL curves (within 14 percent) and are usually on the conservative side. At shorter girder spacings, AASHTO becomes unconservative by about 3 to 9 percent depending on the span length. AASHTO appears to be adequate for design.

Figure 11 compares the shear distribution factors for STRUDL, AASHTO, and OHBDC for exterior girders. Figure 11a shows the variation with span length. This figure shows that all methods have no significant variation with span length.

Figure 11b shows the variation in the shear distribution factor with changing girder spacing for exterior girders. STRUDL shows a 14 percent variation with girder spacing at the 30-ft span length. OHBDC varies 38 percent with girder spacing and differs from STRUDL by as much as 31 percent on the conservative side and 11 percent on the unconservative side.

The exterior girder curves for AASHTO are conservative compared with STRUDL for practically all bridges studied. This conservatism is generally less than 10 percent, except for the 30-ft span (not shown here).

FIELD STUDIES

The finite element method is today a well-accepted method of analysis. However, any method of analysis

or modeling technique requires some degree of approximation when applied to a real structure. Thus it was prudent to verify the modeling assumptions made in the finite element analysis used to generate the data base for SALOD. A total of eight spans were tested, two of each of the following types:

1. Prestressed concrete girder bridges,
2. Steel girder bridges,
3. T-beam bridges, and
4. Flat slab bridges.

All of the bridges were simple span and tested under static load conditions. Strain and deflection data were taken near midspan using a data acquisition system. Complete details on the testing program and evaluation of results are available elsewhere (2).

CONCLUSIONS AND RECOMMENDATIONS

Parameter studies were done for prestressed concrete girder bridges covering a wide range of span lengths and girder spacings. Comparisons of OHBDC, AASHTO, and SALOD flexural distribution factors for interior girders show that, unlike AASHTO, both SALOD and OHBDC exhibit significant variation with span length. Both OHBDC and SALOD show the same percentage change in the distribution factors with changing girder spacing. However, OHBDC is generally about 8 percent unconservative compared with SALOD because of model-

ing differences. AASHTO is conservative compared with SALOD except at short span lengths.

For exterior girders, the OHBDC flexural distribution factors tend to be more sensitive to changing girder spacing than is SALOD or AASHTO. The simple-beam criterion used by AASHTO is a good representation of the flexural distribution characteristics of exterior girders.

In the design of prestressed concrete girders, considering the combined effect of shear and moment in the quarter-span region, distribution factors should be computed using the following guidelines:

1. Use the AASHTO criteria for computing shear distribution factors.

2. Use the SALOD program for computing flexural distribution factors. This procedure should give sufficiently accurate results for most prestressed concrete girder bridges. However, it should be noted that AASHTO shear distribution factors may be unconservative at short girder spacings.

The SALOD program used influence surfaces developed using the finite element method. A series of tests (2) was conducted to validate the modeling techniques used in developing the influence surfaces for the SALOD program. The test program was believed to generally confirm the applicability of the finite element modeling techniques used in SALOD as a useful tool for predicting the moments in bridges for purposes of analysis and design.

ACKNOWLEDGMENTS

The authors would like to acknowledge the cooperative efforts of the Florida Department of Transportation in making this research possible. In addition to providing financial support, the FDOT provided equipment and personnel essential for the field-testing phase of the research. Also, FDOT personnel were most helpful in implementing the computer programs on their computer system.

The authors would also like to express their appreciation to John E. Hachey, a former graduate student at the University of Florida, who did much of the programming on the original version of SALOD.

REFERENCES

1. C.O. Hays and J.E. Hachey. Lateral Distribution of Wheel Loads on Highway Bridges Using the Finite Element Method. Structures and Materials Research Report 84-3. Engineering and Industrial Experiment Station, University of Florida, Gainesville, Dec. 1984.
2. C.O. Hays and P. Foley. Field Studies on Lateral Distribution of Wheel Loads on Highway Bridges. Structures and Materials Research Report 85-3. Engineering and Industrial Experiment Station, University of Florida, Gainesville, Aug. 1985.
3. STRUDL User Manual. McDonnell Douglas Automation Company, St. Louis, Mo., Oct. 1983.
4. Building Code Requirements for Reinforced Concrete. ACI 318-83. Committee 318, American Concrete Institute, Detroit, Mich., 1983.
5. C.N. Kostem. Overloading Behavior of Beam-Slab Highway Bridges. Fritz Engineering Laboratory Report 387B.8. Bethlehem, Pa., July 1977.
6. K.C. Natesaiyer. Influence Surfaces for Highway Bridge Decks. M.S. thesis. University of Florida, Gainesville, 1984.
7. A.F. Alani and J.E. Breen. Verification of Computer Simulation Methods for Slab and Girder Bridge Systems. Report 115-1F. Center for Highway Research, The University of Texas at Austin, Aug. 1971.
8. C. Shieh and H.A. Sawyer. Inelastic Analysis of Prestressed Girder Bridge. Final Report D651-DF. Engineering and Industrial Experiment Station, University of Florida, Gainesville, 1975.
9. C.N. Kostem and E.S. DeCastro. Effects of Diaphragms on Lateral Load Distribution in Beam-Slab Bridges. In Transportation Research Record 645, TRB, National Research Council, Washington, D.C., 1977, pp. 6-9.
10. M.W. Self. Experimental Investigation of the Influence of an Interior Diaphragm on the Behavior of a Model Prestressed Concrete Bridge Under Static and Dynamic Loading. Report D602. Engineering and Industrial Experiment Station, University of Florida, Gainesville, July 1969.
11. C.O. Hays and A.J. Berry. Further Analytical Studies on Lateral Distribution of Wheel Loads on Highway Bridges. Structures and Materials Research Report 85-2. Engineering and Industrial Experimental Station, University of Florida, Gainesville, Aug. 1985.
12. P.M. Kuzio. Effects of Skew Angle on Simple Span Bridge Decks Under Simulated Truck Loading. M.S. thesis. University of Florida, Gainesville, 1984.
13. Ontario Highway Bridge Design Code 1983. 2nd ed. Highway Engineering Division, Ontario Ministry of Transportation and Communications, Toronto, Ontario, Canada, 1983.
14. Ontario Highway Bridge Design Code Commentary 1983. 2nd ed. Highway Engineering Division, Ontario Ministry of Transportation and Communications, Toronto, Ontario, Canada, 1983.
15. B. Bakht, M.S. Cheung, and T.S. Aziz. Application of a Simplified Method of Calculating Longitudinal Moments to the Ontario Highway Bridge Design Code. Canadian Journal of Civil Engineering, Vol. 6, 1979.
16. A.R. Cusens and R.P. Pama. Bridge Deck Analysis. John Wiley and Sons, Inc., New York, 1975.
17. R. West. The Use of Grillage Analogy for the Analysis of Slab and Pseudoslab Bridge Decks. Research Report 21. Cement and Concrete Association, London, England, 1973.
18. Standard Specifications for Highway Bridges. 13th ed. AASHTO, Washington, D.C., 1984.
19. Interim Specifications, Bridges, 1979. AASHTO, Washington, D.C., 1979.

The opinions, findings, and conclusions expressed in this paper are those of the authors and not necessarily those of the State of Florida Department of Transportation.

Publication of this paper sponsored by Committee on General Structures.

Application of Microcomputers in Bridge Design

RONALD A. LOVE, FURMAN W. BARTON, and WALLACE T. McKEEL, Jr.

ABSTRACT

The use of microcomputers in bridge design activities in state transportation departments was evaluated through contacts with 32 state agencies. Although present use of microcomputers was found to be limited, subsequent research showed that the current generation of 16-bit machines offers significant advantages in complementing existing computing facilities in a manner that fully uses the power of both mainframe and microcomputer. The ability of microcomputers to run large bridge design applications in a stand-alone mode was demonstrated by successfully downloading and converting four mainframe programs. Running design and analysis programs in a stand-alone mode frees the mainframe CPU and increases access to software that can be run repetitively without consideration of mainframe costs. When access to larger applications on the mainframe is required, the microcomputer used as an intelligent terminal can process input data locally and send them to the mainframe for processing. Output data, in return, can be downloaded to the microcomputer and reviewed off-line or input into microcomputer applications such as spreadsheets or graphics packages for further processing.

Computer applications in engineering design have had a dramatic effect on the analysis and design process in general. Automating analysis and design procedures has relegated much of the computational burden to machines, allowing the engineer more time to evaluate alternatives and assume a more creative design and decision-making role. Although the role computers play may vary from one organization to another, their effect has been revolutionary.

The manner in which computers are utilized in the design divisions of state departments of transportation is not standardized and varies greatly. Most of the software developed for design calculations within bridge divisions was designed for implementation on large mainframe computers. Bridge designers, in large measure, have access to these programs via terminals, and this has created little demand for other computer configurations such as microcomputers. However, recent developments in microcomputer design have resulted in microcomputers that have stand-alone capabilities that rival those of mini-computers and mainframes and that also possess versatile communications capability.

There still appears to be considerable difference of opinion about the most appropriate role for microcomputers in bridge design applications. Many bridge divisions, which have their own large computer and several terminals, find their present configuration satisfactory and see no reason to incur the additional expense of microcomputers. Other bridge engineers, however, are required to use centralized state computer facilities that are sometimes shared by other state agencies. The inconvenience of gaining access, the high cost of computing and other charges, and excessive turnaround time may not be acceptable. These engineers see the new generation of microcomputers as a cost-effective and

preferred alternative for using much of the bridge design software available. In Virginia, as in many other states, many bridge design activities have been decentralized in district offices across the state. The present generation of microcomputers would appear to meet most of the computational needs of these offices. These smaller computers could supplement the mainframe, possibly using downloaded, smaller programs, in a more efficient mode of operation. The many advantages of microcomputers, such as powerful computing capability, stand-alone capability, communications capability, and cost-effectiveness, make them a powerful element in engineering computation.

It is useful and timely to evaluate the manner in which microcomputers are used in other states and to suggest the role that they may play in the future. Such information could assist bridge engineers and administrators in state departments of transportation in making decisions about the use of microcomputers.

The objective of this study was to examine the current and future role of microcomputers in bridge design applications within state departments of transportation. The focus was on the use of microcomputers, as a complement to present computing configurations, to increase productivity and enhance cost-effectiveness.

The manner in which bridge engineers currently use computers for design and analysis was evaluated by contacting a number of state and federal agencies including bridge divisions in several states. These bridge divisions were surveyed to determine their present computer configurations used for bridge design applications and their current and projected uses of microcomputers. The capabilities of the present generation of 16-bit microcomputers were evaluated for bridge design applications, several microcomputers were used to run typical bridge design software, and comparisons of performance were noted. The feasibility of converting current bridge design software from mainframes to microcomputers was evaluated through actual conversions of existing software. After examination and study of the information collected and the tests performed, the potential for increased usage of microcomputers in bridge design activities was evaluated.

R.A. Love and F.W. Barton, Department of Civil Engineering, University of Virginia, Charlottesville, Va. 22903. W.T. McKeel, Jr., Virginia Highway and Transportation Research Council, University of Virginia, Charlottesville, Va. 22903. Current address for R.A. Love: G.W. Beilfuss and Associates, Inc., 700 East Butterfield Road, Suite 220, Lombard, Ill. 60148.

MICROCOMPUTER USE IN STATE BRIDGE DIVISIONS

To determine trends in microcomputer use, an informal telephone survey of bridge divisions in various state departments of transportation was conducted, and a total of 32 states were contacted:

Alabama	Massachusetts	Pennsylvania
California	Michigan	South Carolina
Colorado	Minnesota	South Dakota
Connecticut	Mississippi	Tennessee
Delaware	Montana	Texas
Florida	Nebraska	Vermont
Georgia	New Jersey	Virginia
Illinois	New York	Washington
Iowa	North Carolina	West Virginia
Kentucky	Ohio	Wisconsin
Louisiana	Oklahoma	

Initial contacts were based on prior knowledge of microcomputer usage in these states; subsequently, other states involved in microcomputer usage were identified. Additional information on states using microcomputers for bridge design-related activities was obtained from FHWA.

The survey consisted of targeting a knowledgeable person within a state bridge division or computer division and asking the following questions.

1. What kind of computer system is used for bridge design and analysis?
2. Do your engineers and designers have computer access through
 - a. Direct access via a terminal?
 - b. Submitting data using data entry forms (data actually entered and program run by others)?
3. Do you use microcomputers in bridge design?
4. If not, do you plan to purchase microcomputers in the near future for use in bridge design activities?
5. Do you use your microcomputer as
 - a. A stand-alone unit?
 - b. An intelligent terminal linked to a larger computer?
6. What kinds of bridge design programs are run on your microcomputer?
7. Can a list of these programs be made available?
8. Are your design programs
 - a. Written in-house?
 - b. Purchased from outside vendors?
9. What programming languages are used for programs written in-house?
10. Have you converted any programs currently running on a larger computer to run on your microcomputer?
11. If so, how was the program converted?
 - a. Method of downloading used.
 - b. Type of compiler or interpreter used.
12. Is increased use of microcomputers planned for the future? If so, what are your plans (e.g., upgrade to more powerful machines, microcomputer-aided design systems)?

The questions were designed to determine the current mainframe computing environment, to assess the level of satisfaction with this environment, to identify current utilization of microcomputers in bridge design applications, and to evaluate the attitudes and perceptions of engineers regarding the usefulness of microcomputers in design. Finally, plans for future implementation of microcomputers were discussed. A summary of the responses to the survey is given in Table 1.

As a result of this survey, several conclusions

were drawn. First, the large majority of states uses mainframe computers in their bridge design and analysis work. A total of 30 out of 32 states, or 94 percent, use mainframes as their primary computing resource. The two remaining states use minicomputers. However, in almost all instances, the bridge divisions that use mainframes share them with other state agencies under some type of time-sharing arrangement.

Almost all bridge design groups (94 percent) have direct access to the computer through terminals located within the design group. In addition, some states with remote design locations, such as Pennsylvania, have terminal access at the district level. Through terminal access, the engineers are able to run mainframe applications in either interactive or batch mode, review the results, modify input if desired, and rerun the application. Some states, such as Michigan and Delaware, use screen forms packages that simplify data entry at the terminal by creating the actual input form for a given program on the terminal screen. Most states with computer configurations of this type expressed the belief that it served their computing needs well. Eleven of the 30 states with terminal access to a mainframe or minicomputer indicated that it served their computing needs completely and therefore those states showed little or no interest in using microcomputers.

However, the majority of the respondents did see some need for improvement of their computing environment. Reasons cited included slow turnaround time on time-shared systems, a desire for better access to software, and insufficient access to terminals connected to the mainframe. Of the 21 states that indicated a need for improvement in computer access, 9 including Virginia have begun using microcomputers in bridge design activities, although for the most part specific plans have not been developed (see Table 1).

The manner in which microcomputers are currently used for bridge design purposes varies widely from state to state. For example, in Montana, microcomputers are used almost exclusively for bridge design and analysis. Design and analysis programs previously run on IBM minicomputers were converted from their original FORTRAN coding to BASIC and adapted to an IBM-PC. In South Dakota, and as part of this project in Virginia, FORTRAN bridge design and analysis programs were downloaded from a mainframe computer and adapted to run on IBM-PC (or compatible) microcomputers using available microcomputer FORTRAN compilers. Ohio uses an IBM-PC 3270 networked to its mainframe and is in the process of developing some specialized bridge design-related applications. New Jersey, taking a similar approach, has recently purchased several IBM-PCs that will have communications capability with their mainframe via modems. These microcomputers were purchased to satisfy the needs of remote design locations for access to the mainframe and for stand-alone computing capability.

Other states are currently using microcomputers in bridge-related areas but to a lesser extent. New York uses microcomputers for project management functions and for field data collection and review. Future uses may include overload permit and splice design applications. Massachusetts currently uses an IBM-PC for field data collection and expressed intentions to use it for additional bridge design applications in the future. In Vermont an IBM-PC AT, to be delivered in the near future, will be the primary computer used for bridge design applications.

In addition to the states already using or beginning to use microcomputers, nine other states have indicated a desire to begin using them in the near future. Common among the responses from these states was an uncertainty about exactly what the capabilities

TABLE 1 Summary of Responses to Questions 1-4

State	Principal Computer Used for Bridge Design	Access to Mainframe via Terminals	Microcomputer Used for Bridge Design	Plans to Use Micros in Future for Bridge Design Applications
Alabama	MF	Yes	No	Yes
California	MF	Yes	No	Yes ^d
Colorado	MF	Yes	No	No
Connecticut	MF	Yes	No	No
Delaware	MF	Yes	No ^b	No
Florida	MF	Yes	No	Yes ^d
Georgia	MN	Yes	No	Yes ^d
Illinois	MF	Yes	No	Yes ^a
Iowa	MF	Yes	No	Yes ^a
Kentucky	MF	Yes	No ^c	Yes ^a
Louisiana	MF	Yes	No ^d	No
Massachusetts	MF	Yes	Yes ^e	Yes
Michigan	MF	Yes	No	No
Minnesota	MF	Yes	No	Yes ^a
Mississippi	MF	Yes	No	Yes
Montana	MN	Yes	Yes	
Nebraska	MF	Yes	No	No
New Jersey	MF	Yes	Yes	
New York	MF	Yes	Yes ^b	Yes ^f
North Carolina	MF	Yes	No	No
Ohio	MF	Yes	Yes	
Oklahoma	MF	Yes	No	No
Pennsylvania	MF	Yes	No ^b	No
South Carolina	MF	Yes	No	No
South Dakota	MF	Yes	Yes	
Tennessee	MF	Yes	No	No
Texas	MF	Yes	No	No
Vermont	MF	No	Yes	
Virginia	MF	No	Yes	
Washington	MF	Yes	Yes	Yes ^a
West Virginia	MF	Yes	No	No
Wisconsin	MF	Yes	No	Yes ^g

Note: MF = mainframe, MN = minicomputer.

^aPlans not defined at present.

^bMicrocomputers are used for spread sheets, word processing, data base management, and the like.

^cMicrocomputers are used for planning.

^dMicrocomputers are used in roadway design.

^eMicrocomputers currently used for field data collection.

^fMicrocomputers would be used more for construction management, overload permit, and splice design

work; "number crunching" would still be done on mainframe.

^gCould possibly get involved with microcomputers if they demonstrate the ability to run large-scale programs in an efficient manner.

ties of microcomputers are when used in bridge design and analysis applications. Some engineers expressed doubts about the ability of these machines to handle large programs; doubts also arose about how the integrity of software would be maintained when it was distributed among several users.

Clearly there is a need to better define the role that microcomputers can play in bridge design at the state level. Several instances have been cited of private design firms in which proper implementation of microcomputers as a complement to present computer configurations has served to increase productivity and decrease overall computing costs. This should also be true in bridge design applications.

MICROCOMPUTER HARDWARE AND SOFTWARE

The hardware components of microcomputers, namely central processing unit (CPU), keyboard, and cathode ray tube (CRT), are becoming generally familiar, but specific hardware details and capabilities may not be so familiar. The current generation of 16-bit microcomputers generally uses one of three types of central processor, the Intel 8086, the Intel 8088, or the Motorola 68000 (1). The 8086 is a true 16-bit processor in that it moves data through a 16-bit data bus and processes 16 bits at a time. The 8088 moves data through an 8-bit bus and processes 16 bits at a time. The Motorola 68000 CPU, the most powerful of the three, handles data through a 16-bit data bus but processes 32 bits at a time. Internal memory is classified into two types, read-only mem-

ory (ROM) and random access memory (RAM). The ROM is factory installed and is read when the computer is turned on; it is permanent and cannot be altered by the computer operator. RAM is temporary memory and accessible to the user; it gives microcomputers their real power because it determines the size of applications that can be run. Four different 16-bit microcomputers were available for use during this project and are given in Table 2.

In addition to internal memory capabilities, microcomputers also have mass storage capability that enables them to access vast amounts of data outside the CPU. Mass storage memory usually refers to floppy diskettes or hard disks. Storage capacity on 5 1/4-in. floppy diskettes can range from 320 kilobytes (kb) to more than one megabyte. In general, floppy diskettes provide a reliable and portable form of mass storage, though lacking in access speed and overall storage capability. Hard disks provide much greater storage capacities and access data at significantly higher speeds than floppy drives. Hard disk capacities of 20 megabytes and more are common and some allow removal of the disks in a fashion similar to floppy diskettes. Although much more expensive than floppy drives, hard disk drives are becoming more commonplace as user requirements expand. The microcomputers used in this project all had mass storage capacity of 329 kb using double-sided, double-density floppy disk drives.

Another type of mass storage is commonly known as disk emulation or RAM disk. A RAM disk is created by software that in effect partitions unused RAM into what the computer treats as an additional disk

TABLE 2 Microcomputers Used

Attribute	Description
Zenith Z-151 (Marketed by NBI)	
Word length	16-bit
Processor	Intel 8088
Operating system	MS-DOS
Installed RAM	384 kb
Mass storage	Two 360-kb DS/DD disk drives
IBM Personal Computer	
Word length	16-bit
Processor	Intel 8088
Operating system	PC-DOS; CP/M; UCSD P-System
Installed RAM	596 kb
Mass storage	Two 360-kb DS/DD disk drives
COMPAQ Portable Computer	
Word length	16-bit
Processor	Intel 8088
Operating system	MS-DOS; CP/M86; UCSD P-System
Installed RAM	256 kb
Mass storage	Two 360-kb DS/DD disk drives
AT&T Personal Computer 6300	
Word length	16-bit
Processor	Intel 8086
Operating system	MS-DOS
Installed RAM	512 kb
Mass storage	Two 360-kb DS/DD disk drives

drive. This form of mass storage provides the fastest access time because there are no mechanical drive parts involved, such as read-and-write heads. However, RAM disks are limited in capacity to whatever RAM is not used during the application.

In general, it is far more important to consider software than hardware capabilities. The most fundamental piece of software is the operating system that ties the CPU and memory to the display, keyboard, and disks. Some of the different operating systems available for the 16-bit microcomputers are MS-DOS, CP/M-86, and the UCSD P-System for single-tasking operations and Unix from Bell Labs, MP/M (an advanced version of CP/M), Pick, and Oasis for multi-tasking.

In this study, four different microcomputers were used and MS-DOS version 2.11 was the operating system used on all four machines (Table 2). Two capabilities of MS-DOS, which served well when running the large FORTRAN bridge design programs encountered in this project, were: (a) output files could be spooled to the printer while program execution continued and (b) batch capabilities allowed several program runs without an operator present. Because the execution time of some programs on microcomputers is slow relative to larger machines, the batch capability is a distinct benefit.

The ability of the 16-bit microcomputers to handle a wide variety of programming languages is further indication of their computing power and versatility. Most of these machines come with a BASIC interpreter, but there are also several dozen compilers available for a variety of languages. A fairly complete listing of these compilers and languages, taken from Ruby (2), follows.

PASCAL compilers

1. Turbo PASCAL (Borland International)
2. PASCAL/MT+ (Digital Research)
3. Micro Concurrent PASCAL (Enertec, Inc.)
4. UCSD PASCAL Compiler (IBM)
5. IBM PC PASCAL Compiler 2.0

6. MS PASCAL (Microsoft)
7. PASCAL 86/88 (Real-Time Computer Science Corporation)
8. UCSD PASCAL Compiler (Softech Microsystems)
9. Concurrent PASCAL 8086 (Soft Machines, Inc.)
10. SBB PASCAL (Software Building Blocks)

BASIC compilers

1. CRASIC Compiler 2.0 (Digital Research)
2. BASIC Compiler (IBM)
3. ATV/BASIC (LanTech Systems, Inc.)
4. BASIC Compiler (Microsoft)
5. Business BASIC
6. BASIC Compiler (Quantum Software Systems)
7. BASIC Compiler (Softech Systems)
8. BASIC (Supersoft)
9. Squish (Versaterm Systems, Ltd.)

BASIC interpreters

1. BI-286 1.4 (Control-C)
2. BASIC Interpreter (Microsoft)

Combined BASIC compilers and interpreters

1. APC BASIC (American Planning Corporation)
2. MegaBASIC
3. HAI*BAS (Holland Automation USA, Inc.)
4. Professional BASIC (Morgan Computing Company, Inc.)
5. Better BASIC (Summit Software Technology, Inc.)

Modula-2 compilers

1. Logitech Modula-2/86 (Logitech, Inc.)
2. Modula-2 for the IBM-PC (Modula Corporation)
3. M2M-PC (Modula Research Institute)
4. Volition Systems Modula-2 (Volition Systems)

APL interpreters

1. IBM-PC APL (IBM)
2. Sharp APL/PC (I.P. Sharp Associates, Ltd.)
3. APL*PLUS/PC (STSC, Inc.)
4. WATCOM APL (WATCOM Products, Inc.)

FORTRAN compilers

1. FORTRAN 77 (Digital Research)
2. FORTRAN 77 Compiler (IBM)
3. FORTRAN Compiler 2.0
4. FORTRAN Compiler (Microsoft)
5. 87 FORTRAN/RTOS (MicroWare, Inc.)
6. FORTRAN 86/88 (Real-Time Computer Science Corporation)
7. FORTRAN 77 (Quantum Software Systems, Inc.)
8. FORTRAN 77 (Softech Microsystems)
9. FORTRAN Compiler (Supersoft)
10. Professional FORTRAN (IBM)
11. R/M FORTRAN (Ryan-McFarland)

FORTH compilers and interpreters

1. HSFORTH 2.01 (Harvard Softworks)
2. PC/FORTH 3.0 (Laboratory Microsystems, Inc.)
3. PC/FORTH+ 3.0
4. MMSFORTH (Miller Microcomputer Services)
5. MVP-FORTH PAD (Mountain View Press)
6. FORTH-32 (Quest Research)

C compilers

1. C Compiler (C-Systems)
2. C Compiler (C Ware)
3. CC 86 (Control-C Software)

4. C86 (Computer Innovations, Inc.)
5. Small-C:PC (Custom Software)
6. Digital Research C3 (Digital Research)
7. Lattice C Compiler (Lifeboat Associates)
8. Aztec C 86 1.06D (Manx Software Systems)
9. MWC-85 (Mark Williams Company)
10. C Compiler (Microsoft)
11. C Compiler (Quantum Software Systems, Inc.)
12. Instant C (Rational Systems)
13. C 86/88 (Real-Time Computer Science Corporation)
14. C Compiler (Supersoft, Inc.)
15. C Compiler (Telecon Systems)
16. C Compiler (Whitesmith's, Ltd.)

COBOL compilers

1. COBOL Compiler (Digital Research)
2. MBP COBOL Compiler (MBP Software Systems Technology)
3. Level II COBOL Compiler 2.6 (Micro Focus, Inc.)
4. Personal COBOL
5. COBOL Compiler (Microsoft)
6. RM/COBOL (Ryan-McFarland)

In this study, FORTRAN was used for all of the applications and the Microsoft FORTRAN compiler was the most convenient to use. The MS-FORTRAN compiler conforms to subset FORTRAN as described in ANSI X3.9-1978 and also contains extensions to the standard. These extensions are listed in the MS-FORTRAN User's Guide, Appendix A (3). Minimizing use of these extensions increased portability and allowed the bridge design programs to be run easily on other microcomputers and the University of Virginia's Cyber mainframe.

APPLICATION SOFTWARE

With the tremendous growth in microcomputer hardware has come a corresponding growth in application software and software vendors. The number of application programs for civil engineering and construction alone has become so large that they are catalogued in Hunt's Directory (4), a good source of software for potential bridge applications. Currently the majority of vendor-supplied programs is analysis packages rather than design applications because design programs typically require more upkeep because of code changes. A review of several software sources determined that, in the area of bridge design, few design applications were available. Design packages that were found included three bridge design systems for small bridges, a pier design program, a pile design program, an influence line generation program, and several coordinate geometry programs. However, almost every conceivable type of structural analysis program was available for all makes of microcomputers. These analysis packages ranged from simple-beam analysis to full-feature integrated finite element analysis packages.

Most states perform in-house software development for their mainframe applications; because the use of microcomputers is not great, similar software development for them is limited. A few state bridge divisions that currently use microcomputers in design, such as Montana, Ohio, and Virginia, develop some software in-house. Such programs are typically written in BASIC, although Montana has converted several bridge design applications from a FORTRAN code running on an IBM 5100 minicomputer to BASIC for use on an IBM-PC. The following list gives typical bridge design applications developed in this manner.

1. Bridge centerline grade (Virginia)

2. Steel beam or girder section properties in negative moment region (Virginia)
3. Steel beam or girder section properties (Virginia)
4. Critical moments and shears (Virginia)
5. Concrete section analysis (Virginia)
6. Live load reactions on pier or abutment (Virginia)
7. Bolted beam/girder splice design and analysis (Virginia)
8. Concentric curve skewed bridge geometry (Virginia)
9. Bearing stiffener design or analysis (Virginia)
10. Transverse stiffener design or analysis (Virginia)
11. Straight roadway skewed bridge geometry and elevations along lines (Virginia)
12. Various programs to determine bridge geometry and elevations (Montana)
13. Various programs to determine bent and girder reactions due to various standard and nonstandard loadings (Montana)
14. Slab analysis by working stress design or ultimate stress design (Montana)
15. Prestressed beam analysis (Montana)
16. Prestressed bulb T-beam analysis (Montana)
17. Welded plate girder analysis (Montana)
18. Two-column bent programs (Montana)
19. Coordinant geometry program (Montana)
20. Beam splice design (Ohio)
21. Crane loading program (Ohio)
22. Analysis of composite rolled beam (Ohio)

Most of these programs are small and designed to perform rather specialized functions. Although a useful first step, they do not fully meet the need of bridge divisions for general application programs to run on microcomputers.

Potentially one of the most attractive schemes for development of microcomputer software for bridge design applications is the downloading and conversion of existing mainframe programs. There are several advantages to having the ability to run large-scale converted mainframe bridge design software on a microcomputer. First, it provides greater flexibility to the engineer. Applications can be run at any time without the need for access to a mainframe. A state bridge division may be only one of several state agencies that must share time on a mainframe; thus, depending on demand, computer access may not always be possible because of low priority. Also, microcomputers can insulate bridge designers from the inconveniences of unscheduled mainframe downtimes. The converted programs will also be familiar to the users. Programs that were converted as part of this study used the same input and output format as those run on the mainframe. In states in which design activities are carried out at remote locations, microcomputers can provide an efficient and relatively inexpensive means of distributing computer power. The high costs of communicating with mainframes over telephone lines can be minimized. There are also other benefits to be realized. Converting mainframe bridge design software to microcomputer use will ease demand on the mainframe and allow more processor time for other, larger agency applications.

As part of this study, several attempts at downloading and converting mainframe programs were made. These conversions provided a means of identifying problems and the level of effort required. With the assistance of the Bridge Division and the Information Systems Division of the Virginia Department of Highways and Transportation, copies of the following bridge design problems were obtained.

1. Prestressed Concrete I-Beam Design and Analysis Program
2. Steel Girder Design and Analysis Program (composite)
3. Deck Slab Design Program
4. Critical Moments and Shears on a Simple Span for Moving Loads
5. Bridge Geometry Program
6. Georgia Continuous Beam Program
7. Georgia Pier Program
8. SIMON (a complete design system for steel bridge girders)

Successful conversions were made on the first four programs, but a number of problems were encountered in attempting to convert the remaining programs. First, most programs currently run on mainframes have been around for a long time and are written in early versions of FORTRAN. Some programs, such as the Bridge Geometry Program, were originally written in assembly language and then converted to FORTRAN. Still others were written such that they required machine-dependent software. These types of problems require extensive changes in coding. Major portions of some of the programs, which were not converted, would have had to be completely rewritten. Another obstacle to program conversions can be the programming technique of the original programmer. An example of this occurred in both the Georgia Continuous Beam and the George Pier programs. These are long programs with few subroutines; this causes problems because large programs usually must be broken into groups of subroutines to be compiled on a microcomputer, and programs without subroutines may require major alterations to existing code. A final obstacle to converting mainframe programs to the microcomputer is program size. Some programs are simply too large to be converted for use on the present generation of 16-bit microcomputers.

The bridge design application programs used in this project consisted of a Prestressed Concrete I-Beam Design and Analysis Program, a Steel Girder Design and Analysis Program, a Deck Slab Design Program, and a Critical Moments and Shears Program. These programs are currently used by the Bridge Division of the Virginia Department of Highways and Transportation on an IBM 3084 mainframe computer. All four of these programs are written in FORTRAN and were converted from mainframe use for use on microcomputers. As an example of the type of bridge design applications that the 16-bit microcomputers are capable of running, two of the larger programs (Prestressed Beam and Steel Girder) were used to run example problems.

Two different example problems were selected for each program and these were run on four different microcomputers and on an additional machine equipped with an 8087 math coprocessor chip. Details of these runs are given in Table 3. Also, Table 3 gives the program source file size and executable run file size for the Prestressed Beam and Steel Girder programs. The Prestressed Beam Program is a fairly long program with approximately 3,000 FORTRAN statements in the source file and an executable run file size of 161,480 bytes. This size program would certainly not run on the earlier 8-bit machines. Theoretically, an IBM-PC with full RAM capacity of 640 kb could run an application program of comparable size. The data in Table 3 indicate not only that programs of significant size do run on the 16-bit microcomputers but also that they execute in a reasonably short time.

Program size is only one of the factors that affect program execution. Another factor that will affect execution time is the type of CPU employed by the microcomputer. The IBM-PC, the Compaq Portable, and the Zenith-151 all use the Intel 8088 CPU. Com-

TABLE 3 Bridge Design Program Characteristics Illustrating Memory Capacity and Execution Time

Test Problem	Execution Time (sec)				
	Zenith Z-151	IBM-PC	COMPAQ Portable	AT&T PC	COMPAQ W/8087
Prestressed Concrete I-Beam Design and Analysis Program ^a					
PB1 ^b	54	43	43	33	36
PB2 ^c	57	46	47	35	38
Steel Girder Design and Analysis Program ^d					
SG1 ^e	30	24	24	20	20
SG2 ^f	88	74	75	50	36

^aFORTRAN statements in source file: 2,961 and executable file size: 161,480 bytes.

^bDesign of a standard AASHTO type 5 beam with standard HS-20 loading. (See Appendix B for input form)

^cDesign of a non AASHTO beam for HS-20 loading and additional concentrated dead loads. (See Appendix B)

^dFORTRAN statements in source file: 896, and executable file size: 90,360 bytes.

^eComplete analysis of an interior bridge girder of composite construction. (See Appendix B)

^fThree separate complete designs of an interior composite bridge girder at web depths of 48 in., 51 in., and 54 in. (See Appendix B)

parison of test results for the two programs on the IBM and Compaq machines shows virtually identical execution times; however, execution time on the Zenith Z-151 is about 20 percent slower. The probable causes of this are differences in the basic input-output system and elsewhere in the system architecture of the machines (5). The execution times for the test problems using the AT&T PC with the 8086 CPU turned out to be faster than those of the 8088 machines. This is not surprising because the 8086 moves data to and from the CPU through a 16-bit data bus versus an 8-bit bus on the 8088 machines.

Another hardware feature that may have a dramatic effect on program execution time is the 8087 math coprocessor. The test problems in Table 3 show a decrease in execution time of up to 60 percent using an 8087. The extent to which the 8087 math coprocessor will decrease execution time depends largely on the math processing requirements of the program at hand. In general, the more "number crunching" required, the more benefit will be realized from the 8087. All of the bridge design software of this project, and most available commercially, will be able to take advantage of an 8087. There are certain disadvantages, however, to using the 8087: It draws a significant percentage of the power supplied to the system board of a microcomputer and also dissipates a significant amount of heat. Excessive power consumption and heat dissipation can cause erratic operation of the disk drives, memory malfunctions, periodic lockup of the computer, unsafe heat buildup inside the computer cabinet, and possible eventual burnout of the power supply. It has been found that most combinations of the expansion cards with an 8087 will allow safe operation of the microcomputer, but, because of the possible detrimental effects, each individual microcomputer system should be properly evaluated before adding the 8087 coprocessor (5).

It has been noted that a RAM disk may offer increased efficiencies for running certain programs. To illustrate the performance of a RAM disk, the same test problems from Table 3 were run using a RAM disk. The results of the new runs are given in Table 4. The amount of storage in the RAM disk drive varied among machines depending on available RAM. Enough storage was allocated for the RAM disks to allow the executable run files and the input and output files to be stored. This permits direct comparison of the results summarized in Tables 3 and 4. Comparison of the results in Table 4 with those of Table 3 shows

TABLE 4 Comparison of Bridge Design Program Execution Times Using a RAM Disk for Input and Output

Test Problem	Execution Time (sec)				
	Zenith Z-151	IBM-PC	COMPAQ Portable	AT&T PC	COMPAQ W/8087
Prestressed Concrete I-Beam Design and Analysis Program					
PB1	— ^a	24	— ^a	12	— ^a
PB2	— ^a	27	— ^a	14	— ^a
Steel Girder Design and Analysis Program					
SG1	16	12	12	7	9
SG2	83	59	59	28	22

^aInsufficent memory exists to simultaneously create an emulated disk drive and run the program.

that disk emulation significantly decreases execution time in all cases. These decreased execution times can be attributed wholly to decreased input-output time and the decreased time required for the programs to be loaded into memory (no mechanical drive components are involved).

Whether application software is purchased, developed in-house, or converted from mainframe programs, considerations such as maintenance, portability, and distribution control cannot be neglected. Many of the mainframe programs used for bridge design applications in Virginia and other states are shared among states. The state that developed a given program usually assumes responsibility for maintaining the program and implementing major changes. If one of these programs has been converted for microcomputer use, subsequent changes must be transferred to the converted version. This may prove difficult if changes are not well documented and if the conversion requires extensive source code modifications.

Changes in computing technology or outgrowing present computing facilities, or both, may necessitate a future changeover to more powerful and sophisticated microcomputers. This can have a drastic effect on currently used software if software portability has not been considered. When software is being planned, the potential for future migration of programs to other computers must be considered. One way to maximize portability is to use standard features of standard programming languages and minimize the use of proprietary languages. In cases in which individual users continue to write programs, portability can be maximized by imposing guidelines for program development. These guidelines should specify the languages and operating systems that can be used. Complete program documentation should also be required.

A major consideration that has become intrinsically associated with microcomputers is control over the distribution of software. Microcomputers have ushered in the age of truly distributed computing power, and associated with this distribution of computing power is the distribution of software. Some form of control is necessary to properly manage this distribution and to maintain the integrity of common software used within an organization. However, excessive control may serve to stifle use of the software and result in reduced efficiency.

Information and examples given thus far make it clear that the current generation of microcomputers possesses sufficient computing power to be seriously considered as an alternative to mainframe computers for bridge design applications and that there is considerable interest in such utilization. As this interest translates into microcomputer implementation, more and more microcomputer bridge design and

analysis software will become available. It has already been noted that considerable programming of small design aids has been and is taking place, and, in Virginia and South Dakota, some conversion of mainframe software is taking place. These microcomputer programs should be available for sharing among the state bridge divisions. The following converted mainframe programs are currently available and can be obtained by contacting the bridge division in the appropriate state.

1. Prestressed Concrete I-Beam Design and Analysis (standard AASHTO and nonstandard simple-span bridge girders) (Virginia)
2. Steel Bridge Girder Design and Analysis (Virginia)
3. Deck Slab Design (Virginia)
4. Critical Moments and Shears on a Simple Span (Virginia)
5. Georgia Bent Program (South Dakota)
6. Continuous Span Prestressed Concrete Bridge Girder Design (South Dakota)
7. PCA Reinforced Concrete Column Design (South Dakota)

SCENARIOS FOR MICROCOMPUTER IMPLEMENTATION

How and when a state DOT bridge design unit should start using microcomputers depend on several factors. Basically, microcomputer use should be considered whenever present computing capabilities require enhancement such as additional computing power, distribution of computing power, and addition of communications capabilities.

The basic computing configurations for 16-bit microcomputers are either as stand-alone operation or as intelligent terminals linked to mainframes. In a stand-alone mode the microcomputer can operate independently and provide the engineer with a means of using a significant computing resource without the disadvantages of a time-shared mainframe system. The advantages of using a microcomputer as an intelligent terminal are numerous. Indeed, the ability to use a microcomputer in this mode is an example of how microcomputers can complement existing computer configurations in an efficient and cost-effective manner. The key here is the ability of the microcomputer to communicate with a mainframe computer. Communication enables the engineer both to complement mainframe operations with the microcomputer capabilities and to use mainframe resources to expand microcomputer power. A number of communications packages are available that allow engineers to communicate with virtually any mainframe system. In this mode the microcomputer can be used to run applications that are, at present, too large for microcomputer implementation. Also, off-line preparation of data represents a potential for considerable cost savings.

When both personnel and machine costs are considered, the costs of communicating between terminals and the mainframe becomes a relatively large portion of the total computation cost because the cost of computing is decreasing while those of communication and personnel continue to rise (6). Applications that use microcomputers to assist in the preparation of data and speed communications to the mainframe show great potential. However, there are a number of costs inherent in microcomputer implementation that go beyond the initial purchase price. These costs include service and maintenance costs, training costs, and additional hardware and software costs.

A major cost consideration is that related to training. For example, it may be necessary to form and staff internal user support groups. Other training-associated costs may include the value of the

time it takes individual users to learn how to operate the computer, the value of productivity lost while the engineers become computer proficient, the cost of time lost attempting to train persons who never become computer proficient, and even the cost of time lost when skilled users interrupt their own work to assist less skilled users with a problem (7). The bottom line with training costs is that time is much more expensive than hardware or software.

One of the major obstacles to large-scale microcomputer implementation by bridge design groups is divergence from traditional computerization norms. Much computing in typical bridge design groups is done through a mainframe controlled by a computer systems group. The type of support required by microcomputer implementation will require some level of involvement by a computer systems group. The expertise these groups possess in computer hardware systems, and software development and maintenance, will be necessary for proper microcomputer implementation and support. However, for proper microcomputer implementation, changes in traditional attitudes toward computing will be necessary and these groups may, at least initially, be reluctant to accept changes necessitated by the most efficient microcomputer implementation.

Scenarios for microcomputer implementation will vary from state to state because of differences in present computing configurations and the level of satisfaction with these systems. Future computing needs will also play a major role. In states in which mainframe access is good all the way down to the district level and the level of satisfaction is high, microcomputers may play a minor role at best. However, in states in which engineers are hampered in their access to a mainframe or dissatisfied with the service they receive, microcomputers can be a distinct benefit. Their usefulness is bound only by the imagination of the engineers and their ability to modify problem-solving techniques and office procedures to harness the computer's power more effectively (6).

SUMMARY

In this study an effort was made to assess the present overall computer configurations used in state DOT bridge design groups; to determine present utilization of microcomputers in these groups; to illus-

trate applications of microcomputers in bridge design activities; and, finally, to develop scenarios for the application of microcomputers in bridge design. The feasibility of downloading and converting mainframe programs and the ability of microcomputers to run large bridge design applications efficiently in a stand-alone mode were demonstrated.

The development of microcomputers signals a new era in computer use. The significant computing power they possess, along with their relatively low cost compared with traditional large computers, has assured their success. Their use is being constantly explored in many business and engineering applications. Many state department of transportation bridge design groups are in a position to make full use of microcomputer capabilities, and some states are already beginning to do so. Although there are many serious organizational and financial considerations, a well-planned computing system with microcomputers that complement existing mainframes can significantly improve computing methods and increase efficiency and productivity.

REFERENCES

1. C. Lu. Microcomputers: The Second Wave. High Technology, Sept./Oct. 1982, pp. 36-52.
2. D. Ruby. With Expanding Options, Who's Programming In-House and With What Languages. PC WEEK, Aug. 28, 1984.
3. Microsoft FORTRAN Compiler For the MS-DOS Operating System, Users Guide & Reference Manual. Microsoft Corporation, Bellevue, Wash., 1984.
4. A.J. Hunt, ed. Hunts Directory of Microcomputer Software and Services. Pleasant Hill, Calif., 1984.
5. C. DeVoney. IBM's Personal Computer. Que Corporation, Indianapolis, Ind., 1983.
6. G.W. Davies. Microcomputers in Civil Engineering. In Transportation Research Record 932, TRB, National Research Council, Washington, D.C., 1983, pp. 20-23.
7. Cutting Through The Hidden Costs of Computing. Personal Computing, Oct. 1984, pp. 122-129.

Publication of this paper sponsored by Committee on General Structures.

Simplified Method for Estimating Thermal Stresses in Composite Bridges

M. SOLIMAN and JOHN B. KENNEDY

ABSTRACT

The North American codes of practice do not specify a temperature distribution throughout the depth of composite bridge superstructures; furthermore, no temperature differentials are given for accurately assessing the thermal stresses induced in such bridges. A realistic temperature distribution and temperature differentials are proposed in this paper. Simple formulas are deduced for use in the design office for estimating the thermal stresses in the concrete deck slab as well as in the steel girders in simple- and continuous-span composite bridges. It is shown that thermal stresses can be quite significant and should be included in the design of bridges.

Thermal stresses caused by temperature variation through the depth of a composite bridge can be relatively large compared with dead or live load stresses; such variation has been shown (1,2) to be nonuniform in composite concrete deck slab-on-steel beam bridges. These thermal stresses are known to cause considerable damage in structures (3-5); their presence will magnify the development of cracks in the concrete deck slab and thus in time cause corrosion of the steel reinforcing and the steel beams and deterioration of the concrete by allowing the seepage of salt-laden water. State-of-the-art surveys of thermal stresses in bridges were carried out by Reynolds and Emanuel (6) and more recently by Imbsen and Vandershaf (7). Surprisingly, none of the North American codes of practice provides guidance for the estimation of thermal stresses, or for the temperature distribution through the depth of the composite section; AASHTO (8) recently presented a range of temperature variation in bridges to account for the expansion movement but not for estimating thermal stresses.

The results reported in this paper are based on earlier work (9-11) that investigated the temperature distribution and temperature differentials through the depth of the composite section; simple formulas, suitable for the design office, are derived for estimating the thermal stresses in simple- and continuous-span bridges.

ANALYSIS

Following Zuk (9,12,13), the method of analysis is based on the following assumptions:

1. Plane sections remain plane after any temperature change;
2. The concrete deck slab is restrained in the transverse direction of the composite beam by the adjacent beam;
3. Perfect interaction exists between the concrete deck slab and the steel beam;
4. Both concrete and steel are elastic;
5. Temperature distribution is constant longi-

tudinally and transversely along the beam but non-uniform throughout the depth;

6. Temperature of the reinforcing steel is the same as that of the surrounding concrete, and the concrete deck slab is symmetrically reinforced;

7. Fatigue stresses are negligible; and

8. The concrete deck slab and the steel beams are homogeneous and isotropic.

Temperature differentials through the depth of the composite section give rise to shearing forces (F) and couples (Q) at the interface between the concrete deck slab and the steel beams as shown in Figure 1(a). The resulting longitudinal strains at the bottom of the concrete deck slab and at the top of the steel beam can be shown to be (12)

$$\epsilon_{xc} = [2(1 - \nu^c)/A_c E_c] [2F - (3Q/2a)] + [(1 + \nu)/2a] \alpha_c \int_{-a}^{+a} (T_{y1} - T_o) dy_1 + [3(1 + \nu)/2a^2] \alpha_c \int_{-a}^{+a} (T_{y1} - T_o) y_1 dy_1 \quad (1)$$

$$\epsilon_{xs} = -(Qd_1/I_s E_s) - (F/E_s) [(d_1^2/I_s) + (1/A_s)] + (\alpha_s/A_s) \int_{-d_1}^{d_2} (T_y - T_o) b_y dy - (d_1 \alpha_s/I_s) \int_{-d_1}^{d_2} (T_y - T_o) b_y y dy \quad (2)$$

where

- $\epsilon_{sc}, \epsilon_{xs}$ = total longitudinal strain at bottom of concrete deck slab and at top of steel beam, respectively;
- F = interface shearing force, shown in Figure 1(a);
- Q = interface couple, shown in Figure 1(a);
- a = one-half concrete deck slab thickness;
- w = slab width;
- α_c, α_s = concrete and steel thermal expansion coefficients, respectively;
- y_1 = distance from the centroid of the concrete deck slab to a fiber where the induced thermal stresses are determined, shown in Figure 1(b);
- y = distance from the centroid of the steel section to a fiber where the thermal stresses are determined, shown in Figure 1(b);
- b_y = width of steel section at distance y, shown in Figure 1(b);

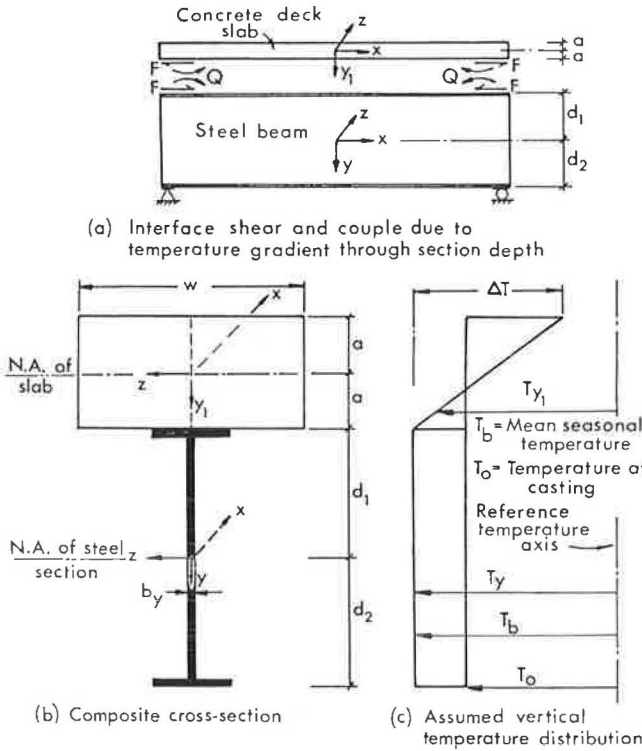


FIGURE 1 Interface shear and couple and assumed vertical temperature distribution.

- E_c, E_s = concrete and steel modulus of elasticity, respectively;
- A_s = area of the steel section;
- J_s = moment of inertia of the steel section;
- T_o = initial temperature at time of construction;
- T_{y1} = temperature of any fiber within the concrete deck slab, shown in Figure 1(c);
- d_1, d_2 = distance from top and bottom fibers in the steel section, respectively, measured from the centroid of the steel section, shown in Figure 1(b); and
- ν = Poisson's ratio of the concrete deck slab.

The shearing force (F) and the couple (Q) are determined from the compatibility conditions; namely, the strain and the radius of curvature for both the concrete deck slab and the steel beams must be the same at the interface. Thus equating Equations 1 and 2 for strain leads to

$$AF + BQ = [-(1 + \nu)/2a] \alpha_c \left[\int_{-a}^a (T_{y1} - T_o) dy_1 + (3/a) \int_{-a}^a (T_{y1} - T_o) y_1 dy_1 \right] + \alpha_s \left[(1/A_s) \int_{-d_1}^{d_2} (T_y - T_o) b_y dy - (d_1/I_s) \int_{-d_1}^{d_2} (T_y - T_o) b_y y dy \right] \quad (3)$$

where A and B are coefficients defined in the Appendix. To deduce the radius of curvature for the concrete deck slab at the interface, difference in strains at the midplane of the slab and the bottom of the slab must be calculated. Such a difference in strains due to temperature change is given by

$$\Delta \epsilon_{xc1} = [3(1 + \nu)/2a^2] \alpha_c \int_{-a}^a (T_{y1} - T_o) y_1 dy_1 \quad (4)$$

and the difference in strains due to F and Q is

$$\Delta \epsilon_{xc2} = [3(1 - \nu^2)/2a^2 w E_c] (Fa - Q) \quad (5)$$

Hence the total difference in strain becomes

$$\Delta \epsilon_{xc} = \Delta \epsilon_{xc1} + \Delta \epsilon_{xc2} \quad (6)$$

From geometry the radius of curvature of the concrete deck slab is equal to the ratio $a/\Delta \epsilon_{xc}$; thus the radius of curvature (R_c) of the slab at the interface becomes

$$R_c = (a/\Delta \epsilon_{xc}) + a \quad (7)$$

The radius of curvature of the steel beam at the interface can be deduced from the moment on the steel beam given by

$$M_s = Fd_1 + Q + \alpha_s E_s \int_{-d_1}^{d_2} (T_y - T_o) b_y y dy \quad (8)$$

From the flexural formula, $(1/R) = (M/EI)$, the radius of curvature of the steel beam at the interface becomes

$$R_s = (E_s I_s / M_s) - d_1 \quad (9)$$

The last terms in Equations 7 and 9 are relatively quite small and therefore may be ignored without significant error. With this simplification, equating R_c to R_s yields an equation of the form:

$$KF + RQ = E_c E_s w \left[3(1 + \nu) \alpha_c I_s \int_{-a}^a (T_{y1} - T_o) y_1 dy_1 - 2a^3 \alpha_s \int_{-d_1}^{d_2} (T_y - T_o) b_y y dy \right] \quad (10)$$

where the coefficients K and R are as defined in the Appendix. F and Q can be explicitly determined from Equations 3 and 10 for any given temperature distribution through the depth of the cross section.

TEMPERATURE DIFFERENTIALS

From an extensive review of the pertinent literature, it was found that the most realistic and simple temperature distribution through the composite section is the one-dimensional distribution shown in Figure 1(c); the upper portion of the distribution is linear through the depth of the concrete deck slab, and the lower portion is uniform through the depth of the steel beams. On the basis of previous results (7), the temperature differential (ΔT) between the top of the concrete deck slab and the bottom of the steel beam can be assumed to be as given in Table 1. The maximum temperature differentials pertain to the case

TABLE 1 Recommended Values for Temperature Differential, ΔT

ΔT	Summer ($^{\circ}F$)	Winter ($^{\circ}F$)
Maximum	40	20
Minimum	-7.5	-7.5

in which the concrete deck slab is exposed to the sun's radiation during the summer and winter, which results in a deck slab that is warmer than the steel beams; the minimum temperature differentials refer to the case in which the concrete deck slab is suddenly drenched with cold rain or snow and thus cools at a faster rate than the steel beams.

It can be shown (14) that for the linear uniform temperature distribution shown in Figure 1(c) Q and F can be expressed as

$$Q = \Delta T k_1 - (T_b - T_o)k_2 \tag{11}$$

$$F = (T_b - T_o)k_3 - Qk_4 \tag{12}$$

where

ΔT = temperature differential between the top and the bottom surfaces of the concrete deck slab;

T_b = maximum (or minimum) seasonal temperature obtained from a map of isotherms;

T_o = temperature at casting of concrete; and

$k_1, k_2 \dots$ = constants with values presented in Tables 2-7 for different steel beam sections, recommended by the U.S. Department of Transportation (15); three concrete deck slab thicknesses; and different concrete compressive strengths.

Explicit expressions for $k_1, k_2 \dots$ are given in the Appendix. The moment (M_s) in the steel beam, acting as an individual element, is

$$M_s = Fd_1 + Q \tag{13}$$

When F and Q are known, the thermal stresses in the concrete deck slab and in the steel beams can be calculated from (12)

$$\begin{aligned} \sigma_{xc} = & (F/2aw) + [3(Fa - Q)y_1/2a^3w] - [\alpha_c E_c / (1 - \nu)] (T_{y_1} - T_o) \\ & + [\alpha_c E_c / 2a(1 - \nu)] \int_{-a}^{+a} (T_{y_1} - T_o) dy_1 \\ & + [3\alpha_c E_c / 2a^3(1 - \nu)] y_1 \int_{-a}^{+a} (T_{y_1} - T_o) y_1 dy_1 \end{aligned} \tag{14}$$

$$\begin{aligned} \sigma_{xs} = & -\alpha_s E_s (T_y - T_o) + (\alpha_s E_s / A_s) \int_{-d_1}^{d_2} (T_y - T_o) b_y dy \\ & + (\alpha_s E_s / I_s) \int_{-d_1}^{d_2} (T_y - T_o) b_y dy + (Q / I_s) y \\ & + F [(d_1 / I_s) y - (1 / A_s)] \end{aligned} \tag{15}$$

$$\sigma_{zc} = \nu \sigma_{xc} - \alpha_c E_c (T_{y_1} - T_o) \tag{16}$$

where

σ_{xc}, σ_{xs} = thermal stresses induced through the depth of the concrete deck slab and the steel beams in the longitudinal direction (x), respectively, and

σ_{zc} = thermal stress induced through the depth of the concrete deck slab in the transverse direction (z).

For the assumed linear uniform temperature distribution in Figure 1(c), Equations 14 and 15 reduce to

$$\sigma_{xc} = (F/2aw) - (Q/I_c) y_1 + (Fa/I_c) y_1 \tag{17}$$

$$\sigma_{xs} = (-F/2aw) + (Q/I_s) y + (Fd_1/I_s) y \tag{18}$$

where I_c is the moment of inertia of the concrete deck slab about its own centroid.

TABLE 2 Thermal Coefficients k_1 to k_4 for $f'_c = 3$ ksi

Steel Section	k_1 for 2a =			k_2 for 2a =			k_3 for 2a =			k_4 for 2a =		
	7 in.	8 in.	9 in.	7 in.	8 in.	9 in.	7 in.	8 in.	9 in.	7 in.	8 in.	9 in.
36x300	-13.46	-17.68	-22.40	-0.19	-0.22	-0.23	0.03	0.04	0.05	-0.13	-0.10	-0.08
36x280	-13.11	-17.22	-21.83	-0.18	-0.20	-0.22	0.03	0.04	0.05	-0.13	-0.10	-0.07
36x260	-12.72	-16.71	-21.19	-0.17	-0.19	-0.20	0.03	0.04	0.04	-0.12	-0.09	-0.07
36x245	-12.43	-16.33	-20.72	-0.16	-0.18	-0.19	0.03	0.04	0.04	-0.12	-0.09	-0.07
36x230	-12.12	-15.93	-20.24	-0.15	-0.17	-0.17	0.03	0.04	0.04	-0.12	-0.09	-0.06
36x210	-11.48	-15.10	-19.20	-0.13	-0.14	-0.15	0.03	0.03	0.04	-0.11	-0.08	-0.06
36x194	-11.17	-14.73	-18.78	-0.12	-0.13	-0.13	0.03	0.03	0.04	-0.10	-0.07	-0.05
36x182	-10.92	-14.41	-18.40	-0.12	-0.12	-0.12	0.03	0.03	0.04	-0.10	-0.07	-0.05
36x170	-10.65	-14.08	-17.99	-0.11	-0.11	-0.11	0.03	0.03	0.03	-0.10	-0.07	-0.05
36x160	-10.41	-13.77	-17.61	-0.10	-0.11	-0.10	0.03	0.03	0.03	-0.09	-0.06	-0.04
36x150	-10.20	-13.50	-17.29	-0.10	-0.10	-0.09	0.03	0.03	0.03	-0.09	-0.06	-0.04
36x135	-9.71	-12.90	-16.55	-0.08	-0.08	-0.08	0.02	0.03	0.03	-0.08	-0.05	-0.03
33x221	-11.83	-15.51	-19.66	-0.14	-0.16	-0.16	0.03	0.04	0.04	-0.11	-0.08	-0.06
33x201	-11.39	-14.96	-18.99	-0.13	-0.14	-0.14	0.03	0.03	0.04	-0.11	-0.08	-0.06
33x141	-9.83	-12.99	-16.60	-0.09	-0.09	-0.08	0.02	0.03	0.03	-0.08	-0.06	-0.04
33x130	-9.52	-12.61	-16.13	-0.08	-0.08	-0.07	0.02	0.03	0.03	-0.08	-0.05	-0.03
33x118	-9.16	-12.16	-15.58	-0.07	-0.07	-0.06	0.02	0.02	0.03	-0.07	-0.04	-0.03
30x116	-8.96	-11.82	-15.07	-0.06	-0.06	-0.05	0.02	0.02	0.03	-0.07	-0.04	-0.02
30x108	-8.70	-11.50	-14.67	-0.06	-0.05	-0.04	0.02	0.02	0.02	-0.06	-0.04	-0.02
30x99	-8.42	-11.15	-14.24	-0.05	-0.04	-0.03	0.02	0.02	0.02	-0.06	-0.03	-0.02
27x94	-8.16	-10.74	-13.63	-0.05	-0.04	-0.02	0.02	0.02	0.02	-0.05	-0.03	-0.01
27x84	-7.84	-10.35	-13.14	-0.04	-0.03	-0.01	0.02	0.02	0.02	-0.05	-0.02	-0.01
24x94	-7.93	-10.36	-13.04	-0.04	-0.03	-0.02	0.02	0.02	0.02	-0.05	-0.03	-0.01
24x84	-7.63	-9.99	-12.57	-0.04	-0.02	-0.01	0.02	0.02	0.02	-0.04	-0.02	-0.00
24x76	-7.37	-9.66	-12.16	-0.03	-0.02	0.00	0.02	0.02	0.02	-0.04	-0.02	0.00
24x68	-7.10	-9.31	-11.71	-0.02	-0.01	0.01	0.02	0.02	0.02	-0.03	-0.01	0.01
24x62	-6.80	-8.92	-11.21	-0.02	0.00	0.02	0.01	0.02	0.02	-0.02	0.00	0.01
21x55	-6.55	-8.60	-10.78	-0.01	0.00	0.02	0.01	0.01	0.01	-0.01	0.00	0.02
21x68	-6.80	-8.83	-10.97	-0.02	-0.01	0.01	0.02	0.02	0.02	-0.03	-0.01	0.01
21x62	-6.60	-8.56	-10.63	-0.01	0.00	0.02	0.01	0.02	0.02	-0.02	0.00	0.01
21x50	-6.08	-7.88	-9.73	0.00	0.01	0.03	0.01	0.01	0.01	-0.01	0.01	0.02
21x44	-5.84	-7.55	-9.29	0.00	0.02	0.04	0.01	0.01	0.01	0.00	0.02	0.03
18x55	-5.97	-7.61	-9.28	-0.01	0.01	0.03	0.01	0.01	0.02	-0.01	0.01	0.02
18x50	-5.78	-7.37	-8.95	-0.00	0.01	0.03	0.01	0.01	0.01	0.00	0.02	0.03

TABLE 3 Thermal Coefficients k_1 to k_4 for $f'_c = 4$ ksi

Steel Section	k_1 for $2a =$			k_2 for $2a =$			k_3 for $2a =$			k_4 for $2a =$		
	7 in.	8 in.	9 in.	7 in.	8 in.	9 in.	7 in.	8 in.	9 in.	7 in.	8 in.	9 in.
36x300	-14.18	-18.63	-23.63	-0.19	-0.22	-0.23	0.04	0.04	0.05	-0.13	-0.10	-0.07
36x280	-13.82	-18.16	-23.04	-0.18	-0.20	-0.22	0.04	0.04	0.05	-0.12	-0.09	-0.07
36x260	-13.41	-17.62	-22.38	-0.17	-0.19	-0.20	0.03	0.04	0.05	-0.12	-0.09	-0.07
36x245	-13.10	-17.23	-21.89	-0.16	-0.18	-0.19	0.03	0.04	0.04	-0.12	-0.09	-0.06
36x230	-12.78	-16.82	-21.40	-0.15	-0.17	-0.17	0.03	0.04	0.04	-0.11	-0.08	-0.06
36x210	-12.11	-15.95	-20.32	-0.13	-0.14	-0.14	0.03	0.04	0.04	-0.10	-0.07	-0.05
36x194	-11.80	-15.58	-19.90	-0.12	-0.13	-0.13	0.03	0.03	0.04	-0.10	-0.07	-0.05
36x182	-11.54	-15.25	-19.50	-0.12	-0.12	-0.12	0.03	0.03	0.04	-0.09	-0.07	-0.05
36x170	-11.26	-14.91	-19.09	-0.11	-0.11	-0.11	0.03	0.03	0.03	-0.09	-0.06	-0.04
36x160	-11.00	-14.59	-18.70	-0.10	-0.10	-0.10	0.03	0.03	0.03	-0.09	-0.06	-0.04
36x150	-10.79	-14.31	-18.37	-0.09	-0.10	-0.09	0.03	0.03	0.03	-0.08	-0.06	-0.04
36x135	-10.29	-13.69	-17.60	-0.08	-0.08	-0.07	0.02	0.03	0.03	-0.07	-0.05	-0.03
33x221	-12.47	-16.37	-20.79	-0.14	-0.16	-0.16	0.03	0.04	0.04	-0.11	-0.08	-0.06
33x201	-12.02	-15.80	-20.09	-0.13	-0.14	-0.14	0.03	0.04	0.04	-0.10	-0.07	-0.05
33x141	-10.41	-13.78	-17.64	-0.09	-0.09	-0.08	0.03	0.03	0.03	-0.08	-0.05	-0.03
33x130	-10.08	-13.38	-17.15	-0.08	-0.07	-0.06	0.02	0.03	0.03	-0.07	-0.05	-0.03
33x118	-9.71	-12.92	-16.58	-0.07	-0.06	-0.05	0.02	0.03	0.03	-0.07	-0.04	-0.02
30x116	-9.49	-12.56	-16.03	-0.06	-0.06	-0.04	0.02	0.03	0.03	-0.06	-0.04	-0.02
30x108	-9.23	-12.22	-15.61	-0.06	-0.05	-0.03	0.02	0.02	0.03	-0.06	-0.03	-0.02
30x99	-8.94	-11.87	-15.17	-0.05	-0.04	-0.02	0.02	0.02	0.02	-0.05	-0.03	-0.01
27x94	-8.66	-11.42	-14.51	-0.04	-0.03	-0.02	0.02	0.02	0.02	-0.05	-0.02	-0.01
27x84	-8.33	-11.01	-13.99	-0.04	-0.02	-0.01	0.02	0.02	0.02	-0.04	-0.02	0.00
24x94	-8.41	-11.01	-13.86	-0.04	-0.03	-0.01	0.02	0.02	0.02	-0.05	-0.02	0.01
24x84	-8.10	-10.62	-13.37	-0.03	-0.02	0.00	0.02	0.02	0.02	-0.04	-0.02	0.00
24x76	-7.84	-10.28	-12.94	-0.03	-0.01	0.01	0.02	0.02	0.02	-0.03	-0.01	0.00
24x68	-7.55	-9.91	-12.46	-0.02	-0.01	0.01	0.02	0.02	0.02	-0.03	-0.01	0.01
24x62	-7.24	-9.51	-11.94	-0.01	0.00	0.02	0.01	0.02	0.02	-0.02	0.00	0.01
21x55	-6.98	-9.16	-11.48	-0.01	0.01	0.03	0.01	0.01	0.01	-0.01	0.01	0.02
21x68	-7.23	-9.38	-11.66	-0.02	0.00	0.02	0.02	0.02	0.02	-0.02	0.00	0.01
21x62	-7.02	-9.11	-11.29	-0.01	0.00	0.03	0.02	0.02	0.02	-0.02	0.00	0.02
21x50	-6.48	-8.39	-10.34	0.00	0.02	0.04	0.01	0.01	0.01	0.00	0.02	0.03
21x44	-6.23	-8.04	-9.86	0.00	0.02	0.04	0.01	0.01	0.01	0.01	0.02	0.03
18x55	-6.34	-8.08	-9.83	0.00	0.01	0.04	0.01	0.01	0.02	0.00	0.01	0.03
18x50	-6.15	-7.82	-9.48	0.00	0.02	0.04	0.01	0.01	0.01	0.00	0.02	0.03

TABLE 4 Thermal Coefficients k_1 to k_4 for $f'_c = 5$ ksi

Steel Section	k_1 for $2a =$			k_2 for $2a =$			k_3 for $2a =$			k_4 for $2a =$		
	7 in.	8 in.	9 in.	7 in.	8 in.	9 in.	7 in.	8 in.	9 in.	7 in.	8 in.	9 in.
36x300	-14.62	-19.21	-24.37	-0.19	-0.22	-0.23	0.04	0.04	0.05	-0.12	-0.09	-0.07
36x280	-14.25	-18.72	-23.78	-0.18	-0.20	-0.22	0.04	0.04	0.05	-0.12	-0.09	-0.07
36x260	-13.82	-18.18	-23.11	-0.17	-0.19	-0.20	0.04	0.04	0.05	-0.12	-0.09	-0.06
36x245	-13.51	-17.77	-22.61	-0.16	-0.18	-0.18	0.03	0.04	0.05	-0.11	-0.08	-0.06
36x230	-13.18	-17.36	-22.10	-0.15	-0.17	-0.17	0.03	0.04	0.04	-0.11	-0.08	-0.06
36x210	-12.49	-16.47	-21.01	-0.13	-0.14	-0.14	0.03	0.04	0.04	-0.10	-0.07	-0.05
36x194	-12.18	-16.10	-20.58	-0.12	-0.13	-0.13	0.03	0.04	0.03	-0.10	-0.07	-0.05
36x182	-11.91	-15.76	-20.18	-0.12	-0.12	-0.12	0.03	0.04	0.03	-0.09	-0.06	-0.04
36x170	-11.63	-15.41	-19.76	-0.11	-0.11	-0.11	0.03	0.03	0.04	-0.09	-0.06	-0.04
36x160	-11.37	-15.09	-19.36	-0.10	-0.10	-0.10	0.03	0.03	0.03	-0.08	-0.06	-0.04
36x150	-11.15	-14.81	-19.02	-0.09	-0.10	-0.09	0.03	0.03	0.03	-0.08	-0.05	-0.03
36x135	-10.64	-14.18	-18.25	-0.08	-0.08	-0.07	0.02	0.03	0.03	-0.07	-0.05	-0.03
33x221	-12.86	-16.90	-21.47	-0.14	-0.16	-0.16	0.03	0.04	0.04	-0.11	-0.08	-0.05
33x201	-12.40	-16.32	-20.76	-0.13	-0.14	-0.14	0.03	0.04	0.04	-0.10	-0.07	-0.05
33x141	-10.76	-14.26	-18.27	-0.09	-0.08	-0.07	0.03	0.03	0.03	-0.07	-0.05	-0.03
33x130	-10.43	-13.85	-17.77	-0.08	-0.07	-0.06	0.02	0.03	0.03	-0.07	-0.04	-0.03
33x118	-10.05	-13.38	-17.19	-0.07	-0.06	-0.05	0.02	0.03	0.03	-0.06	-0.04	-0.02
30x116	-9.82	-13.00	-16.61	-0.06	-0.06	-0.04	0.02	0.03	0.03	-0.06	-0.04	-0.02
30x108	-9.55	-12.66	-16.19	-0.06	-0.05	-0.03	0.02	0.02	0.03	-0.05	-0.03	-0.01
30x99	-9.26	-12.30	-15.74	-0.05	-0.04	-0.02	0.02	0.02	0.02	-0.05	-0.03	-0.01
27x94	-8.97	-11.84	-15.04	-0.04	-0.03	-0.01	0.02	0.02	0.02	-0.05	-0.02	-0.01
27x84	-8.63	-11.42	-14.51	-0.03	-0.02	0.00	0.02	0.02	0.02	-0.04	-0.02	0.00
24x94	-8.70	-11.40	-14.36	-0.04	-0.03	-0.01	0.02	0.02	0.02	-0.04	-0.02	0.00
24x84	-8.39	-11.00	-13.86	-0.03	-0.02	0.00	0.02	0.02	0.02	-0.04	-0.01	0.00
24x76	-8.12	-10.65	-13.41	-0.03	-0.01	0.01	0.02	0.02	0.02	-0.03	-0.01	0.01
24x68	-7.83	-10.28	-12.92	-0.02	0.00	0.02	0.02	0.02	0.02	-0.02	0.00	0.01
24x62	-7.51	-9.86	-12.38	-0.01	0.00	0.03	0.01	0.02	0.02	-0.01	0.00	0.02
21x55	-7.25	-9.51	-11.90	-0.01	0.01	0.03	0.01	0.01	0.01	-0.01	0.01	0.02
21x68	-7.49	-9.72	-12.07	-0.02	0.00	0.02	0.02	0.02	0.02	-0.02	0.00	0.01
21x62	-7.28	-9.44	-11.69	-0.01	0.01	0.03	0.02	0.02	0.02	-0.01	0.01	0.02
21x50	-6.72	-8.70	-10.71	0.00	0.02	0.04	0.01	0.01	0.01	0.00	0.02	0.03
21x44	-6.46	-8.33	-10.21	0.01	0.02	0.04	0.01	0.01	0.01	0.01	0.02	0.03
18x55	-6.57	-8.37	-10.16	0.00	0.02	0.04	0.01	0.02	0.02	0.00	0.02	0.03
18x50	-6.37	-8.10	-9.80	0.00	0.02	0.04	0.01	0.01	0.01	0.00	0.02	0.03

TABLE 5 Thermal Coefficients k_1 to k_4 for $f'_c = 6$ ksi

Steel Section	k_1 for $2a =$			k_2 for $2a =$			k_3 for $2a =$			k_4 for $2a =$		
	7 in.	8 in.	9 in.	7 in.	8 in.	9 in.	7 in.	8 in.	9 in.	7 in.	8 in.	9 in.
36x300	-14.84	-19.50	-24.76	-0.19	-0.22	-0.23	0.04	0.04	0.05	-0.12	-0.09	-0.07
36x280	-14.46	-19.01	-24.15	-0.18	-0.20	-0.22	0.04	0.04	0.05	-0.12	-0.09	-0.07
36x260	-14.04	-18.46	-23.48	-0.17	-0.19	-0.20	0.04	0.04	0.05	-0.11	-0.08	-0.06
36x245	-13.72	-18.06	-22.98	-0.16	-0.18	-0.18	0.04	0.04	0.05	-0.11	-0.08	-0.06
36x230	-13.39	-17.64	-22.47	-0.15	-0.17	-0.17	0.03	0.04	0.04	-0.11	-0.08	-0.06
36x210	-12.69	-16.74	-21.36	-0.13	-0.14	-0.14	0.03	0.04	0.04	-0.10	-0.07	-0.05
36x194	-12.37	-16.36	-20.93	-0.12	-0.13	-0.13	0.03	0.04	0.04	-0.09	-0.07	-0.04
36x182	-12.10	-16.03	-20.53	-0.12	-0.12	-0.12	0.03	0.03	0.04	-0.09	-0.06	-0.04
36x170	-11.82	-15.67	-20.10	-0.11	-0.11	-0.11	0.03	0.03	0.04	-0.09	-0.06	-0.04
36x160	-11.56	-15.34	-19.70	-0.10	-0.10	-0.10	0.03	0.03	0.03	-0.08	-0.05	-0.04
36x150	-11.33	-15.07	-19.36	-0.09	-0.09	-0.09	0.03	0.03	0.03	-0.08	-0.05	-0.03
36x135	-10.82	-14.43	-18.58	-0.08	-0.08	-0.07	0.03	0.03	0.03	-0.07	-0.04	-0.03
33x221	-13.06	-17.17	-21.82	-0.14	-0.16	-0.16	0.03	0.04	0.04	-0.10	-0.07	-0.05
33x201	-12.60	-16.58	-21.11	-0.13	-0.14	-0.14	0.03	0.04	0.04	-0.10	-0.07	-0.05
33x141	-10.94	-14.51	-18.59	-0.08	-0.08	-0.07	0.03	0.03	0.03	-0.07	-0.05	-0.03
33x130	-10.61	-14.10	-18.09	-0.08	-0.07	-0.06	0.02	0.03	0.03	-0.07	-0.04	-0.02
33x118	-10.23	-13.62	-17.51	-0.07	-0.06	-0.05	0.02	0.03	0.03	-0.06	-0.04	-0.02
30x116	-9.99	-13.24	-16.91	-0.06	-0.05	-0.04	0.02	0.03	0.03	-0.06	-0.03	-0.02
30x108	-9.72	-12.89	-16.49	-0.05	-0.05	-0.03	0.02	0.02	0.03	-0.05	-0.03	-0.01
30x99	-9.43	-12.53	-16.03	-0.05	-0.04	-0.02	0.02	0.02	0.02	-0.05	-0.02	-0.01
27x94	-9.12	-12.05	-15.32	-0.04	-0.03	-0.01	0.02	0.02	0.02	-0.04	-0.02	-0.01
27x84	-8.79	-11.63	-14.77	-0.03	-0.02	0.00	0.02	0.02	0.02	-0.04	-0.02	0.00
24x94	-8.85	-11.60	-14.62	-0.04	-0.03	-0.01	0.02	0.02	0.02	-0.04	-0.02	0.00
24x84	-8.54	-11.20	-14.11	-0.03	-0.02	0.00	0.02	0.02	0.02	-0.03	-0.01	0.00
24x76	-8.27	-10.85	-13.65	-0.02	-0.01	0.01	0.02	0.02	0.02	-0.03	-0.01	0.01
24x68	-7.97	-10.47	-13.15	-0.02	0.00	0.02	0.02	0.02	0.02	-0.02	0.00	0.01
24x62	-7.65	-10.05	-12.61	-0.01	0.01	0.03	0.01	0.02	0.02	-0.01	0.00	0.02
21x55	-7.39	-9.69	-12.12	-0.01	0.01	0.03	0.01	0.01	0.01	-0.01	0.01	0.02
21x68	-7.63	-9.90	-12.29	-0.01	0.00	0.03	0.02	0.02	0.02	-0.02	0.00	0.02
21x62	-7.41	-9.61	-11.90	-0.01	0.01	0.03	0.02	0.02	0.02	-0.01	0.01	0.02
21x50	-6.85	-8.86	-10.89	0.00	0.02	0.04	0.01	0.01	0.01	0.00	0.02	0.03
21x44	-6.58	-8.49	-10.38	0.01	0.02	0.05	0.01	0.01	0.01	0.01	0.02	0.03
18x55	-6.68	-8.51	-10.33	0.00	0.02	0.04	0.01	0.02	0.02	0.00	0.02	0.03
18x50	-6.48	-8.24	-9.96	0.00	0.02	0.04	0.01	0.01	0.01	0.00	0.02	0.03

TABLE 6 Thermal Coefficients k_1 to k_4 for $f'_c = 7$ ksi

Steel Section	k_1 for $2a =$			k_2 for $2a =$			k_3 for $2a =$			k_4 for $2a =$		
	7 in.	8 in.	9 in.	7 in.	8 in.	9 in.	7 in.	8 in.	9 in.	7 in.	8 in.	9 in.
36x300	-14.89	-19.57	-24.85	-0.19	-0.22	-0.23	0.04	0.04	0.05	-0.12	-0.09	-0.07
36x280	-14.51	-19.08	-24.24	-0.18	-0.20	-0.22	0.04	0.04	0.05	-0.12	-0.09	-0.07
36x260	-14.09	-18.53	-23.56	-0.17	-0.19	-0.20	0.04	0.04	0.05	-0.11	-0.08	-0.06
36x245	-13.77	-18.12	-23.06	-0.16	-0.18	-0.18	0.04	0.04	0.05	-0.11	-0.08	-0.06
36x230	-13.44	-17.70	-22.55	-0.15	-0.17	-0.17	0.03	0.04	0.04	-0.11	-0.08	-0.06
36x210	-12.74	-16.80	-21.44	-0.13	-0.14	-0.14	0.03	0.04	0.04	-0.10	-0.07	-0.05
36x194	-12.42	-16.43	-20.02	-0.12	-0.13	-0.13	0.03	0.04	0.04	-0.09	-0.07	-0.04
36x182	-12.15	-16.09	-20.61	-0.12	-0.12	-0.12	0.03	0.03	0.04	-0.09	-0.06	-0.04
36x170	-11.86	-15.74	-20.18	-0.11	-0.11	-0.11	0.03	0.03	0.04	-0.09	-0.06	-0.04
36x160	-11.60	-15.40	-19.78	-0.10	-0.10	-0.10	0.03	0.03	0.03	-0.08	-0.05	-0.04
36x150	-11.38	-15.13	-19.44	-0.09	-0.09	-0.09	0.03	0.03	0.03	-0.08	-0.05	-0.03
36x135	-10.87	-14.49	-18.66	-0.08	-0.08	-0.07	0.03	0.03	0.03	-0.07	-0.04	-0.03
33x221	-13.11	-17.23	-21.91	-0.14	-0.16	-0.16	0.03	0.04	0.04	-0.10	-0.07	-0.05
33x201	-12.64	-16.64	-21.19	-0.13	-0.14	-0.14	0.03	0.04	0.04	-0.10	-0.07	-0.05
33x141	-10.98	-14.57	-18.67	-0.08	-0.08	-0.07	0.03	0.03	0.03	-0.07	-0.05	-0.03
33x130	-10.65	-14.15	-18.16	-0.08	-0.07	-0.06	0.03	0.03	0.03	-0.07	-0.04	-0.02
33x118	-10.27	-13.68	-17.58	-0.07	-0.06	-0.05	0.02	0.03	0.03	-0.06	-0.04	-0.02
30x116	-10.03	-13.29	-16.98	-0.06	-0.05	-0.04	0.02	0.03	0.03	-0.06	-0.03	-0.02
30x108	-9.75	-12.95	-16.55	-0.05	-0.05	-0.03	0.02	0.02	0.03	-0.05	-0.03	-0.01
30x99	-9.46	-12.58	-16.10	-0.05	-0.04	-0.02	0.02	0.02	0.02	-0.05	-0.02	-0.01
27x94	-9.16	-12.10	-15.38	-0.04	-0.03	-0.01	0.02	0.02	0.02	-0.04	-0.02	-0.01
27x84	-8.83	-11.68	-14.84	-0.03	-0.02	0.00	0.02	0.02	0.02	-0.04	-0.01	0.00
24x94	-8.89	-11.65	-14.68	-0.04	-0.03	0.00	0.02	0.02	0.02	-0.04	-0.02	0.00
24x84	-8.57	-11.25	-14.16	-0.03	-0.02	0.00	0.02	0.02	0.02	-0.03	-0.01	0.00
24x76	-8.30	-10.89	-13.71	-0.02	-0.01	0.01	0.02	0.02	0.02	-0.03	-0.01	0.01
24x68	-8.01	-10.51	-13.21	-0.02	-0.00	0.02	0.02	0.02	0.02	-0.02	0.00	0.01
24x62	-7.68	-10.09	-12.66	-0.01	0.01	0.03	0.01	0.02	0.02	-0.01	0.00	0.02
21x55	-7.42	-9.73	-12.17	-0.01	0.01	0.03	0.01	0.01	0.01	-0.01	0.01	0.02
21x68	-7.66	-9.94	-12.34	-0.01	0.00	0.03	0.02	0.02	0.02	-0.02	0.00	0.02
21x62	-7.44	-9.65	-11.95	-0.01	0.01	0.03	0.02	0.02	0.02	-0.01	0.01	0.02
21x50	-6.88	-8.89	-10.94	0.00	0.02	0.04	0.01	0.01	0.01	0.00	0.02	0.03
21x44	-6.61	-8.52	-10.42	0.01	0.02	0.05	0.01	0.01	0.01	0.01	0.02	0.03
18x55	-6.71	-8.55	-10.37	0.00	0.02	0.04	0.01	0.02	0.02	0.00	0.02	0.03
18x50	-6.51	-8.27	-10.00	0.00	0.02	0.04	0.01	0.01	0.01	0.00	0.02	0.03

TABLE 7 Thermal Coefficients k_1 to k_4 for $f'_c = 8$ ksi

Steel Section	k_1 for $2a =$			k_2 for $2a =$			k_3 for $2a =$			k_4 for $2a =$		
	7 in.	8 in.	9 in.	7 in.	8 in.	9 in.	7 in.	8 in.	9 in.	7 in.	8 in.	9 in.
36x300	-14.79	-19.43	-24.67	-0.19	-0.22	-0.23	0.04	0.04	0.05	-0.12	-0.09	-0.07
36x280	-14.41	-18.95	-24.07	-0.18	-0.20	-0.22	0.04	0.04	0.05	-0.12	-0.09	-0.07
36x260	-13.99	-18.40	-23.39	-0.17	-0.19	-0.20	0.04	0.04	0.05	-0.12	-0.08	-0.06
36x245	-13.67	-17.99	-22.89	-0.16	-0.18	-0.18	0.03	0.04	0.05	-0.11	-0.08	-0.06
36x230	-13.34	-17.57	-22.38	-0.15	-0.17	-0.17	0.03	0.04	0.04	-0.11	-0.08	-0.06
36x210	-12.65	-16.68	-21.28	-0.13	-0.14	-0.14	0.03	0.04	0.04	-0.10	-0.07	-0.05
36x194	-12.33	-16.30	-20.85	-0.12	-0.13	-0.13	0.03	0.04	0.04	-0.09	-0.07	-0.05
36x182	-12.06	-15.97	-20.45	-0.12	-0.12	-0.12	0.03	0.03	0.04	-0.09	-0.06	-0.04
36x170	-11.78	-15.61	-20.02	-0.11	-0.11	-0.11	0.03	0.03	0.04	-0.09	-0.06	-0.04
36x160	-11.51	-15.28	-19.62	-0.10	-0.10	-0.10	0.03	0.03	0.03	-0.08	-0.06	-0.04
36x150	-11.29	-15.01	-19.28	-0.09	-0.09	-0.09	0.03	0.03	0.03	-0.08	-0.05	-0.03
36x135	-10.78	-14.37	-18.50	-0.08	-0.08	-0.07	0.03	0.03	0.03	-0.07	-0.04	-0.03
33x221	-13.01	-17.11	-21.74	-0.14	-0.16	-0.16	0.03	0.04	0.04	-0.10	-0.07	-0.05
33x201	-12.55	-16.52	-21.03	-0.13	-0.14	-0.14	0.03	0.04	0.04	-0.10	-0.07	-0.05
33x141	-10.89	-14.45	-18.52	-0.09	-0.08	-0.07	0.03	0.03	-0.03	-0.07	-0.05	-0.03
33x130	-10.56	-14.04	-18.01	-0.08	-0.07	-0.06	0.02	0.03	0.03	-0.07	-0.04	-0.02
33x118	-10.19	-13.57	-17.43	-0.07	-0.06	-0.05	0.02	0.03	0.03	-0.06	-0.04	-0.02
30x116	-9.95	-13.18	-16.84	-0.06	-0.05	-0.04	0.02	0.03	0.03	-0.06	-0.03	-0.02
30x108	-9.68	-12.84	-16.42	-0.05	-0.05	-0.03	0.02	0.02	0.03	-0.05	-0.03	-0.01
30x99	-9.39	-12.47	-15.96	-0.05	-0.04	-0.02	0.02	0.02	0.02	-0.05	-0.02	-0.01
27x94	-9.09	-12.00	-15.25	-0.04	-0.03	-0.01	0.02	0.02	0.02	-0.04	-0.02	-0.01
27x84	-8.75	-11.58	-14.71	-0.03	-0.02	0.00	0.02	0.02	0.02	-0.04	-0.02	0.00
24x94	-8.82	-11.56	-14.56	-0.04	-0.03	-0.01	0.02	0.02	0.02	-0.04	-0.02	0.00
24x84	-8.50	-11.15	-14.05	-0.03	-0.02	0.00	0.02	0.02	0.02	-0.03	-0.01	0.00
24x76	-8.23	-10.80	-13.59	-0.02	-0.01	0.01	0.02	0.02	0.02	-0.03	-0.01	0.01
24x68	-7.94	-10.42	-13.10	-0.02	-0.00	0.02	0.02	0.02	0.02	-0.02	0.00	0.01
24x62	-7.62	-10.00	-12.55	-0.01	0.01	0.03	0.01	0.02	0.02	-0.01	0.00	0.02
21x55	-7.35	-9.65	-12.07	-0.01	0.01	0.03	0.01	0.01	0.01	-0.01	0.01	0.02
21x68	-7.59	-9.86	-12.24	-0.01	0.00	0.02	0.02	0.02	0.02	-0.02	0.00	0.01
21x62	-7.38	-9.57	-11.85	-0.01	0.01	0.03	0.02	0.02	0.02	-0.01	0.01	0.02
21x50	-6.82	-8.82	-10.85	0.00	0.02	0.04	0.01	0.01	0.01	0.00	0.02	0.03
21x44	-6.56	-8.45	-10.34	0.01	0.02	0.05	0.01	0.01	0.01	0.01	0.02	0.03
18x55	-6.66	-8.48	-10.29	0.00	0.02	0.04	0.01	0.02	0.02	0.00	0.02	0.03
18x50	-6.46	-8.21	-9.92	0.00	0.02	0.04	0.01	0.01	0.01	0.00	0.02	0.03

The thermal stresses given by Equations 17 and 18 are for simply supported composite bridges. In the case of continuous composite bridges the resultant thermal stresses are obtained by superimposing the thermal stresses given by Equations 17 and 18 and the stresses induced by the presence of the intermediate supports; these latter stresses are derived from the redundant moments resulting from continuity, as shown in Figure 2. This will be illustrated in the design example given later.

DISCUSSION

The adopted maximum and minimum temperature differentials (ΔT) for both summer and winter, given in Table 1, are based on shade air temperatures found from maps of isotherms for the particular construction site considered. These temperature differentials were chosen to represent the most unfavorable conditions expected, as proposed by Zuk (13) and confirmed by Emanuel and Hulsey (1). The suggested minimum temperature differentials in summer and winter of -7.5°F compare favorably with those given by the British Standards BS 5400 (16) and with the values calculated by Emanuel and Hulsey (1) using a finite element analysis. Although the maximum temperature differential of 40°F for summer is higher than the 25°F given in BS 5400 (16), it is in good agreement with the value obtained by Emanuel and Hulsey (1).

Both German specifications DIN 1072 and DIN 1078 (17) have suggested a linear temperature distribution through the section depth from the top of the concrete deck slab to the soffit of the steel beam; however, because the diffusivity of the steel is much higher than that of the concrete, such a temperature distribution is unrealistic compared with the one adopted herein (14). The use of Tables 2 through 7 for the constants k_1 to k_4 in estimating the thermal

stresses will be demonstrated by the following worked example.

Worked Example

It is necessary to estimate the thermal stresses induced in a two-span continuous concrete composite bridge with the following characteristics:

- Length of span = 80 ft;
- Effective concrete deck slab width (w) = 96 in.;
- Concrete deck slab thickness ($2a$) = 8 in.;
- $f'_c = 8$ ksi;
- f_y for WF 36x245 steel beam of grade A36 = 36 ksi;
- $E_s = 20 \times 10^3$ ksi;
- $E_c = 3.9 \times 10^3$ ksi (private communication from D.W. Pfeifer, Portland Cement Association, May 1970);
- $m = 7.44$;
- Poisson's ratio of concrete (ν) = 0.2; and
- $\alpha_c = 5.5 \times 10^{-6}/^\circ\text{F}$.

With reference to Figure 1(c), $T_o = 60^\circ\text{F}$ and $T_b = 85^\circ\text{F}$ maximum in summer and -22°F minimum in winter.

Solution

There are four cases of temperature variations through the depth of the section that have to be considered. However, for brevity only Case (iv), shown in Figure 3(a), will be given in detail here; the same procedure will apply to the other three cases. From geometry of the composite section, $A_c = 768$ in.²; $I_c = 4,096$ in.⁴; $A_s = 72.1$ in.²; $I_s = 16,100$ in.⁴; and moment of inertia of transformed composite section (I_t) = 37,283 in.⁴. Using Table 7

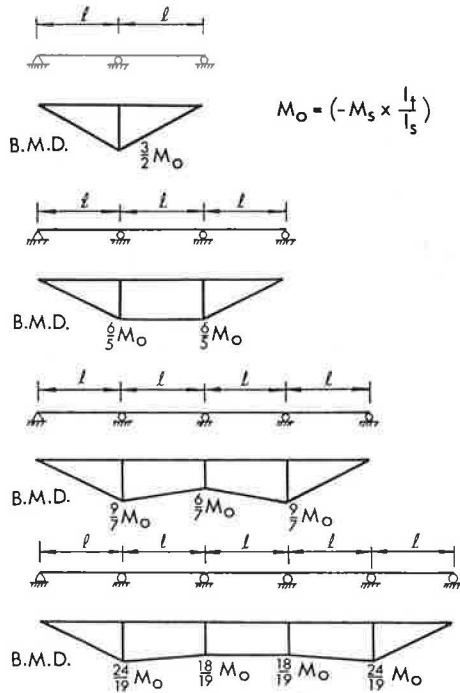


FIGURE 2 Redundant bending moments in continuous beams caused by temperature change.

for $F_c^1 = 8 \text{ ksi}$, $(2a) = 8 \text{ in.}$, yields $k_1 = -17.99 \text{ kip-in.}$, $k_2 = -0.18 \text{ kip-in.}$, $k_3 = 0.04 \text{ kip.}$, and $k_4 = -0.08$. Thus, from Equations 11-13,

$$Q = (40)(-17.99) - (85 - 60)(-0.18) = -715.10 \text{ kip-in.}$$

$$F = (85 - 60)(0.04) - (-715.10)(-0.08) = -56.21 \text{ kips}$$

$$M_s = (-56.21)(18.04) + (-715.10) = -1,729.13 \text{ kip-in.}$$

From Equations 17 and 18, the thermal stresses induced (with the intermediate pier support assumed removed) are

$$\sigma_{xc} \begin{matrix} \text{top} \\ \text{bottom} \end{matrix} = \begin{matrix} -4 \\ +4 \end{matrix} \left\{ \begin{matrix} (-56.21/768) - (-715.10/4096) \\ + [(-56.21)(4)/4096] \end{matrix} \right\} = \begin{matrix} -0.55 \text{ ksi} \\ 0.41 \text{ ksi} \end{matrix}$$

$$\sigma_{xs} \begin{matrix} \text{top} \\ \text{bottom} \end{matrix} = \begin{matrix} -18.04 \\ +18.04 \end{matrix} \left\{ \begin{matrix} (56.21/72.1) + [(-56.21)(18.04)/16100] \\ + (-715.10/16100) \end{matrix} \right\} = \begin{matrix} 2.72 \text{ ksi} \\ -1.16 \text{ ksi} \end{matrix}$$

Because of the thermal strains and the presence of the intermediate pier support, the redundant moment at the pier support for a two-span continuous bridge is (Figure 2)

$$M_R = (3/2)(-M_s)(l_t/l_s) \tag{19}$$

or

$$M_R = (3/2)(1729.13)(37283/16100) = 6,006.26 \text{ kip-in.}$$

The resulting stresses from $\sigma = (M/I)y$ are

$$\sigma_{xc} \begin{matrix} \text{top} \\ \text{bottom} \end{matrix} = [6,006.26/37283(7.44)] \begin{matrix} -13.06 \\ -5.06 \end{matrix} = \begin{matrix} -0.28 \text{ ksi} \\ -0.11 \text{ ksi} \end{matrix}$$

$$\sigma_{xs} \begin{matrix} \text{top} \\ \text{bottom} \end{matrix} = (6,006.26/37283) \begin{matrix} -5.06 \\ 31.02 \end{matrix} = \begin{matrix} -0.82 \text{ ksi} \\ +5.00 \text{ ksi} \end{matrix}$$

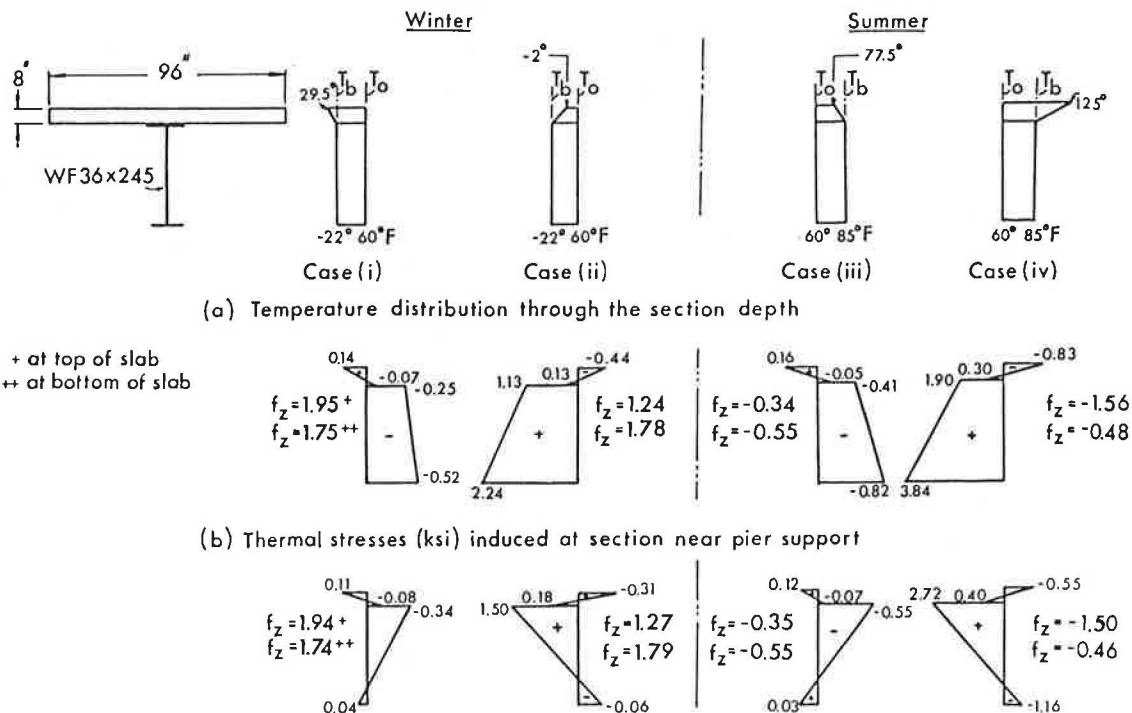


FIGURE 3 Induced thermal stresses in the bridge design example.

Thus the resultant thermal stresses at a section near the pier support become

$$\sigma_{xc} \left. \begin{array}{l} \text{top} \\ \text{bottom} \end{array} \right\} = \begin{array}{l} -0.55 - 0.28 = -0.83 \text{ ksi} \\ 0.41 - 0.11 = 0.30 \text{ ksi} \end{array}$$

$$\sigma_{xs} \left. \begin{array}{l} \text{top} \\ \text{bottom} \end{array} \right\} = \begin{array}{l} 2.72 - 0.82 = 1.90 \text{ ksi} \\ -1.16 + 5.00 = 3.84 \text{ ksi} \end{array}$$

The thermal stresses in the concrete deck slab in the transverse direction are calculated from Equation 16 as

$$\sigma_{zc} \left. \begin{array}{l} \text{top} \\ \text{bottom} \end{array} \right\} = \begin{array}{l} (0.2)(-0.83) - (5.5)(10^{-6})(3.9)(10^3)(125 - 60) = -1.56 \text{ ksi} \\ (0.2)(0.30) - (5.5)(10^{-6})(3.9)(10^3)(85 - 60) = -0.48 \text{ ksi} \end{array}$$

The induced thermal stresses for the other three cases, (i) to (iii), are presented in Figure 3(b). The thermal stresses at sections near the outer supports are shown in Figure 3(c). These results indicate that significant tensile thermal stresses can develop in the concrete deck slab in the longitudinal direction not only at the top of the concrete deck slab but also at its bottom. Furthermore, the transverse stresses in the deck slab, which result from thermal variations, can be quite large and are likely to cause severe longitudinal cracking of the concrete deck unless adequately reinforced.

SUMMARY AND CONCLUSIONS

A simple method of analysis is presented for estimating the thermal stresses in composite concrete deck slab-on-steel beam bridges; the method can be applied to both simple spans and continuous spans. The results are based on a realistic temperature distribution through the depth of the bridge section and on accepted maximum and minimum temperature differentials for summer and winter. From the results given it can be concluded that

- The magnitude of the longitudinal thermal stresses in composite bridges can be significant compared with stresses due to dead and live loads.

- The thermal stresses induced in the concrete deck slab in the transverse direction can exceed the tension capacity of the concrete by several fold; therefore additional steel reinforcements are necessary in the transverse direction to guard against the formation of longitudinal cracks in the concrete deck.

ACKNOWLEDGMENTS

This work was supported by the Natural Sciences and Engineering Research Council of Canada under Grant 1869.

REFERENCES

1. J.H. Emanuel and J.L. Hulsey. Temperature in Composite Bridges. *Journal of the Structural Division, ASCE*, Vol. 104, No. ST1, Jan. 1978.
2. M.H. Naruoka and T. Yamaguti. The Measurement of the Temperature of the Interior of the Reinforced Concrete Slab of the Shigita Bridge and Presumption of Thermal Stresses. *Proc., Symposium on the Stress Measurements for Bridge and Structures, Japanese Society for Promotion of Science, Tokyo, Japan, Dec. 1957, pp. 109-115.*

3. I.G. White. Non-Linear Differential Temperature Distribution in Concrete Bridge Structures: A Review of Current Literature. Report 525. Cement and Concrete Association, Wexham Springs, Slough, Berkshire, England, 1979.
4. F. Leonhardt and W. Lippoth. Folgerungen aus Schäden an Spannbetonbrücken. *Beton- und Stahlbetonbau*, Vol. 65, No. 10, Oct. 1970, pp. 231-244.
5. M.J.N. Priestley. Effects of Transverse Temperature Gradients on Bridges. Report 394. Ministry of Works, Wellington, New Zealand, Sept. 1972.
6. J.C. Reynolds and J.H. Emanuel. Report of the Subcommittee on the State-of-the-Art Survey of the Task Committee on Composite Construction of the Committee on Metals of the Structural Division. *Journal of the Structural Division, ASCE*, Vol. 100, Part 1, May 1974.
7. R.A. Imbsen and D.E. Vandershaf. Thermal Effects in Concrete Bridge Superstructures. In *Transportation Research Record 950*, TRB, National Research Council, Washington, D.C., Vol. 1, 1984, pp. 70-76.
8. Standard Specifications for Highway Bridges. 13th ed. AASHTO, Washington, D.C., 1983.
9. W. Zuk. Thermal Behavior of Composite Bridges-- Insulated and Uninsulated. In *Highway Research Record 76*, HRB, National Research Council, Washington, D.C., 1965, pp. 231-253.
10. C. Berwanger. Thermal Stresses in Composite Bridges. *Proc., ASCE Specialty Conference on Steel Structures, Engineering Extension Series, No. 15, University of Missouri-Columbia, 1970, pp. 27-36.*
11. C Berwanger and Y. Symko. Thermal Stresses in Steel-Concrete Composite Bridges. *Canadian Journal of Civil Engineering*, Vol. 2, No. 1, 1975.
12. W. Zuk. Thermal and Shrinkage Stresses in Composite Beams. *Journal of the American Concrete Institute*, Vol. 58, Sept. 1961.
13. W. Zuk. Simplified Design Check of Thermal Stresses in Composite Highway Bridges. In *Highway Research Record 103*, HRB, National Research Council, Washington, D.C., 1965, pp. 10-13.
14. M.H. Soliman. Long-Term Losses in Prestress and Thermal Effect in Composite Steel: Concrete Structures with Prestressed Decks. M.A.Sc. thesis. University of Windsor, Windsor, Ontario, Canada, 1985.
15. Standard Plans for Highway Bridges: Structural Steel Superstructures. FHWA, U.S. Department of Transportation, Vol. II, 1982.
16. Steel, Concrete, and Composite Bridges, Part I: General Statement. British Standard BS 5400. British Standards Institution, Crowthorne, Berkshire, England, 1978.
17. K. Roik and J.H. Haensel. Composite Bridge Design in Germany. U.S.-Japan Joint Seminar on Composite Construction, ASCE Conference Proceedings, Seattle, Wash., July 1984.

APPENDIX

The explicit expressions for the thermal coefficients k_1 , k_2 , k_3 , and k_4 are as follows:

$$k_1 = [AC_2/(AR-KB)]$$

$$k_2 = [KC_1/(AR-KB)]$$

$$k_3 = (C_1/A)$$

$$k_4 = B/A$$

where

$$C_1 = -(1 + \nu) \alpha_c + \alpha_s,$$

$$C_2 = -(1 + \nu) \alpha_c w I_s E_s E_c a^2,$$

$$A = (1/E_s A_s) + (d_1^2/I_s E_s) + [2(1 - \nu^2)/w a E_c],$$

$$B = (d_1/E_s I_s) - [1.5(1 - \nu^2)/a^2 w E_c],$$

$$K = 2w d_1 a^3 E_c - 3(1 - \nu^2) a I_s E_s, \text{ and}$$

$$R = 2w a^3 E_c + 3(1 - \nu^2) I_s E_s.$$

Publication of this paper sponsored by Committee on General Structures.

Multi-Increment Cost-Allocation Methodology for Bridges

AH-BENG TEE, KUMARES C. SINHA, and EDWARD C. TING

ABSTRACT

In this paper is presented an overview of a bridge cost-allocation procedure that uses data from bridges built in the state of Indiana between 1980 and 1983. The framework of the present analysis was based on the incremental concept with modification at various steps in the allocation process such that a larger number of cost increments were obtained. A technique is discussed for obtaining a large number of cost increments in order to render the economies-of-scale problem associated with the incremental methodology insignificant. The quantitative correlation between study vehicle classification and AASHTO vehicles was based on the relative effect of both axle loading and axle spacing of each vehicle on continuous-span bridges. The cost responsibility of each vehicle class was determined first on the basis of its structural and geometric requirements and then on the relative frequency with which it uses the bridges. A discussion of the approach employed in the distribution of the bridge construction, bridge replacement, and bridge rehabilitation cost is presented.

There are several methods of allocating bridge costs in the literature. However, the most commonly used and widely accepted methodology for structural cost-allocation analysis is classical incremental analysis (1-6). Although the concept of classical incremental analysis for bridge cost allocation is well documented, the approach for developing the various bridge cost functions in the allocation process varies among studies. The bridge cost-allocation process discussed in this paper is also based on the classical incremental framework but with modification at various steps. Presented herein is a multi-increment cost-allocation process based on data from bridges built in Indiana between 1980 and 1983.

VEHICULAR CLASSIFICATION AND DESIGN LOADING

Vehicles that use the Indiana highway system were categorized into 14 basic classifications (Table 1).

School of Civil Engineering, Purdue University, Lafayette, Ind. 47907.

Each class was further divided into various weight groups. For the purpose of incremental analysis, with the exception of the live loads, all loads and forces were handled in the same manner as the original bridge. The live loads that represented the weight of the moving traffic were modified to reflect a range of different types of vehicles. According to AASHTO bridge specifications (7), traffic-related loadings can be represented by standard trucks or by equivalent lane loads. The trucks specified are designated with an H prefix followed by a number indicating the total weight of the trucks in tons for the two-axle trucks or with an HS prefix followed by a number indicating the weight of the tractor in tons for the tractor-trailer combinations. The AASHTO bridge specification provides only five classes of design loading, namely, HS 20, HS 15, H 20, H 15, and H 10. Other loadings required for the present analysis can be obtained by proportionally changing the weights of the designated trucks (7). The modified AASHTO live loadings and the corresponding lane loadings used in the present study are shown in Figure 1. The cost functions of each bridge element were

TABLE 1 Adopted Vehicle Classification (9)

Class	Description
1	Small passenger automobiles
2	Standard and compact passenger automobiles and panel and pickup trucks
3	Buses
4	Two-axle trucks (2 S and 2 D)
5	Automobiles with one-axle trailers
6	Three-axle single-unit trucks
7	2 S1 tractor-trailers
8	Automobiles with two-axle trailers
9	Four-axle single-unit trucks
10	3 S1 tractor-trailers
11	2 S2 tractor-trailers
12	3 S2 tractor-trailers
13	Other five-axle vehicles
14	Six or more axles

then computed on the basis of the previously mentioned set of design loadings.

CORRELATION BETWEEN AASHTO VEHICLES AND STUDY VEHICLES

It is to be noted that the design trucks are different from the trucks seen operating on the highways.

They are trucks with configurations that would simulate the most severe live loads on a structure. Therefore the correlation between the design vehicles and the study vehicle classes should be viewed as a critical task in any structural cost-allocation study. Without a proper procedure for matching the design vehicles with the study vehicle classes, any attempt to improve computational precision would be limited because the accuracy of the cost functions in terms of design vehicles would not be maintained when converted into the study vehicle classes. Many studies (1-4,6) used gross vehicle weight to establish the relationship between AASHTO vehicles and study vehicles. The use of gross vehicle weight neglects axle load distribution and axle spacing.

Maryland (8,5) used a more rational method in establishing this correlation because it incorporated both axle loading and axle spacing in its analysis. However, the vehicles were analyzed on simply supported single-span bridges of varying span length rather than on continuous-span bridges. The results obtained by using simply supported simple spans would involve approximations when extended to continuous-span bridges.

Because most bridges have continuous spans, the quantitative correlations between study vehicles and AASHTO design vehicles were based on continuous-span

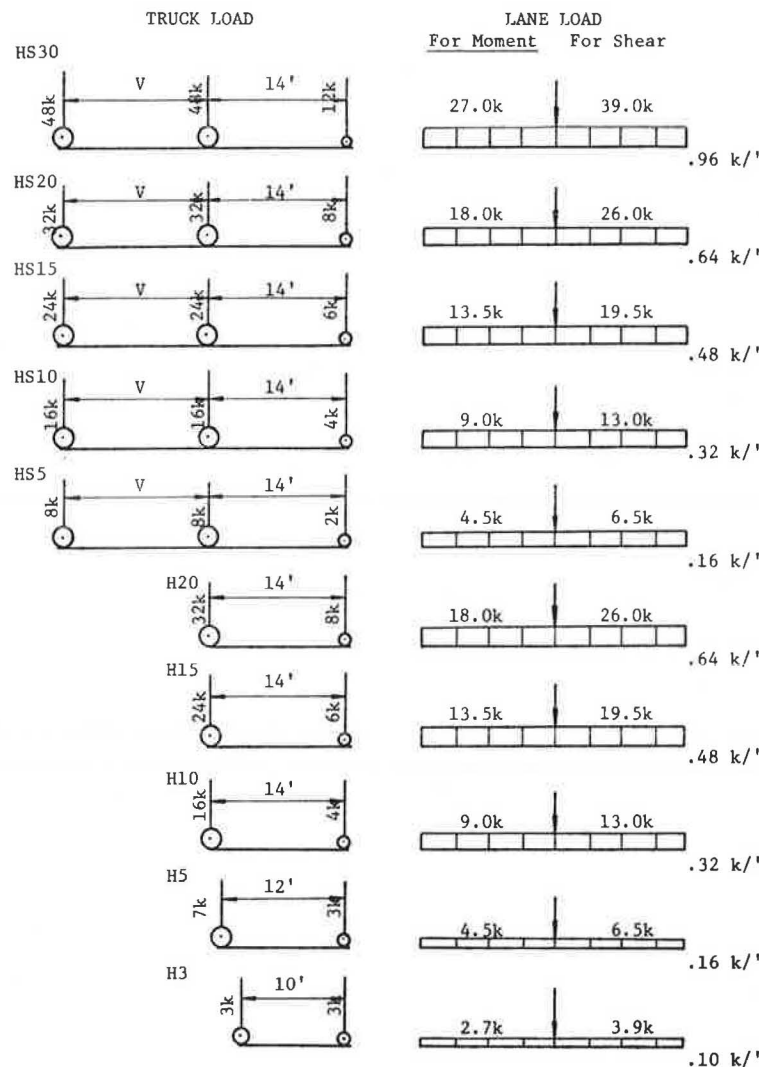


FIGURE 1 Modified AASHTO live loading configurations for bridge incremental designs.

bridges of varying span lengths. Figure 2 shows a flow chart of such an analysis. This approach required knowledge of the axle loads and the axle spacings of each vehicle weight group. It is to be noted that each vehicle within each subweight group may have different axle loading and axle spacing because vehicles were grouped according to their high-

way use and damage criteria. Therefore, an average value for both the axle loading and the axle spacing of all vehicles in each weight group was used.

Table 2 gives the equivalent AASHTO designation of each study vehicle weight group. Table 3 gives the correspondence of each vehicle weight group with the equivalent AASHTO designation in the correlation matrix.

The correlation between the H and HS trucks was obtained by equating the maximum moments produced on the critical points of bridges. A linear regression analysis was then performed on the results. The regression equation found was $HS = 0.68 H$ with $r^2 = 0.89$.

BRIDGE TYPES

The most recent bridge projects were used in the analysis because they represent modern construction trends and techniques. Bridges in Indiana built within the base period (1980 through 1983) were categorized as follows:

1. Reinforced concrete slab,
2. Prestressed concrete I-beam,
3. Prestressed concrete box-beam,
4. Steel beam, and
5. Steel girder.

Bridges within each category usually have rather similar properties and characteristics. Hence, a representative bridge was selected from each of the five categories. Incremental analyses were performed on each representative bridge using the selected set of design loadings described earlier.

HIGHWAY CLASSIFICATION

In general, the characteristics of a highway are reflected by the bridges constructed on that highway. Bridges on principal arterials have higher design standards than do those on county roads. The following highway classification was used (9):

1. Interstate urban,
2. Interstate rural,
3. State primary,
4. State secondary,
5. County road, and
6. City street.

BRIDGE COST COMPONENTS

Bridge costs were divided into the following components:

1. Superstructure
2. Substructure
 - a. Abutment and pier
 - b. Piling
 - c. Excavation and backfill
3. Railing
4. Drainage system
5. Miscellaneous items

Incremental cost analyses, based on the geometric and structural requirements of the design vehicles, were performed separately on each of the cost components.

COST FUNCTIONS

The design drawings, plans, and bid information were obtained from the Indiana Department of Highways. All of the selected bridges were designed for HS 20 loading. By replacing the HS 20 loading with other

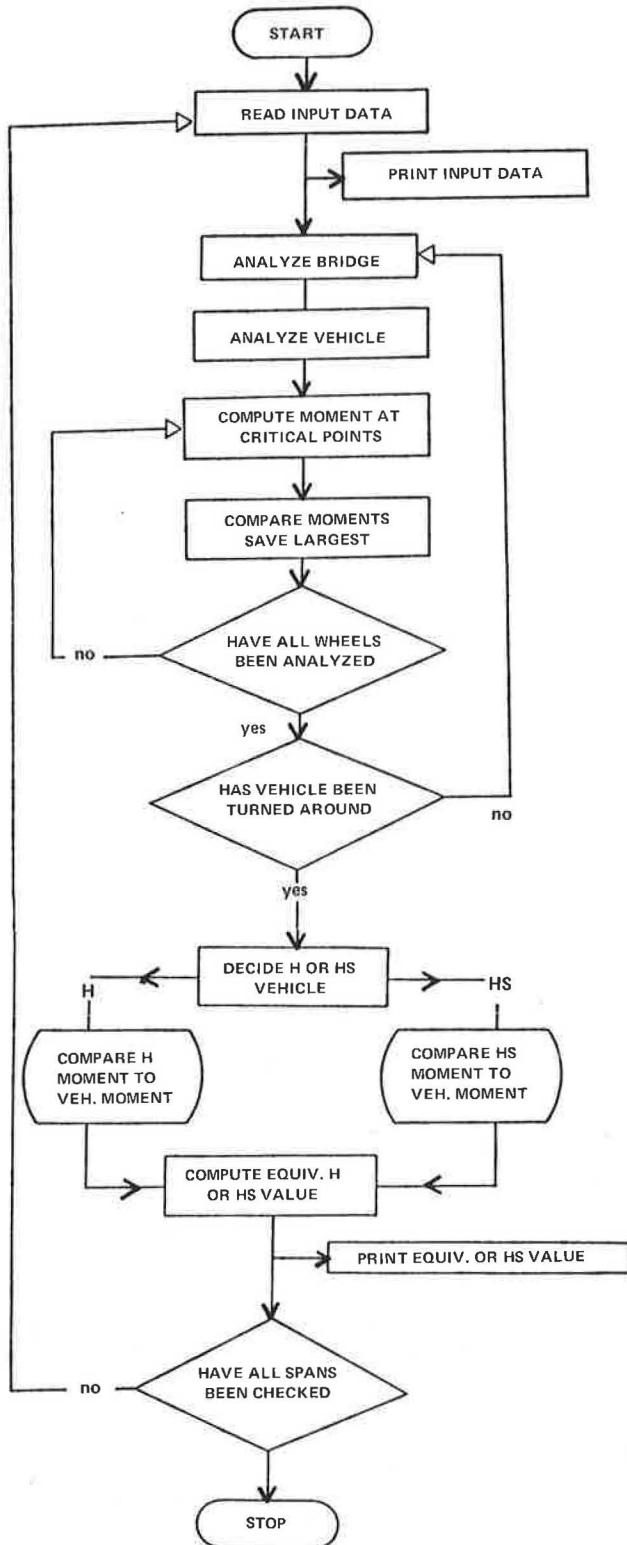


FIGURE 2 Flow diagram for AASHTO loadings and study vehicle classes correlation analysis.

TABLE 2 Study Vehicle Classification and Equivalent AASHTO Designation

Vehicle Type ^a	Gross Weight (kips)	Design Axle Load ^b (kips)						Axle Spacing ^c (ft)					Equivalent AASHTO Vehicle	
		A	B	C	D	E	F	AB	BC	CD	DE	EF		
1	4.0	2.0	2.0					7.2					H 2.9	
2	6.0	3.0	3.0					10.05					H 4.0	
3	30.0	12.0	18.0					31.65					H 17.0	
4	5-10.0	4.5	5.5					11.0					H 8.9	
4	10-15.0	6.5	8.5					13.0					H 9.41	
4	15-20.0	7.7	12.3					14.0					H 12.95	
4	20-25.0	10.2	14.8					15.0					H 15.29	
4	25-30.0	12.0	18.0					17.0					H 17.67	
5	9.0	4.0	4.0	1.0				11.5	8.6				HS 3.0	
6	10-15.0	5.0	6.0	4.0				14.0	4.0				HS 6.0	
6	15-20.0	8.0	6.0	6.0				14.0	4.0				HS 7.0	
6	20-25.0	10.0	7.0	8.0				14.0	4.0				HS 8.0	
6	25-30.0	12.0	8.0	10.0				14.0	4.0				HS 10.0	
6	30-35.0	13.0	10.0	12.0				14.0	4.0				HS 11.0	
6	35-40.0	15.0	12.0	13.0				14.0	4.0				HS 13.0	
7	0-20.0	7.0	8.0	5.0				10.0	16.0				HS 6.0	
7	20-25.0	9.0	10.0	6.0				10.0	17.0				HS 7.0	
7	25-30.0	9.0	11.0	10.0				10.0	18.0				HS 8.0	
7	30-35.0	10.0	13.0	12.0				10.0	21.0				HS 9.0	
8	10.00	4.0	4.0	1.0	1.0			11.5	8.60	5.80			HS 3.50	
9	0-30.0	6.0	6.0	18.0				4.0	40.0				HS 13.0	
9	30-60	16.0	16.0	28.0				4.0	40.0				HS 23.0	
10	0-40.0	13.0	9.0	9.0	9.0			17.30	4.0	21.00			HS 10.0	
11	20-25.0	7.0	8.0	5.0	5.0			10.0	22.0	4.0			HS 7.0	
11	25-30.0	8.0	10.0	6.0	6.0			10.0	22.0	4.0			HS 8.0	
11	30-35.0	9.0	11.0	7.0	8.0			10.0	22.0	4.0			HS 9.0	
11	35-40.0	10.0	14.0	8.0	8.0			10.0	22.0	4.0			HS 10.0	
11	40-45.0	10.0	15.0	10.0	10.0			10.0	22.0	4.0			HS 11.0	
11	45-50.0	10.0	16.0	12.0	12.0			10.0	22.0	4.0			HS 12.0	
11	50-55.0	11.0	18.0	13.0	13.0			10.0	22.0	4.0			HS 14.0	
12	20-25.0	7.0	6.0	6.0	3.0	3.0		10.0	4.0	25.0	4.0		HS 7.0	
12	25-30.0	8.0	7.0	7.0	4.0	4.0		10.0	4.0	25.0	4.0		HS 8.0	
12	30-35.0	9.0	8.0	8.0	5.0	5.0		10.0	4.0	25.0	4.0		HS 9.0	
12	35-40.0	10.0	9.0	9.0	6.0	6.0		10.0	4.0	25.0	4.0		HS 10.0	
12	40-45.0	11.0	10.0	10.0	7.0	7.0		10.0	4.0	25.0	4.0		HS 11.0	
12	45-50.0	12.0	11.0	11.0	8.0	8.0		10.0	4.0	25.0	4.0		HS 12.0	
12	50-55.0	11.0	12.0	12.0	10.0	10.0		10.0	4.0	25.0	4.0		HS 13.0	
12	55-60.0	10.0	13.0	13.0	12.0	12.0		10.0	4.0	25.0	4.0		HS 14.0	
12	60-65.0	10.0	14.0	14.0	13.0	13.0		10.0	4.0	25.0	4.0		HS 15.0	
12	65-70.0	10.0	16.0	16.0	14.0	14.0		10.0	4.0	25.0	4.0		HS 17.0	
12	70-75.0	11.0	17.0	17.0	15.0	15.0		10.0	4.0	25.0	4.0		HS 18.0	
12	75-80.0	12.0	18.0	18.0	16.0	16.0		10.0	4.0	25.0	4.0		HS 19.0	
13	0-40.0	5.0	7.0	12.0	8.0	8.0		9.0	18.0	5.0	11.0		HS 11.0	
13	40-70.0	10.0	18.0	16.0	13.0	13.0		9.0	18.0	5.0	11.0		HS 17.0	
14	0-40.0	8.0	7.0	7.0	8.0	5.0	5.0	10.0	4.0	21.0	5.0	11.0	HS 11.0	
14	40-60.0	9.0	12.0	12.0	13.0	7.0	7.0	10.0	4.0	21.0	5.0	11.0	HS 19.0	
14	60-80	9.0	16.0	16.0	17.0	11.0	11.0	11.0	10.0	4.0	21.0	5.0	11.0	HS 24.0

^a Refer to Table 1 for description of vehicle types.
^b A = first axle, B = second axle, C = third axle, D = fourth axle, E = fifth axle, and F = sixth axle.
^c AB, BC, CD, DE, and EF = distance in feet between adjacent axles.

AASHTO design loadings, bridges of different structural and geometric characteristics were obtained. For the selected bridges, the original specifications, configurations, and materials that were independent of vehicular loadings were retained where appropriate. In areas in which AASHTO specifications governed, those specifications were used in place of the original specifications.

The three lowest bids submitted by contractors were chosen and their itemized unit costs were averaged. The total cost of each bridge cost component was obtained using these itemized unit costs. For each type of bridge and cost component, a cost function of the form shown in Figure 3 was obtained. Next, by dividing the total cost by the deck area, the unit cost per square foot was obtained. Table 4 gives the unit cost per square foot of superstructure by design loading and by bridge type.

It is to be noted that the distribution of each type of bridge is important. For example, there were 30 slab bridges and 50 prestressed box-beam bridges of various dimensions built within the base period. To account for this, the total deck area of all bridges of each bridge type built within the base period (1980 through 1983) was determined and grouped according to highway class. A summary of total deck

area by highway classification and by bridge type is given in Table 5. The cost factors for different AASHTO loadings and by bridge type were then obtained using Equation 1:

$$CF(k) = \left[\sum_{k=1}^{(10)} \sum_{j=1}^{(5)} U(i, k) A(i, j) \right] / \left[\sum_{j=1}^{(5)} U(i, 20) A(i, j) \right] * 100\% \quad (1)$$

where

- i = type of bridge,
- j = type of highway class,
- k = [set of design loadings],
- A(ij) = total deck area for the ith type of bridge and jth highway class, and
- U(ik) = unit cost for the ith bridge type and kth loading.

It is important to note that the interest here is in obtaining cost factors by highway type not by bridge type. The cost factors by highway type should account for the distribution of each bridge type. For instance, certain types of bridges may not be found or may be less predominant on particular types of highway. The cost factors by highway type were

TABLE 3 Correlation Matrix of Study Vehicular Classification and Equivalent AASHTO Designation

AASHTO Classification		Gross Vehicle Weight (kips) of Vehicle Type ^a													
HS	H	1	2	3	4	5	6	7	8	9	10	11	12	13	14
1	1.5														
2	2.9	*	*												
3	4.4														
4	5.9				5-10										
5	7.4								*						
6	8.8				10-15	10-15	0-20								
7	10.3					15-20	20-25	20-25				20-25	20-25		
8	11.8				15-20	20-25	25-30					25-30	25-30		
9	13.2						30-35					30-35	30-35		
10	14.7				20-25	25-30					*	35-40	35-40		
11	16.2		*			30-35						40-45	40-45	0-40	0-40
12	17.7				25-30							45-50	45-50		
13	19.1					35-40				0-30		50-55	50-55		
14	20.6											55-60	55-60		
15	22.1											60-65	60-65		
16	23.5														
17	25.0												65-70	40-70	
18	26.5												70-75		
19	27.9												75-80	40-60	
20	29.4														
21	30.9														
22	32.3									30-60					
23	33.8														
24	35.3														60-80
25	36.8														
26	38.2														
27	39.7														
28	41.2														
29	42.6														
30	44.1														

Note: HS = combination trucks, H = single unit trucks, and * = vehicle class without weight subdivision.
^aRefer to Table 1 for description of vehicles.

obtained by adding the cost factors of each bridge type found on each particular type of highway. For the purpose of illustration, Table 6 gives the bridge cost factors obtained for state secondary highways. A statistical regression analysis was performed on these results and plotted as shown in Figure 4.

BRIDGE COST ALLOCATORS

In the present study, the basic structure is the facility constructed to support the smallest design vehicle. The cost of providing the basic facility should be allocated to all vehicle classes, irre-

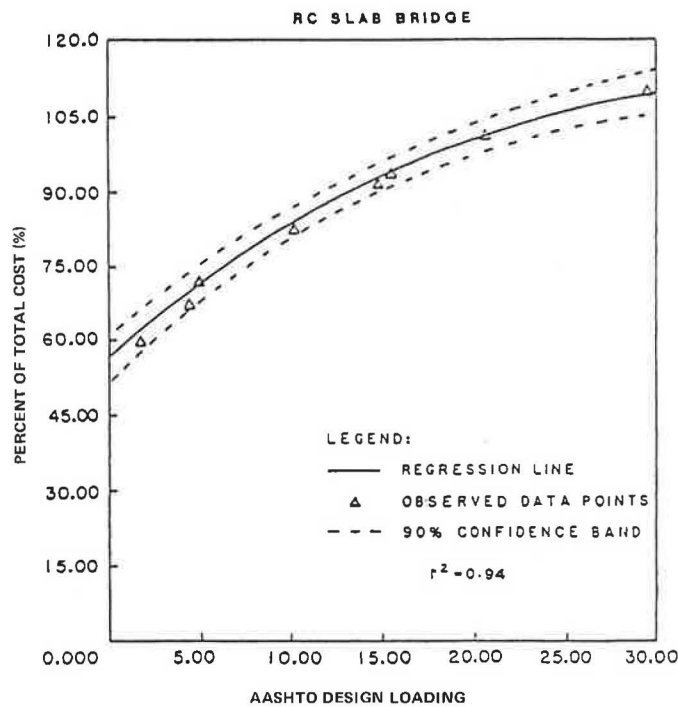


FIGURE 3 Slab bridge superstructure cost function.

TABLE 4 Bridge Superstructure Unit Costs

Bridge Type	Unit Cost (\$/ft ²)									
	H 3	H 5	H 10	H 15	H 20	HS 5	HS 10	HS 15	HS 20	HS 30
Slab	12.19	14.27	17.44	18.73	19.92	16.41	18.61	19.90	21.17	23.03
Box-beam	16.03	17.07	18.25	19.45	20.48	17.87	19.30	20.63	22.31	25.02
I-Beam	14.78	15.53	16.63	17.71	18.62	16.19	17.59	18.75	19.94	22.10
Steel beam	15.71	17.36	20.19	22.91	26.31	19.37	23.16	26.48	29.81	32.73
Steel girder	18.07	19.97	23.22	26.34	30.26	22.85	26.64	30.45	34.29	37.64

TABLE 5 Bridge Deck Area (ft²) Constructed in 1980-1983 by Bridge Type and Highway Classification

Bridge Type	Highway Classification				
	Interstate Urban	Interstate Rural	State Primary	State Secondary	Local Road
Slab	*	*	97,723.60	97,795.40	10,967.50
Box-beam	*	*	18,566.50	4,146.90	*
I-beam	14,464.80	*	188,871.30	126,291.80	2,412.00
Steel beam	17,606.30	29,702.4	133,766.20	72,970.90	*
Steel girder	*	*	171,835.50	91,637.50	*

Note: * = No bridge of this type constructed within the base period.

TABLE 6 Cost Factors for State Secondary Bridge

Bridge Type	Cost by AASHTO Loading Type (\$)									
	H 3	H 5	HS 5	H 10	HS 10	H 15	H 20	HS 15	HS 20	HS 30
Prestressed I-beam	1,192,125	1,395,540	1,604,822	1,705,551	1,819,972	1,831,708	1,946,128	1,948,084	2,070,328	2,252,228
Reinforced concrete slab	66,474	70,788	74,105	75,680	80,035	80,657	84,928	85,550	92,517	103,755
Prestressed box-beam	1,866,592	1,961,311	2,044,664	2,100,232	2,221,473	2,236,628	2,351,553	2,367,971	2,505,629	2,791,049
Continuous steel beam	1,146,372	1,266,774	1,449,932	1,473,282	1,671,763	1,690,006	1,919,864	1,932,269	2,175,263	2,388,337
Continuous steel girder	1,655,889	1,830,000	2,093,916	2,127,822	2,413,731	2,441,223	2,772,950	2,790,361	3,142,249	3,449,236
Total	5,927,452	6,524,413	7,267,439	7,482,567	8,206,974	8,280,222	9,075,423	9,124,231	9,985,982	10,984,605
Percentage of total cost	59	65	73	74	82	83	91	91	100	110

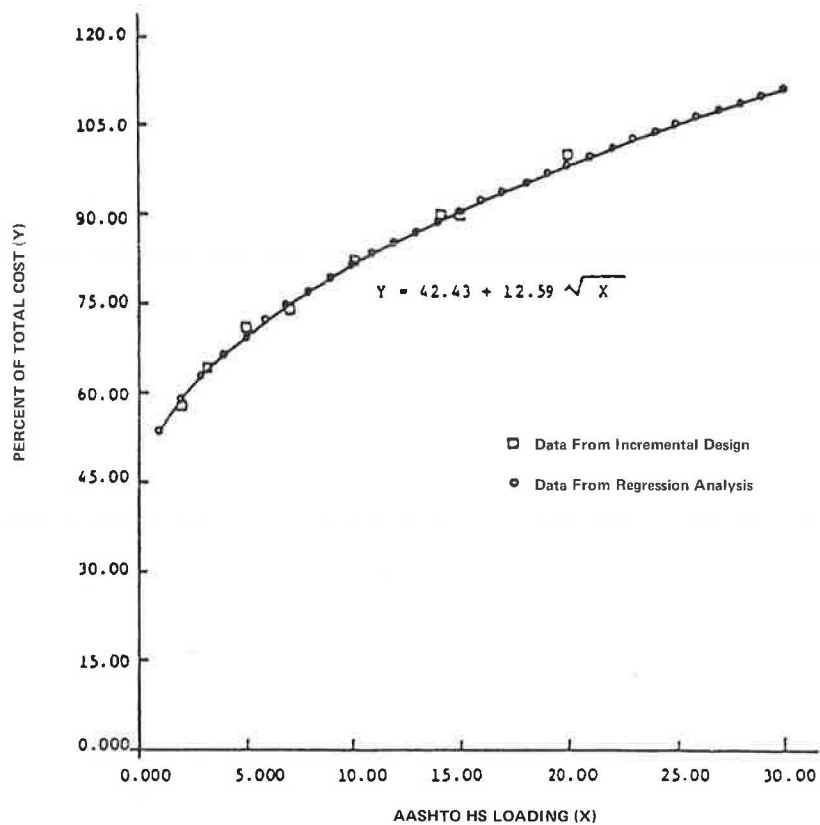


FIGURE 4 Regression equation for state secondary bridges.

TABLE 7 Percentage Distribution of Bridge Rehabilitation Cost by Cost Item and by Highway Class, 1980-1983

	Interstate (rural and urban)	State Primary	State Secondary	Local Road
Superstructure	28.5	29.5	26.2	27.00
Substructure				
Piers and abutments	7	2.6	6.0	5.74
Piling	0.01	0.6	0.13	1.37
Excavation and backfill	9.88	19.6	18.6	18.51
Drainage	0.01	0.10	0.007	0.12
Railing	5.7	3.2	6.50	6.08
Miscellaneous	48.9	44.4	42.50	41.18
Total	100	100	100	100

spective of their size and weight features. The additional cost of providing the additional facility above the basic structure to accommodate heavier vehicles was assigned to the heavier vehicles. Vehicle miles of travel (VMT), which indirectly measures the frequency of the vehicle in a traffic stream, was used as the cost allocator for the basic structural costs and additional facility costs.

TYPES OF BRIDGE PROJECTS

Bridge projects were categorized into bridge construction, bridge replacement, and bridge rehabilitation. Bridges in each category were further divided according to highway type. Next, the itemized unit costs of each project within each project type and highway type were analyzed and grouped according to their cost components described earlier. As an illustration, Table 7 gives the percentage distribution of bridge rehabilitation cost by cost component and by highway class. The cost responsibilities of each vehicle class were then computed according to project type and highway classification for each cost component.

MULTI-INCREMENT COST-ALLOCATION METHOD

The inherent weakness of the incremental concept is the economies-of-scale problem. However, by increasing the number of loading increments, the unequal cost problem would be proportionately reduced. Unfortunately, it was not economically feasible to use a large number of loading increments. For example, suppose that five types of bridges were selected. For each additional loading, there would be five additional hypothetical bridges that would require a large number of design computations. Therefore, an indirect approach to obtaining a large number of design computations was developed.

Initially, bridges were analyzed with a set of AASHTO design loadings to obtain the necessary cost function in the form shown in Figure 5. It was found that seven AASHTO loadings would be sufficient to cover the entire range of study vehicles and would provide the necessary points to plot the cost function accurately.

The next step was to group all study vehicles that produce the same effect on a bridge together. This was done by grouping all vehicles with similar AASHTO designations together (Table 8). The important point here is that all vehicles in the same group basically require the same size bridge and the next higher group will require a slightly larger bridge.

It should be noted that the accuracy of each point derived from careful analysis is more important than the number of points. Each cost function was of the form $Y = a + b/\sqrt{X}$, where a and b were constant and Y and X represented the cost and design increment, respectively. By substituting different values for X into the equation, the additional cost increments could be determined. The graphic way of obtaining the necessary cost increments was through interpolation, as shown in Figure 6.

The last step of the analysis was the distribution of cost responsibilities to all of the study vehicles. For example, in Figure 6, Cost Increment A

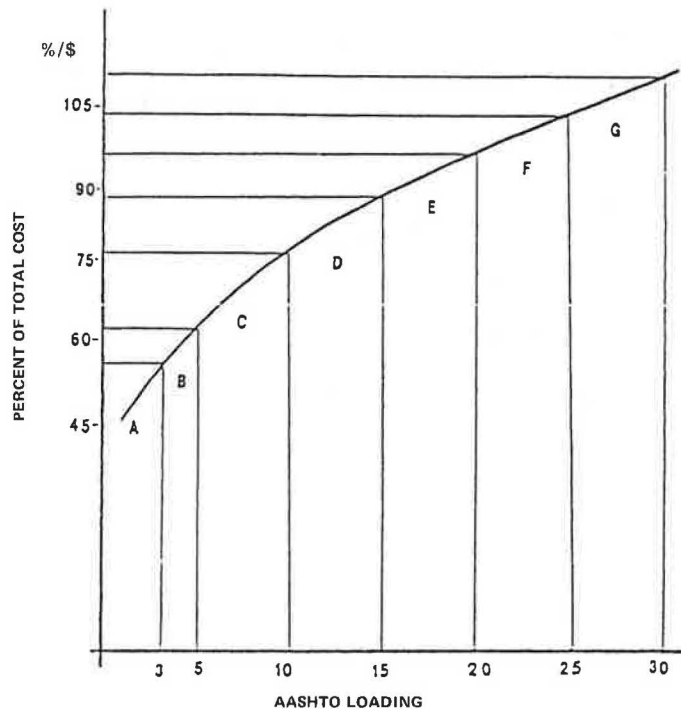


FIGURE 5 Example cost function obtained from the initial set of loading increments.

TABLE 8 Relationship Between AASHTO Design Loadings and Vehicle Class Weight Groups

AASHTO Design Loading	Weight Group
HS 2	[V1:1, V2:1]
HS 3	[V3:1]
HS 4	[V4:1, V8:1]
HS 6	[V4:2, V6:1, V7:1]
HS 8	[V4:3, V6:3, V7:3, V11:2, V12:2]
HS 9	[V7:4, V11:3, V12:3]
HS 10	[V4:4, V6:4, V10:1, V11:4, V12:4]
HS 11	[V3:1, V6:3, V11:5, V12:5, V13:1, V14:1]
HS 12	[V4:5, V11:6, V12:6]
HS 13	[V6:6, V9:1, V12:7]
HS 14	[V11:7, V12:8]
HS 15	[V12:9]
HS 17	[V12:10, V13:2]
HS 18	[V12:11]
HS 19	[V12:12]
HS 20	[V12:13, V14:2]
HS 22	[V9:2]
HS 24	[V14:3]

Note: V = study vehicle designation, number before colon = study vehicle class, and number following colon = position of the study vehicle weight group given in Table 3. HS = AASHTO vehicle designation, and number following HS = AASHTO vehicle index.

was distributed to all vehicles and Cost Increment B was distributed to all vehicles in increments B through R according to their VMT-values. Table 9 gives the data for an example problem, and Table 10 gives the application of the incremental analysis to the example problem. It is to be noted that, for illustrative purposes, only four arbitrary AASHTO loadings were used. This process is repeated for each project type, for each highway type, and for each bridge cost component.

DISCUSSION OF FINDINGS

In Table 11 are given the cost responsibilities of the four generalized vehicle classes determined in

the present study. These results are compared with those of the FHWA study (10). It is to be noted that the definition of the four generalized vehicle classes was not the same in the two studies. Consequently, the results could not be precisely compared. However, it could be concluded that passenger vehicles as a group were responsible for more than 68 percent of the total cost. Such a high figure for passenger vehicles was due to their higher frequency of using the facility (VMT), even though structurally they were responsible for a smaller percentage of the total cost.

SUMMARY AND CONCLUSIONS

As noted earlier, an accurate correlation between design vehicles and study vehicles is important in a structural cost-allocation study. The present study obtained such correlation based on the relative effect of both the axle loading and the axle spacing of each vehicle on a series of continuous-span bridges. Continuous-span bridges were used because most bridges are of this nature.

It is proposed here that the cost of new construction, replacement, and rehabilitation of bridges be distributed on the basis of the relative costs associated with providing the necessary services to each class of vehicle. This is accomplished by

TABLE 9 Cost Allocation Problem Data

AASHTO Loading	Cost Increment (\$ x 10 ⁵)	Cost Allocator (VMT x 10 ⁷)
HS 1	55	45
HS 2	10	20
HS 3	15	25
HS 4	20	10
	100	100

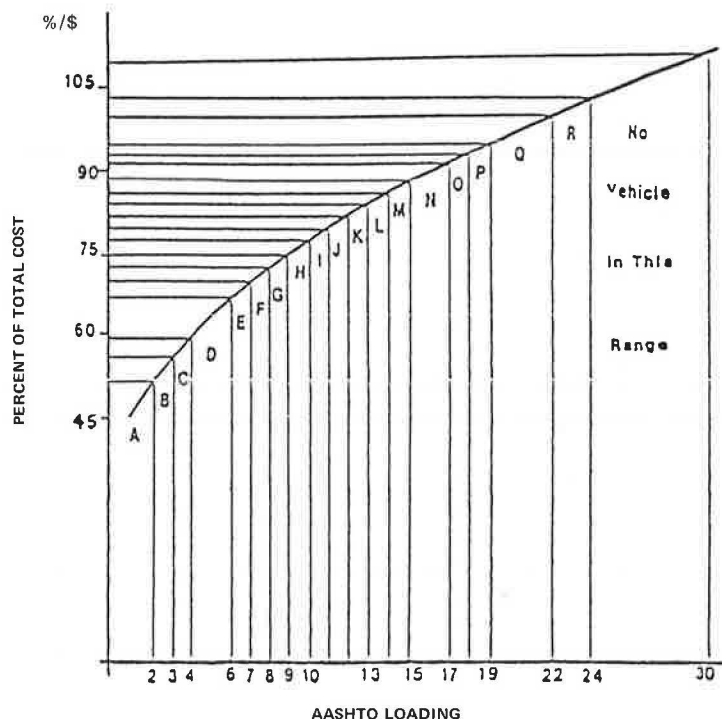


FIGURE 6 Final set of cost increments derived from superimposition of Figure 5 and Table 8.

TABLE 10 Application of Incremental Cost Analysis

	AASHTO Design Vehicle				Total Cost Increment
	HS 1	HS 2	HS 3	HS 4	
First increment	$55 \cdot (45/100) = 24.75$	$55 \cdot (20/100) = 11.0$	$55 \cdot (25/100) = 13.75$	$55 \cdot (10/100) = 5.5$	55
Second increment		$10 \cdot (20/55) = 3.64$	$10 \cdot (25/55) = 4.54$	$10 \cdot (10/55) = 1.82$	10
Third increment			$15 \cdot (25/35) = 10.71$	$15 \cdot (10/35) = 4.29$	15
Fourth increment				$20 \cdot (10/10) = 20$	20
Cost responsibility	24.75	14.64	29.0	31.61	100

TABLE 11 Comparison of Bridge Cost Responsibility Factors (%) of Indiana Study (9) and FHWA Study (10)

Vehicle Type	FHWA Study (1985) ^a		Indiana Study (1983)	
	Recommended Approach ^b	Incremental for All Bridge Costs ^c	State Highways	All Highways ^d
Passenger vehicles	65.02	69.12	68.58	73.18
Buses	1.21	0.94	0.28	1.59
Single-unit trucks	7.67	6.69	6.27	8.28
Combination trucks	27.32	24.19	24.87	17.83

^aFederal Highway Cost-Allocation Study (10), pp. iv-52.

^bAssigns bridge rehabilitation costs to all vehicles as common costs.

^cGroups rehabilitation costs with other structure costs.

^dState highways + county roads + city streets.

grouping the itemized unit costs attributable to each vehicle class according to bridge cost components.

The chief drawback of the incremental cost methodology is the economies-of-scale problem. This problem is particularly pronounced when only a few cost increments are used. Because the number of design analyses required increases with the number of cost increments used, often the tendency is to minimize design analyses and, thereby, cost increments. The proposed multi-increment analysis would reduce the economies-of-scale problem without requiring a large number of design computations.

The cost responsibility of each vehicle class was based first on its structural and geometric requirements and then on the frequency with which it uses the facility. Therefore, from the structural standpoint, passenger automobiles were responsible for only a small portion of the total bridge cost but, because of the high frequency with which they use the facility, they were responsible for a high percentage of total bridge cost.

ACKNOWLEDGMENT

This paper was prepared as part of a Highway Planning and Research study conducted by the Joint Highway

Research Project of Purdue University in cooperation with the Indiana Department of Highways and the Federal Highway Administration. The authors are, however, solely responsible for the content of this paper.

REFERENCES

1. Final Report on the Federal Highway Cost Allocation Study. FHWA, U.S. Department of Transportation, May 1982.
2. Florida Highway Cost Allocation Study. Florida Department of Transportation, Tallahassee, Dec. 1979.
3. Georgia Highway Cost Allocation Study. Georgia Department of Transportation, Atlanta, March 1979.
4. Final Report of the Iowa Highway Cost Allocation Study. Iowa Department of Transportation, Des Moines, 1982.
5. Maryland Cost Allocation Study. University of Maryland, College Park, Feb. 1983.
6. Highway Cost Allocation Study. Final Report. Wisconsin Department of Transportation, Madison, Dec. 1982.
7. Standard Specifications for Highway Bridges. 12th ed. AASHTO, Washington, D.C., 1977.
8. R.D. Schelling. Incremental Cost-Allocation Analysis of Bridge Structures. In Transportation Research Record 900, TRB, National Research Council, Washington, D.C., 1983, pp. 18-26.
9. K.C. Sinha, et al. Indiana Highway Cost-Allocation Study: A Report on Methodology. FHWA/IN/JHRP-84/4. Joint Highway Research Project, Purdue University, Lafayette, Ind.; FHWA, U.S. Department of Transportation, March 1984.
10. Incremental Analysis of Structural Construction Costs. Report FHWA/pl/81/008. FHWA, U.S. Department of Transportation, April 1981.

Publication of this paper sponsored by Committee on General Structures.

Test-to-Failure of a Jack-Arch Bridge

DAVID B. BEAL

ABSTRACT

A 76-year-old jack-arch bridge was tested to failure to obtain information on load capacity and the degree of composite action between the steel beams and concrete deck. This work was started because, despite the good condition of the majority of the 1,300 jack-arch bridges in New York, load-rating estimates indicated that they were inadequate to support modern highway traffic. The most likely explanation for the observed performance of these bridges is that they are resisting loads in ways not considered in design or load-rating calculations. Although these bridges have no mechanical shear-transfer devices to assure composite action, it was suspected that chemical bond and friction were sufficient to provide the observed enhancement in load capacity. The 39-ft-span test structure consisted of six 24-in.-deep I-beams spaced at 36 in. Instrumentation consisted of electrical resistance strain gauges on both flanges at midspan, end rotation measurement devices at the ends of two beams, and deflectometers at midspan. The bridge was loaded to produce a 6-ft region of constant moment at the center of the span. Loads were applied through hydraulic jacks reacting against grouted anchors beneath the structure. It is concluded that full composite action may be assumed in load-rating estimates of jack-arch bridges. Although significant restraint of end rotation was also observed in both tests, a generalization of this restraint to other structures is not possible.

BACKGROUND

Jack-arch bridges are a small but important component of New York State's highway bridge population. More than 1,300 of these bridges, constructed between 1920 and 1940, are currently in service on state and local highway systems. These normally short-span bridges were constructed with steel beams encased in concrete. Curved sheets of corrugated metal, supported on the lower flanges of the beams, were used to form the concrete, producing the "arches." In some structures the lower flange of the beam was also encased in concrete in a separate pour, but this detail is not inherent to the structural form.

In many cases present load capacity of jack-arch bridges is estimated to be less than that required to support modern traffic. This deficiency is not unexpected because the design live load was only 20 tons, in contrast to the 40-ton trucks that are now legal. In addition, frequent pavement overlays have increased the dead load to a level that leaves many structures with little apparent remaining capacity to resist traffic. The difficulty of determining condition of the concrete-encased steel member increases the conservatism of the load rating and thus contributes to low estimates of load capacity.

Despite these apparently justified low load-capacity estimates for jack-arch bridges, many are in good condition and are carrying modern highway loads without distress after many years of service. The most likely explanation for the observed performance of these bridges is that they are resisting loads in ways that were not anticipated during design and that are not now considered in load-rating calculations. At the time jack-arch bridges were being designed, for example, composite action (the steel and concrete participating together in resisting traffic loads and dead loads other than the concrete itself) was

not considered. In general, it was not until the 1950s that composite behavior was included in bridge design calculations. Bridges do not behave compositely just because the designer decides to include such behavior in calculations. In modern construction, a mechanical connection is required between the concrete and steel before composite action can be assumed. Jack-arch bridges, of course, have no mechanical connections and thus cannot be assumed to be composite without experimental justification.

Despite the lack of shear connectors, ample evidence exists that composite action is achieved in many structures. In a test of a truss-bridge floor system (1) the magnitude of the measured strains resulting from application of the test load could be explained only by assuming composite behavior. Unintentional mechanical and chemical bond between the materials provides resistance to slip and permits development of partial composite action at service loads.

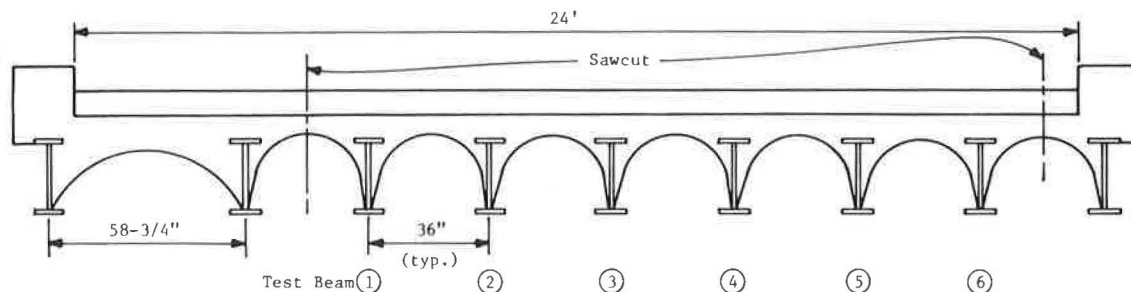
It was recognized that, if composite action is actually achieved in jack-arch bridges, the increase in calculated load capacity would be sufficient, in the majority of cases, to remove all load restrictions. The purpose of the work described in this paper was to determine experimentally the magnitude of composite action, if any, achieved in jack-arch bridges under service loads and under loading to failure.

In an earlier test (2) of a 47-ft-span bridge at Indian Lake, New York, it was concluded, based on measurements of steel strain, deflection, and end rotation, that the full composite section was active in resisting live load. Nevertheless, because that structure was in good condition with no visible deterioration of the concrete, generalization of this result to all jack-arch bridges could not be supported.

TEST STRUCTURE

The test structure reported here was a jack-arch bridge constructed before 1915 to carry east-west

Engineering Research and Development Bureau, New York State Department of Transportation, Albany, N.Y. 12232.



NOTE: See Figs. 2 and 7 for additional dimensions

FIGURE 1 Cross section of the test bridge.

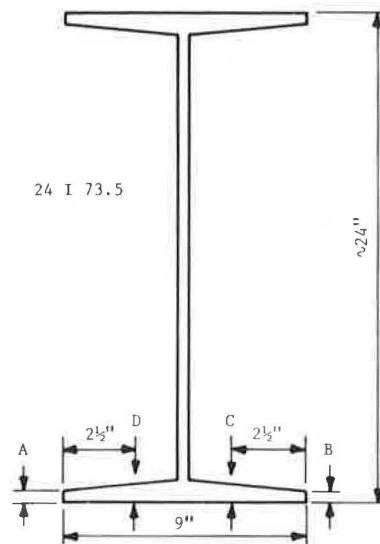
traffic on State Route 217 over North Creek in the town of Mellenville in Columbia County, New York. The bridge's cross section (Figure 1) consisted of nine 24-in.-deep beams spaced at 36 in. except in the north exterior bay, which was 58 3/4 in. The span center-to-center of supports, which are normal to the longitudinal axis of the bridge, was 39 ft.

Condition of the bridge was poor at the time of testing. The general condition rating recommendation for the bridge, based on a May 1982 inspection, was 3. A condition rating of 3 indicates serious deterioration on New York State's scale, which runs from 1 ("potentially hazardous") to 7 ("new condition"). The lower flanges of the steel beams, which had not been encased in concrete, showed section loss due to corrosion of up to 1/4 in. at midspan locations. An HS 20 inventory rating of 4 tons was calculated for the interior beams based on reduced section properties and no composite action for the deteriorated encasement concrete.

To provide a symmetrical section for testing, longitudinal saw cuts were made (Figure 1) to provide a six-beam cross section. Original contract plans were unavailable for the bridge and it was necessary to determine properties of the steel beams from measurement on the exposed lower flanges. These measurements are shown in Figure 2. Beams 2, 4, and 5 showed only minor evidence of rust and were taken as representative of the nominal flange dimensions. These dimensions, the 24-in. section depth, and the pre-1915 construction date identified the section as a 24-in. I-section weighing 73.5 lb/ft, manufactured by Bethlehem Steel (3,p.51). Nominal dimensions for this section are also shown in Figure 2.

The deck was constructed in two pours. The first encased the beams and covered the top flanges by 3 1/4 in. to give a structural deck with a minimum thickness of 5 1/4 in. at the crown of the arches between beams. A concrete wearing surface was placed over the structural deck, varying in thickness from 8 in. at the center to 6 1/2 in. along the curb lines. Cores taken from the deck always broke into two pieces at the cold joint between the two pours. Twelve cores were taken, but only six tests could be performed. Three of these six specimens, because of their short length, were sawed and tested as 4- by 4-in. cubes. The other three, which ranged in height from 6.4 to 7.1 in. (5.65 in. in diameter), were tested as cylinders. All compression test values were factored to be representative of normal 6- by 12-in. cylinders. These tests yielded compressive strengths of 6,610 psi (average of two) for the structural deck and 6,140 psi (average of four) for the wearing surface. The strengths obtained varied considerably, ranging from 4,670 to 7,470 psi, with both extreme values from the wearing surface.

Tension test specimens were cut from the tension and compression flanges of each beam of the test



Beam	A	B	C	D
1	0.37	0.40	0.74	0.53
2	0.55	0.57	0.73	0.78
3	0.35	0.32	0.51	0.52
4	0.53	0.52	0.62	0.66
5	0.53	0.57	0.77	0.73
6	0.42	0.43	0.71	0.74
Nominal	0.51	0.51	0.74	0.74

FIGURE 2 Steel-beam cross section with dimensions.

bridge cross section. Average yield stress of these 12 specimens was 39.2 ksi, with a standard deviation of 3.5 ksi.

TEST PROCEDURE AND INSTRUMENTATION

Response of the bridge to truckloads was determined before destructive testing was performed. Instrumentation for the live-load tests consisted of strain gauges bonded to the tension flanges at midspan of each steel girder.

Instrumentation for the failure test was more elaborate consisting of strain, deflection, and beam-end-rotation measurements. Test loads were applied by jacking against two load-distribution beams, each restrained by four soil anchors. Details of the instrumentation and loading system are given elsewhere (4).

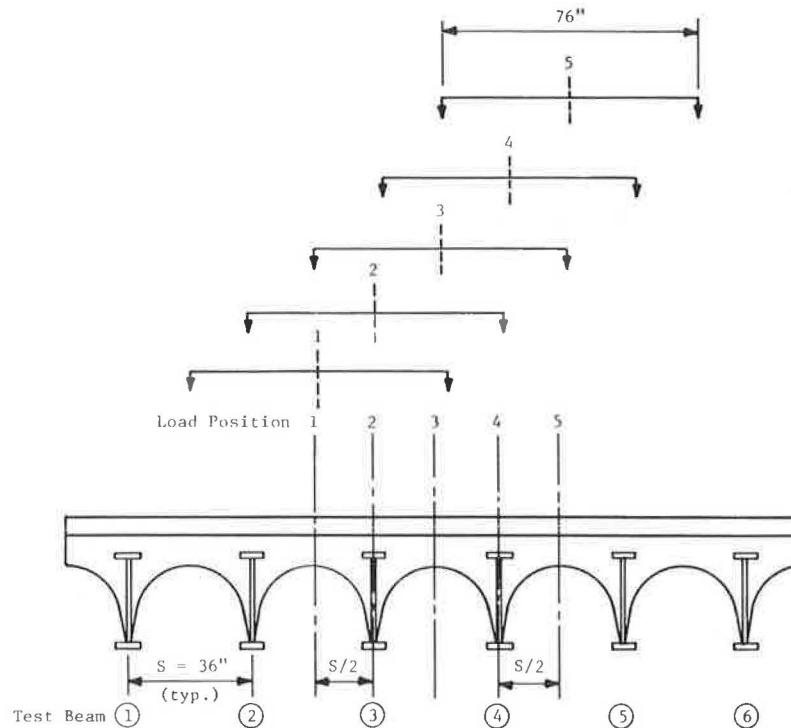


FIGURE 3 Live-load positions.

TEST DATA

Live Loads

Measured tension flange strains in microinches per inch for the load positions shown in Figure 3 are given in Table 1. These values are averages of at least three replicates of the loading. The truck in

TABLE 1 Tension Flange Strain for Live Loads

Beam	Strain ($\mu\text{in./in.}$) at Load Position				
	1	2	3	4	5
1	46	35	27	20	14
2	47	45	33	28	20
3	42	44	43	44	37
4	36	43	43	44	48
5	22	29	38	43	48
6	19	27	37	46	63
Total	212	223	221	225	230

these tests produced a theoretical simple-beam bending moment at the instrumented section of 339.3 kip-ft, in contrast to the AASHTO HS 20 moment of 432.1 kip-ft for this span. Because the measurements were made with the same test vehicle, total moment in the cross section is constant. The results show a trend toward increasing total strain as the load moves toward Beam 6. This trend may result from differences in individual beam section moduli or may be simply the result of random error.

Failure Tests

Average tension and compression flange strains for each beam and load increment are given in Table 2.

These are strains due to the test load only. Total strain is the sum of these values and dead-load strain. When yielding occurs, strains on opposite edges of a flange diverge, and averaging no longer provides a legitimate indication of true strain. It might be expected that this point could be predicted by simply subtracting estimated dead-load strain from yield strain to give test-load strain at the commencement of yielding. Following this procedure, expected test-load strain at first yield would be 1,060 $\mu\text{in./in.}$ (1,370 - 310). The existence of residual stresses, however, introduces a further complication into the analysis. Thus, bottom flange strain averages are reported up to maximum test-load strains of from 320 to 960 psi. Averages were not taken, and no value was reported when the range of the two strains exceeded 10 percent of the average. Individual measured strains for each gauge are given elsewhere (4).

Midspan deflection for each beam is given in Table 3. Deflection at high loads exceeded the range of the displacement measuring devices. A plot of deflection versus load in Figure 4 indicates a bilinear relationship, with the break at a load of about 150 kips. Deflection at failure could not be determined, but permanent set after the load was removed exceeded 6 in. The transverse pattern of deflections was irregular (Figure 5), but this pattern was maintained throughout the range of applied loads.

End rotations measured at the east and west ends of Beams 2 and 5 are shown in Table 4 and Figure 6. It should be noted that end rotations are quite small for loads less than 150 kips but increase rapidly from that point. Total relative displacement of the abutments with respect to the beams was about 1 in. at maximum load. For loads of less than 200 kips, readings indicate that the abutments had moved toward each other by less than 0.2 in.

At maximum load, a failure plane in the slab at the interface of the structural deck and the wearing surface was evident. Although analysis of the test data (as described in the next section) indicates that these slab elements act compositely at low and

TABLE 2 Average Flange Strain

Run	Line Load (kips)	Beam Load (kips)	Strain ($\mu\text{in./in.}$) at Beam											
			1		2		3		4		5		6	
			Top	Bottom	Top	Bottom	Top	Bottom	Top	Bottom	Top	Bottom	Top	Bottom
1	0	0.0	0	0	0	0	0	0	0	0	0	0	0	0
2	10	1.7	-1	15	-15	23	-4	22	-7	25	-7	23	-7	27
3	39	6.5	-33	97	-59	102	-35	120	-41	119	-44	104	-47	118
4	70	11.7	-71	221	-94	221	-75	427	-86	297	-85	241	-93	275
5	-2	-0.2	5	18	-3	9	4	216	1	46	2	45	1	51
6	68	11.3	-78	260	-106	252	-84	490	-96	338	-95	293	-97	327
7	104	17.3	-120	446	-147	399	-131	933	-144	521	-140	508	-145	559
8	13	2.2	-12	39	-19	42	-14	44	-20	48	-18	41	-15	41
9	26	4.3	-20	73	-32	74	-28	86	-35	97	-30	78	-26	83
10	39	6.5	-36	110	-52	112	-43	122	-47	132	-41	112	-40	122
11	52	8.7	-51	151	-69	156	-54	175	-63	185	-59	160	-55	173
12	65	10.8	-62	193	-81	197	-66	218	-76	236	-72	202	-70	222
13	78	13.0	-73	232	-94	234	-76	261	-86	280	-83	240	-80	268
14	91	15.2	-87	277	-109	276	-92	310	-109	336	-103	289	-105	315
15	104	17.3	-101	318	-125	317	-105	362	-120	384	-114	328	-115	366
16	114	19.0	-118	NA	-146	367	-123	NA	-139	440	-133	391	-134	425
17	130	21.7	-130	NA	-162	419	-139	NA	-152	504	-148	513	-153	520
18	143	23.8	-147	NA	-185	488	-167	NA	-182	NA	-176	727	-170	630
19	153	25.5	-168	NA	-211	545	-201	NA	-206	NA	-198	961	-196	722
20	163	27.2	-193	NA	-230	NA	-232	NA	-242	NA	-229	NA	-227	NA
21	179	29.8	-204	NA	-236	NA	-280	NA	-274	NA	-278	NA	-292	NA
22	195	32.5	-241	NA	-274	NA	-332	NA	-332	NA	-338	NA	-364	NA
23	202	33.7	-268	NA	-303	NA	-378	NA	-372	NA	-371	NA	-414	NA
24	218	36.3	-309	NA	-335	NA	-428	NA	-433	NA	-445	NA	-493	NA
25	231	38.5	-323	NA	-370	NA	-478	NA	-480	NA	-506	NA	-568	NA
26	244	40.7	-367	NA	-422	NA	-547	NA	-562	NA	-609	NA	-676	NA
27	254	42.3	-391	NA	-454	NA	-596	NA	-624	NA	-689	NA	-771	NA
28	267	44.5	-434	NA	-520	NA	-676	NA	-764	NA	-835	NA	NA	NA
29	280	46.7	NA	NA	-633	NA	-804	NA	NA	NA	NA	NA	NA	NA
30	296	49.3	NA	NA	-795	NA	-962	NA	NA	NA	NA	NA	NA	NA
31	299	49.8	NA	NA	NA	NA	NA	NA	NA	NA	NA	NA	NA	NA
32	299	49.8	NA	NA	NA	NA	NA	NA	NA	NA	NA	NA	NA	NA
33	20	3.3	NA	NA	NA	NA	NA	NA	NA	NA	NA	NA	NA	NA

Note: Divergence of two flange gauges unacceptably large; NA indicates no average taken.

intermediate load levels, it would be incorrect to include the wearing course in calculation of ultimate capacity.

DATA ANALYSIS

The primary objective of this study was to obtain data useful in developing a load-rating procedure.

Two types of behavior--composite action between the steel and concrete and moment restraint at the supports--would result in an enhancement in strength estimates of jack-arch bridges. Refinements in the estimates of live-load distribution would also be beneficial. The data analysis has been directed to quantifying these forms of behavior.

Effective Section

The effective section resisting load can be determined from the beam-flange strain data obtained during the failure test. The initial approach to defining the effective section assumed full composite behavior and determined an effective modular ratio based on the cross section assumed and the measured tension and compression flange strains. This approach was abandoned when it became clear that, even with a 5-in. deck thickness, comparisons of the analytical and experimental neutral axis locations were inconsistent, regardless of the value assumed for the modular ratio. An approach was required that used the physical and geometric properties of the section tested. The process used conceptualizes the total bending moment carried as the sum of the moments resisted by the steel beam and slab individually, plus a couple formed by the equal and opposite internal thrusts acting at the centroids of these elements. Figure 7 shows these forces and invariant slab dimensions. The arch radius changed 4.5 in. below the crown, and concrete below this level was ignored. In addition to assuming a value for the elastic modulus of the concrete ($n = 8$), it is assumed that curvature of the beam and slab are equal and that the beam thrust calculated from the measured strains is resisted by an equal but opposite thrust in the slab as required for equilibrium. This latter as-

TABLE 3 Deflection

Line Load (kips)	Midspan Deflection (in.) at Beam					
	1	2	3	4	5	6
10	0.015	0.018	0.018	0.016	0.017	0.015
39	0.098	0.106	0.110	0.107	0.115	0.062
70	0.212	0.223	0.228	0.220	0.237	0.145
0	0.002	0.007	0.013	0.015	0.007	0.033
68	0.235	0.246	0.250	0.242	0.263	0.186
104	0.367	0.384	0.392	0.378	0.409	0.302
13	0.040	0.030	0.040	0.040	0.050	0.020
26	0.070	0.070	0.080	0.080	0.090	0.050
39	0.110	0.100	0.110	0.120	0.130	0.100
52	0.160	0.150	0.160	0.150	0.180	0.120
65	0.200	0.190	0.210	0.210	0.230	0.140
78	0.240	0.230	0.250	0.250	0.280	0.200
91	0.280	0.270	0.300	0.300	0.330	0.220
104	0.330	0.310	0.340	0.340	0.380	0.260
114	0.380	0.360	0.400	0.400	0.440	0.320
130	0.450	0.420	0.460	0.460	0.500	0.350
143	0.530	0.500	0.550	0.540	0.590	0.420
153	0.610	0.570	0.630	0.620	0.670	0.420
163	0.710	0.660	0.730	0.720	0.770	0.540
179	0.830	0.780	0.880	0.850	0.910	0.620
195	0.960	0.900	1.020	0.980	1.060	0.730
202	1.110	1.030	1.170	1.120	1.210	0.850
218	1.280	1.160	1.330	1.270	1.370	0.960
231	1.460	1.280	1.510	1.400	1.530	1.130
244	1.670	1.370	1.690	1.490	1.680	1.370

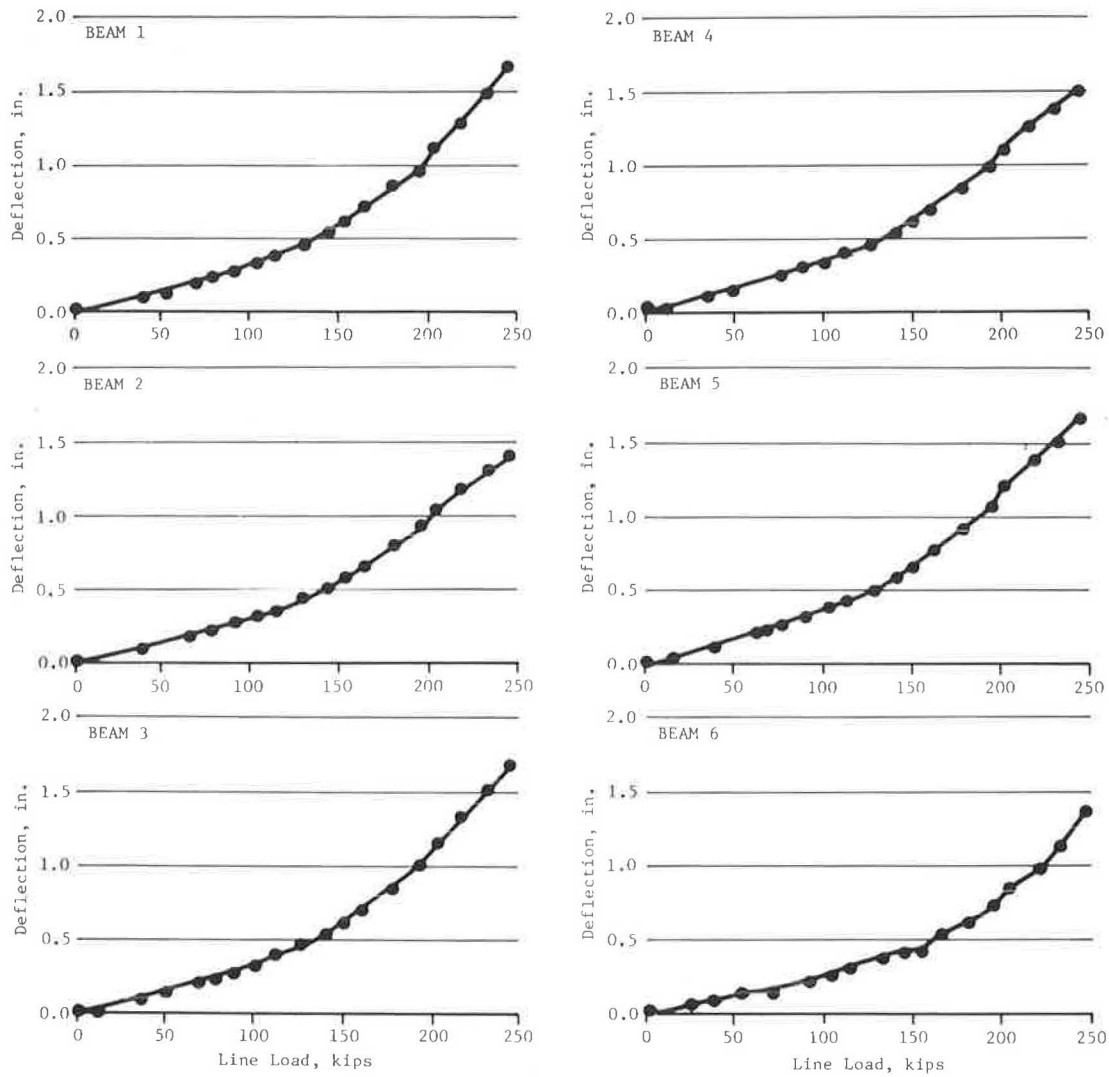


FIGURE 4 Midspan deflections.

sumption is equivalent to assuming that the relative measured displacements of the beams with respect to the abutments did not result in an induced axial beam force. In contrast to ordinary design practice, some tension (for this structure up to 500 psi) has been permitted in the concrete. The appropriate relationships are developed elsewhere (4). From this analysis an effective moment of inertia and the total resist-

TABLE 4 End Rotation

Line Load (kips)	Rotation (radians x 10 ³)			
	2E	2W	5E	5W
13	0.000	-0.050	-0.050	-0.050
26	0.050	-0.050	-0.100	0.050
39	0.250	-0.100	-0.050	0.250
52	0.500	-0.050	-0.100	0.550
65	0.750	0.150	-0.050	0.750
78	1.000	0.500	-0.250	1.050
91	1.250	0.650	-0.300	1.300
104	1.600	0.900	0.650	1.550
114	1.750	1.150	0.550	1.950
130	2.250	1.450	0.450	2.350
143	2.550	1.800	0.250	2.950
153	3.250	2.100	1.500	3.350
163	3.750	2.550	1.300	4.050
179	4.450	3.500	1.050	4.850
195	5.450	4.050	2.500	5.750
202	6.500	4.750	2.200	6.750
218	7.700	5.600	3.750	7.950
231	9.050	6.550	4.650	9.150
244	10.650	8.250	5.150	10.750
254	12.050	9.150	6.050	NA
267	14.450	12.900	7.650	14.250
280	18.950	16.350	10.000	18.550
296	24.050	21.900	13.250	23.150
299	30.450	26.350	26.050	29.650
299	31.850	24.200	39.400	43.450

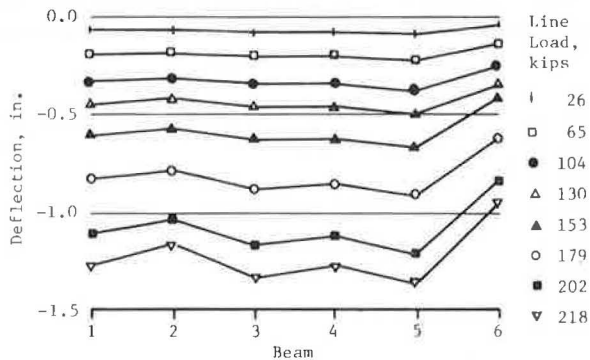


FIGURE 5 Transverse deflection pattern.

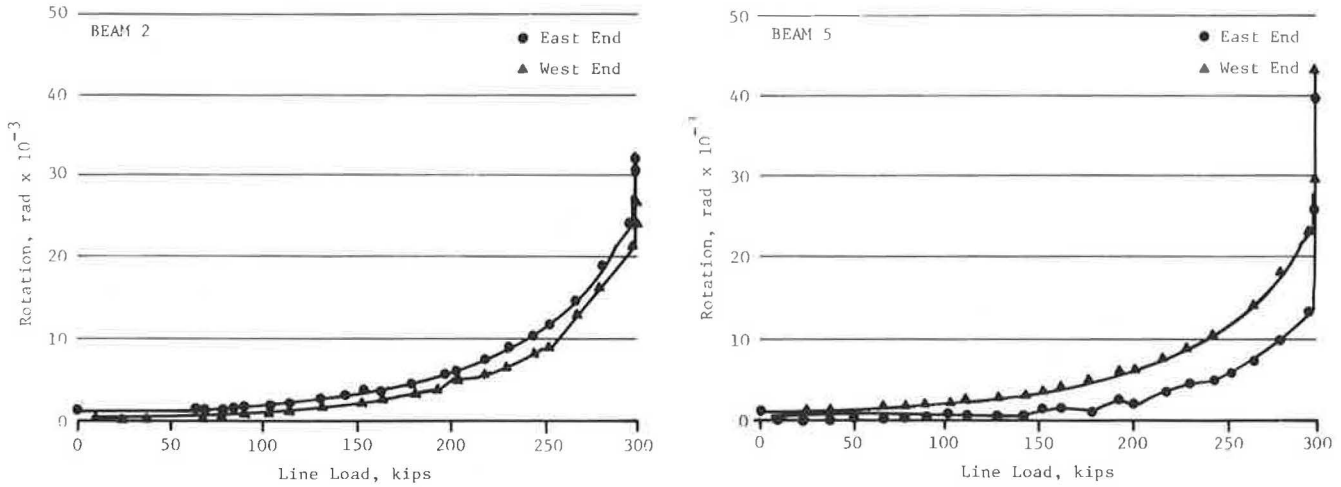


FIGURE 6 End rotation related to line load.

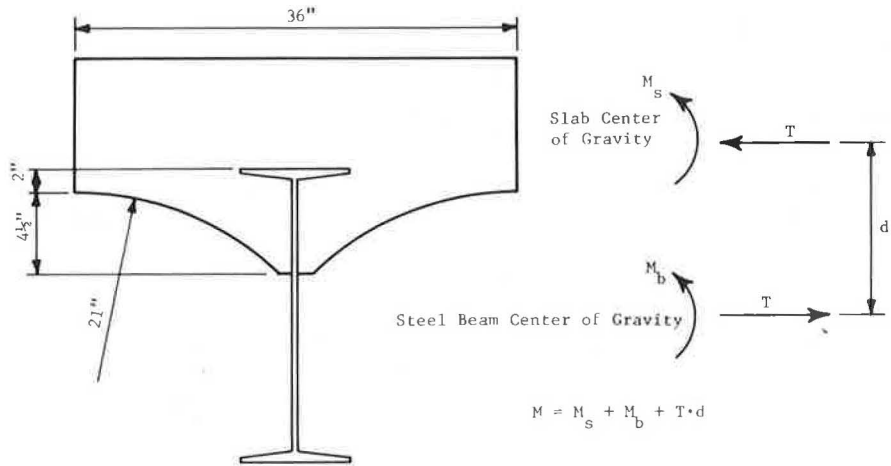


FIGURE 7 Effective section.

ing moment at the measured strain level are obtained. This analysis is, of course, only valid for elastic strains.

Data from the first two loadings (Runs 1 through 7) gave erratic results that are not believed to be representative of true structural behavior and thus were excluded from the reported results:

Beam Properties				
Beam	Slab t (in.)	Flange t (in.)	I _{eff} (in. ⁴)	α
1	11.750	0.62	4,800	0.545
2	12.375	0.74	5,010	0.439
3	13.375	0.50	4,800	0.466
4	13.250	0.63	5,180	0.475
5	13.250	0.74	5,510	0.477
6	12.500	0.71	5,350	0.540

These values are based on data from the final loading of the bridge up to the load providing consistent strains on the edges of the tension flange (104 kips). The effective inertia can be expressed as

$$I_{eff} = \alpha I_c + (1 - \alpha) I_{nc}$$

where the subscripts eff, c, and nc stand for effective, composite, and noncomposite, respectively.

The results of this analysis can also be used to determine the degree of end restraint for this bridge. This is done by comparing static midspan bending moment with estimated bending moment from the strain analysis. This comparison is shown in Figure 8 in which it can be seen that the experimental moments are linear with increasing load and are always less than the static values. Based on this result, the end moment is estimated to be 30 percent of the fixed-end value during the elastic portion of the failure test.

Live Loads

Tension flange strains measured during live-load testing were converted to bending moment using the effective section properties determined from the strain analysis just described. These experimental values were compared with the results from a planar-grid analysis. For this analysis the bridge was assumed to be fixed ended despite the findings from the failure test. It is believed that end moment restraint was partly destroyed during the first increments of the failure loads. It should be noted that the midspan bending moment (assuming a simply supported beam) was only 339 kip-ft--a value exceeded between the first and second failure load increments. In addition, it has been previously noted that the

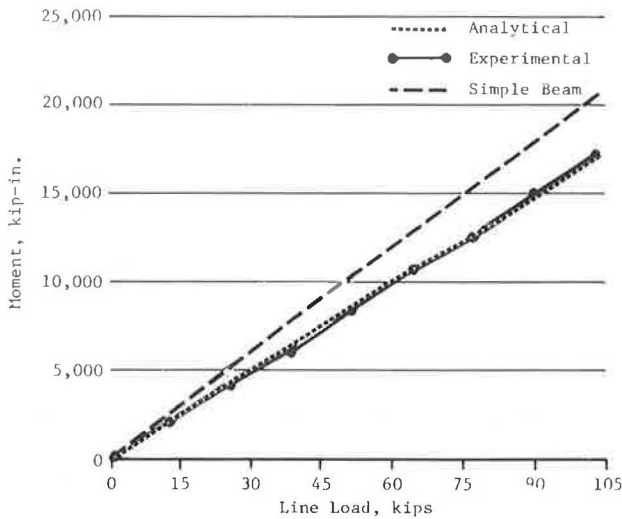


FIGURE 8 Analytical and experimental moments.

structure's behavior under the first increments of failure load was erratic, which indicated a change in behavior.

Figure 9 shows experimental and analytical midspan bending moments for each load position. In general, the analytical values overestimate the experimental moments, and the differences are more prominent on the fascia beams. The total experimental moment for each load position (Figure 10), which theoretically should be constant, varies with load position. Although this variation is not large, it is systematic: the total moment increases as the load position moves across the width of the structure.

Live-load distribution coefficients can be obtained by dividing the beam moments by total moment at the cross section for a particular load position. This structure was so narrow, however, that meaningful values could not be calculated because only one vehicle could be placed at a time.

Failure Loads

End rotation and centerline deflection data are shown in Figures 11 and 12, with calculated values based on the elastic properties determined from the strain results. Values are shown for a simple span and a span restrained with end moments equal to 30 percent of the fixed-end values. For both deformations the restrained solution compares well with the experimental values for lower loads, which supports the findings for effective inertia and end restraint from the strain analysis. Both deformations increase rapidly at a line load of about 150 kips, indicating the initiation of inelastic behavior.

Elastic predictions of beam deflections do not compare well with measured values on an individual basis. Figure 13 shows this comparison for two levels of line load. In general, the analysis overestimates the measured values. Transverse variations in experimental deflection are not reflected in the analytical results, which suggests that the observed variation is a consequence of loss of transverse rather than longitudinal stiffness. Data are insufficient on the possible degradation of concrete properties with location in the structure to make a specific estimate of this effect. It should be noted that transverse variations are small with respect to average values.

Deflection comparisons could be improved by increasing the beam stiffnesses, the amount of end

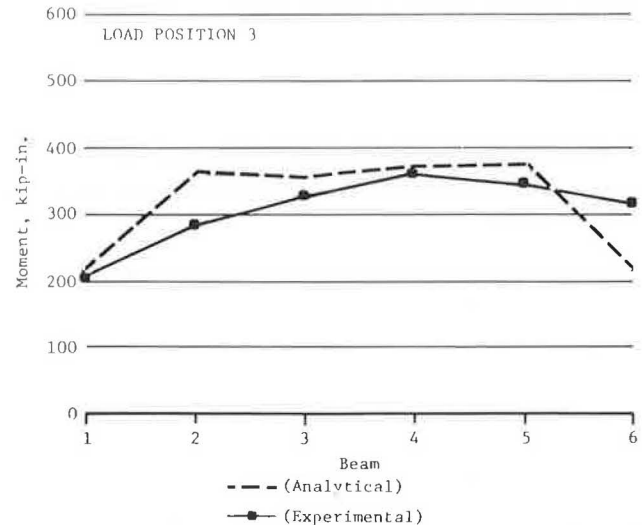
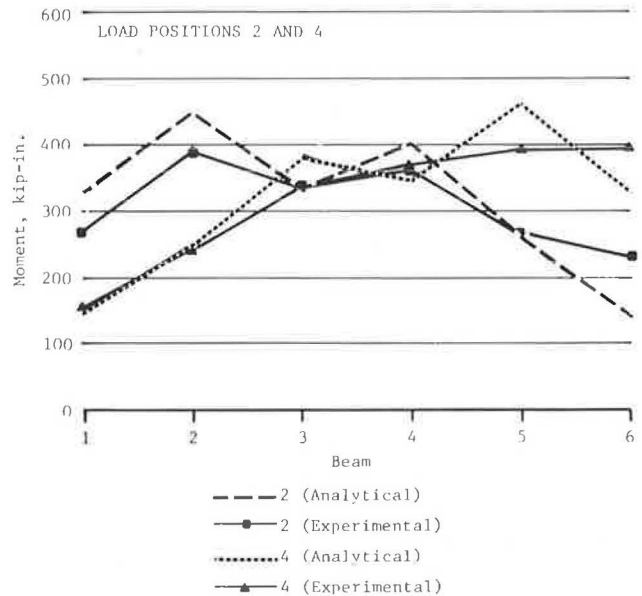
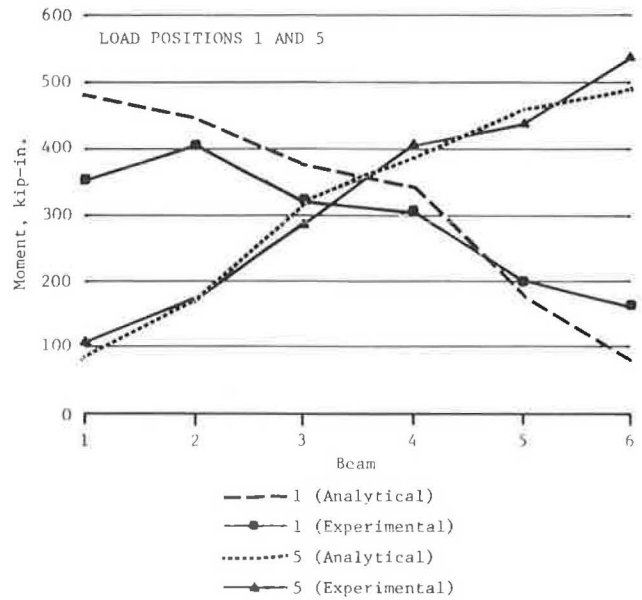


FIGURE 9 Analytical and experimental live-load moments.

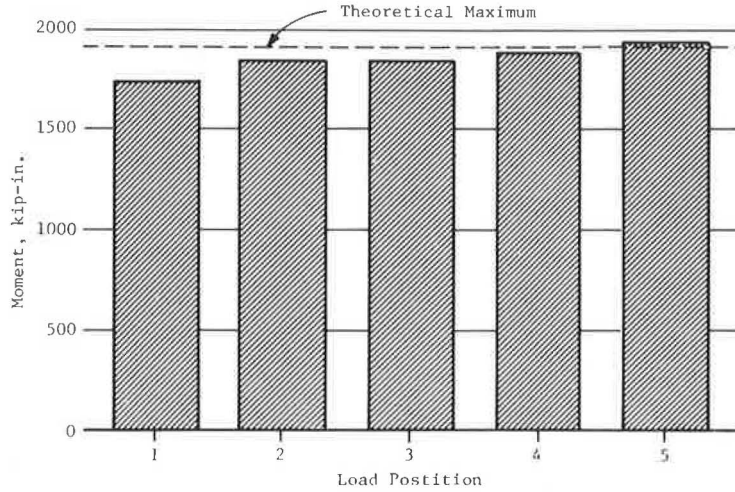


FIGURE 10 Total live-load moments.

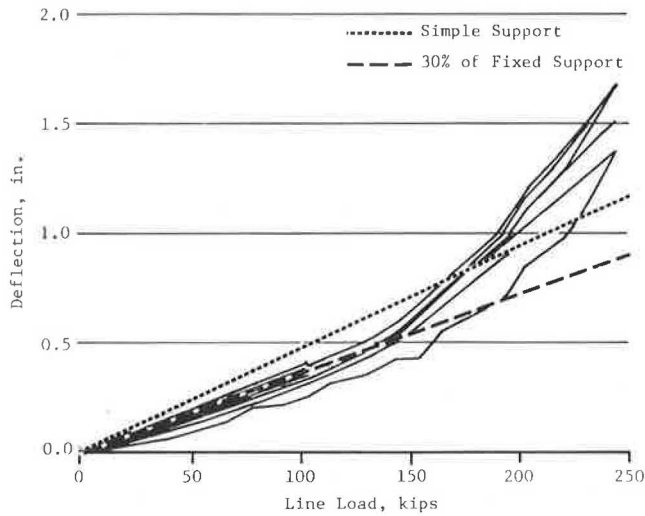


FIGURE 11 Line load related to deflection.

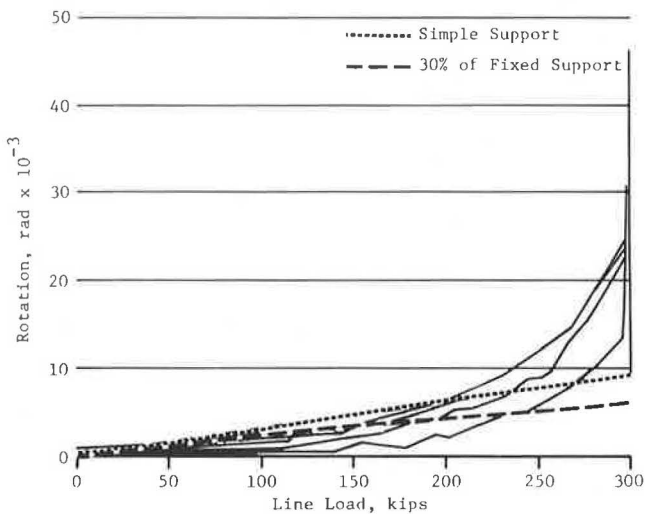


FIGURE 12 Line load related to end rotation.

restraint, or both, but such adjustments are not supported by the strain data. The analytical-to-experimental bending moment comparisons (Figure 14) also show greater transverse variation in the experimental results than are predicted analytically, although these variations are not as pronounced as for deflection. Because the total experimental and analytical moments compare satisfactorily (Figure 8) it is clear that changes in the magnitude of end restraint are unwarranted, because this would have a direct effect on the moment comparisons. Refinements in section properties would have only a minor influence on the strain-to-moment conversion (increasing the inertia would result in increased moment) but would tend to reduce transverse variation in the analytical results. More important, increases in section inertia can only be achieved by decreasing the assumed value for the modular ratio, and the

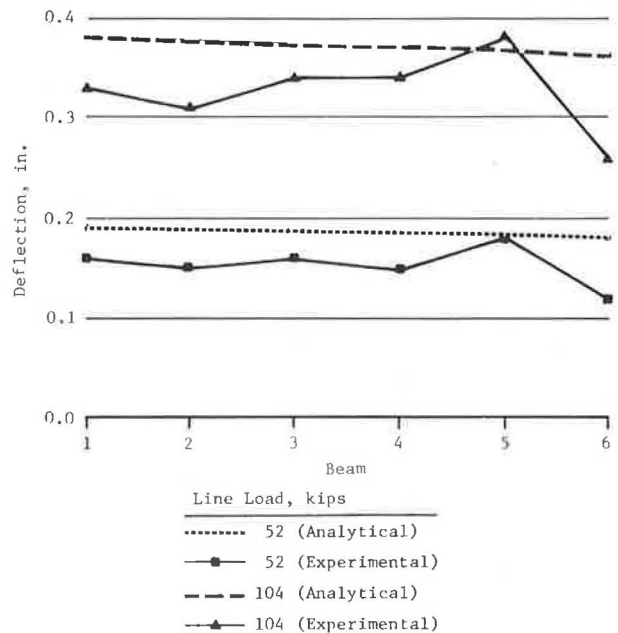


FIGURE 13 Midspan displacement.

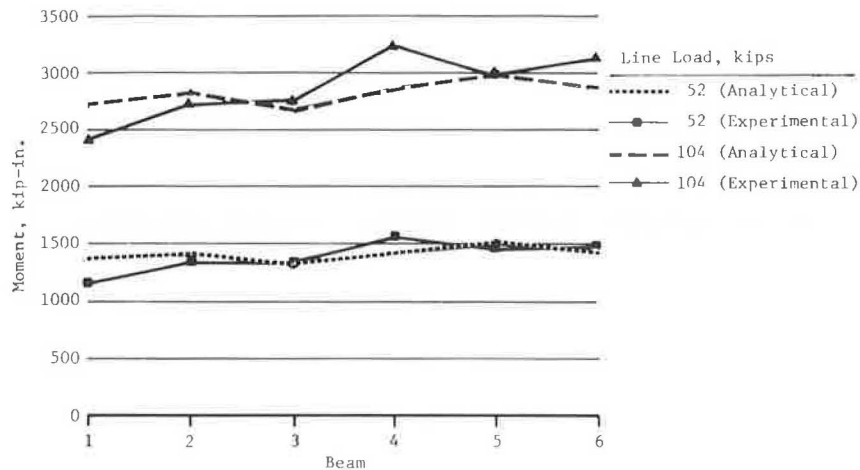


FIGURE 14 Midspan bending moment.

value assumed ($n = 8$) is judged to be the smallest reasonable value for concrete in this condition. Overall comparison of deflection and end rotation data with the analytical estimates supports the validity of the data analysis procedures used for converting measured strain to bending moment and estimating the effective moment of inertia.

Postelastic behavior of this structure has not been investigated in detail because of the lack of full strain data. Delamination of the deck at the interface between the structural and wearing-surface concrete was visible at the maximum load. Because of this delamination the wearing surface should be ignored when estimating the failure load. It should be noted that the maximum load applied to this structure was twice the elastic limit load of 150 kips.

APPLICATION TO LOAD RATING

The procedures used in this study are theoretically correct and produce results that are consistent with observed behavior. Nevertheless, these techniques bear little resemblance to procedures used in conventional design or load-rating practice. It would be unrealistic to expect that a procedure requiring calculation of an effective partly composite section would be received with enthusiasm by engineers working in a production environment. In addition, some criteria would have to be established for maximum allowable concrete tension to permit determination of the effective section depth.

A conventional analysis would compute a tension flange section modulus based on a fully composite section, with tension concrete ignored. For this structure the tension flange strains based on this section and the experimentally determined beam moments overestimate the measured strain by only 3 percent. Despite this good comparison, it should be realized that stiffness of the composite section is at least 25 percent greater than the effective section determined from the measured strains. Nevertheless, estimates of induced stress based on properties of the composite section produce reliable estimates of the true values. This result was also found for the Indian Lake structure tested earlier (2).

The test results show that end restraint equivalent to 30 percent of the fixed-end amount was active for loads of less than 150 kips (equivalent design load with impact = 2.7 HS 20 trucks). For the Indian Lake bridge it was found that full fixity was present for loads less than the service load. Thus

estimates of structural capacity that ignore these effects will be conservative. Generalization of the degree of composite action or the magnitude of end fixity is not possible now, and it is not likely that a technically defensible generalization could ever be produced regardless of the number of bridge tests performed.

Load ratings for the Mellenville bridge have been calculated for the H 15, the HS 20, and the three typical legal load types specified by AASHTO (5, p.50). Those ratings are based on the properties of Beam 3--the most deteriorated beam in the cross section. No end fixity was assumed in these computations. Load-rating factors (load-factor method using properties of Beam 3) for each of these loadings were as follows:

Rating Factors

Vehicle	Inventory	Operating	Service-ability
H 15	1.55	2.58	3.83
HS 20	0.92	1.53	2.27
Type 3	1.26	2.11	3.12
Type 3S2	1.26	2.11	3.12
Type 3-3	1.45	2.42	3.58

Multiplying the rating factor times the rating vehicle weight gives the structure's load capacity for the specific load type. Note that although the inventory rating factor for the HS 20 load is slightly less than unity, posting of the structure would probably not be necessary in view of the ample operating and serviceability ratings.

CONCLUSIONS

Based on the results of failure tests on two jack-arch bridges, the following conclusions can be drawn:

1. Assuming full composite behavior results in conservative estimates of structural behavior.
2. Significant end fixity exists under service load. The effect of this moment restraint is to reduce the midspan bending moment estimated for a simply supported beam.
3. It is not now possible to generalize the prediction of the degree of end fixity to other structures. The source of end fixity for the test structure has not been determined.
4. The test structure remained elastic for loads producing bending moments equivalent to 2.7 HS 20 design vehicles (including impact).

5. A load rating based on the most deteriorated member in the cross section indicates that this structure could have been used safely without posting.

ACKNOWLEDGMENTS

Robert J. Kissane, Civil Engineer II (Physical Research), assisted in planning this test and was responsible for supervising the field work. Wilfred J. Deschamps, Everett W. Dillon, Michael D. Gray, Joel W. Miller, Samuel P. Morris, and Frank P. Pezze installed instrumentation and assisted in monitoring the structure's response to load. Brian Johnson, Student Intern, aided in the data reduction and structural analysis. The research reported was conducted in cooperation with the Federal Highway Administration, U.S. Department of Transportation.

REFERENCES

1. Load Test: Route 30A over Canal. BIN 4021420. Memorandum of May 19, 1983, from W.C. Burnett,

Engineering Research and Development Bureau, to E.V. Hourigan, Structures Design and Construction Division, New York State Department of Transportation, Albany.

2. D.B. Beal. Failure Tests of a Jack Arch Bridge. Research Report 110. Engineering Research and Development Bureau, New York State Department of Transportation, Albany, Feb. 1984.
3. Iron and Steel Beams: 1873 to 1952. American Institute of Steel Construction, New York, N.Y. 1953.
4. D.B. Beal. Load Capacity of a Jack-Arch Bridge. Research Report 129. Engineering Research and Development Bureau, New York State Department of Transportation, Albany, Dec. 1985.
5. Manual for Maintenance Inspection of Bridges 1983. AASHTO, Washington, D.C., 1983.

Publication of this paper sponsored by Committee on Steel Bridges and Committee on Dynamics and Field Testing of Bridges.

Stress State in Coupling Joints of Posttensioned Concrete Bridges

FRIEDER SEIBLE, YURY KROPP, and CHRISTOPHER T. LATHAM

ABSTRACT

Posttensioned continuous concrete bridges have shown unexpected crack patterns in the vicinity of the theoretical inflection point. In particular, box-girder-type cross sections with coupled posttensioning tendons in construction joints at the points of inflection were found to exhibit an increase in the number and width of cracks in the bottom soffit and webs of the bridge superstructure in the coupling joint vicinity. Intensive investigations attribute these cracks to highly nonlinear stress distributions with significant tensile stress content over the depth of the bridge structure due to nonuniform temperature gradients, concentrated anchorage forces, and increased prestress losses. It is shown that a major factor contributing to the tensile stress potential of the nonlinear stress distribution is a significantly reduced compressive stress state caused by the segmental construction and posttensioning sequence. The uniform state of prestress in a concentrically posttensioned concrete member shows reductions of more than half of the initial prestress in the construction and coupling joint vicinity. Combinations of this reduced compression stress field with prestress losses in the couplers or temperature gradients in the bridge deck show theoretical crack development and crack orientation similar to crack patterns encountered in coupling joint vicinities of posttensioned box-girder bridges.

Large cracks and, in one case, even ruptured tendons found during routine bridge inspections in the Federal Republic of Germany in the vicinity of coupling joints of posttensioned continuous bridge structures (1,2) have led to a series of investigations of the behavior of coupling joints.

Coupling joints of posttensioning tendons are common in segmental bridge construction, particularly in construction methods developed and used frequently in Europe, such as incremental launching and span-by-span erection with traveling self-supporting falsework. It was this latter group of bridge structures that showed crack concentrations in the coupling joint vicinity. In the span-by-span construction method (Figure 1) construction joints with couplers for the tendons are generally placed close to the theoretical point of inflection for dead load plus prestressing to minimize reinforcement requirements in the construction joint. Investigations of crack development in this construction joint vicinity, summarized in Seible (1), showed that initial crack development is caused by several factors such as highly nonlinear stress states due to concentrated anchorage forces, unaccounted differences in the actual dead load distribution, temperature gradients, and increased prestress losses in the tendon couplers. When the section has cracked, the reduction in stiffness, and with it higher cyclic stress levels, must be evaluated carefully because changes in tendon geometry due to the lower strength steel of the anchorage-coupler assembly are cause for stress concentrations and lower fatigue limits (1).

An intensive bridge inspection program by the West German Ministry of Transportation (3) of all bridges with coupling joints revealed the results summarized in Table 1. Two kinds of bridge cross sections are

generally used for bridge construction methods that involve coupling joints; namely, box-girders and T-beams with varying numbers of webs and bottom soffit arrangements. Table 1 gives the number of cracked bridge structures encountered, the crack width, and the cracked region for both types of cross section. It can be seen that box-girder sections were found to be more susceptible to cracks in the coupling joint vicinity than T-beam sections, with 30 and 45 percent of the inspected bridge structures showing no cracks, respectively. Cracks wider than one hundredth of an inch (>0.2 mm) were more frequently encountered in box-girder sections and, in particular, in the webs and bottom slab. One example of the encountered crack pattern (2) is shown in Figure 2.

The stress states that lead to these cracks, which are parallel and in close proximity to the coupling and construction joint, need to be investigated. It is the purpose of this paper to study in detail the inherent initial stress state of the coupling joint vicinity, due to the various construction and posttensioning stages, and subsequent combinations with possible stress states, due to prestress losses in the coupler or uniform temperature gradients. These stress states explain crack patterns encountered in the coupling joint vicinity and provide the information necessary to properly design these regions.

NONLINEAR STRESS STATES IN COUPLING JOINTS

Nonlinear stress distributions over the depth of a prestressed concrete member can have various causes that range from local force concentrations in the anchorage zones (4,5) to variable temperature gradients (6). A brief summary of these stresses encountered in the coupling joint region is given in this section. Used as an example is a thin-walled, concentrically prestressed concrete member (Figure 3) erected and posttensioned segmentally.

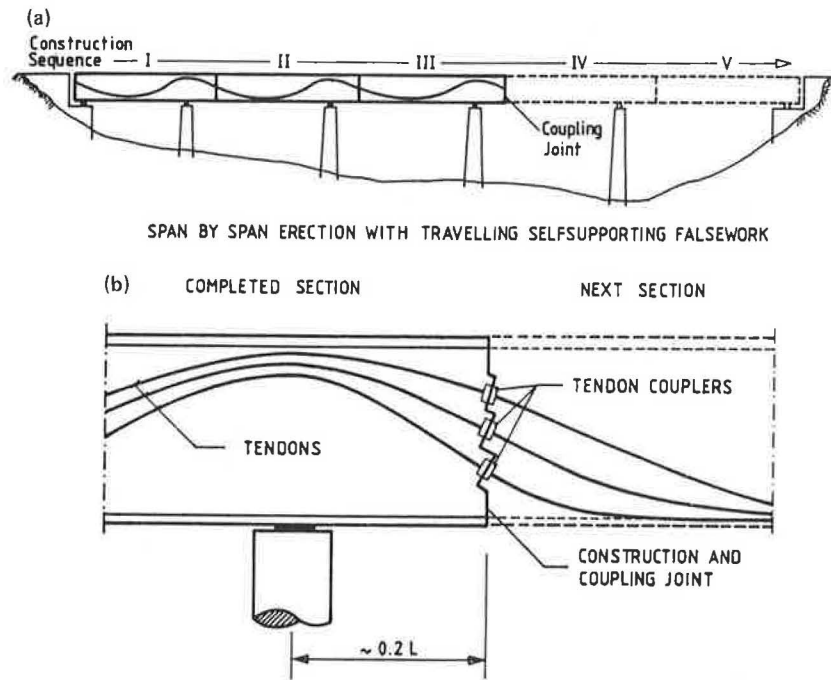


FIGURE 1 Coupling joint: (a) Possible geometry of bridge structure with coupling joints; (b) Coupling joint detail.

Load Conditions Under Investigation

Stress concentrations from tendon anchorages are first present when the initial construction segment is posttensioned and grouted before the formwork is advanced for the construction of the subsequent segment. The stress state is equivalent to the classic case of the infinite half-strip with a concentrated load on the short side (4). To show the accuracy of the chosen linear elastic plane stress model, the splitting stresses are compared with results from Iyengar (5) in Figure 4a normalized with respect to the uniform state of prestress (f_{p0}).

The deformations of the analytical model, which takes advantage of the symmetry in load and geometry along the longitudinal x-axis, are also shown qualitatively in Figures 4a and 4b for the posttensioning

of the initial and subsequent segment, denoted as Case 1 and Case 2, respectively.

Additional load cases considered in this study are the time-dependent prying forces, denoted as Case 3, that result from increased prestress losses in the tendon couplers as derived in detail elsewhere (1) and a uniform moment in the plane of the concrete member, denoted as Case 4, that could originate, for example, from the linear portion of a temperature gradient as discussed in Imbsen and Vandershaf (6) or from a shift in the location of the theoretical point of inflection due to self-weight inaccuracies (7) or time-dependent moment redistributions as discussed elsewhere (1). Although both additional load cases (Cases 3 and 4) are time dependent or environmentally dependent, or both, in nature, the actual load intensity factor

TABLE 1 Crack Development in Coupling Joint Vicinity (2)

Inspected Bridge Structures									
Cross Section	Total	without cracks	crack width [mm]	with cracks*					
				A	B	C	D	E	F
T-Beam	114 (100%)	51 (45%)	cracked region						
			< 0.2	5	34	2	3	1	0
			> 0.2	2	17	2	2	2	0
Box Girder	184 (100%)	54 (30%)	cracked region						
			< 0.2	5	29	32	5	37	6
			> 0.2	1	4	31	3	54	4

* more than one crack pattern can be encountered in one bridge structure

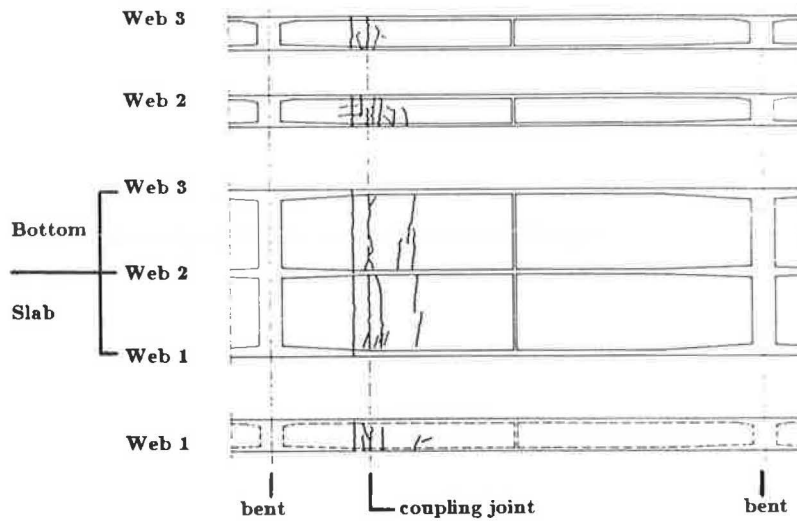


FIGURE 2 Example of crack development in a two-cell box-girder span with coupling joint.

varies for the resulting stress patterns. For Load Case 3, a maximum prying force of 1/2 the initial posttensioning force (P) was selected. This represents a theoretical upper limit for possible prying forces due to increased prestress losses in the tendon coupler as indicated elsewhere (1). The load intensity for Case 4 was chosen to produce maximum tensile extreme fiber stresses of the same magnitude

as the uniform prestress (f_{p0}). In the case of a real bridge structure, prestressing levels of $f_{p0} = 500$ psi (3.5 MN/m^2) are common in the vicinity of the inflection point, and detailed investigations of additional stresses due to temperature differentials, self-weight inaccuracies, and time-dependent force redistributions (8) have shown that actual stress levels of up to 500 psi

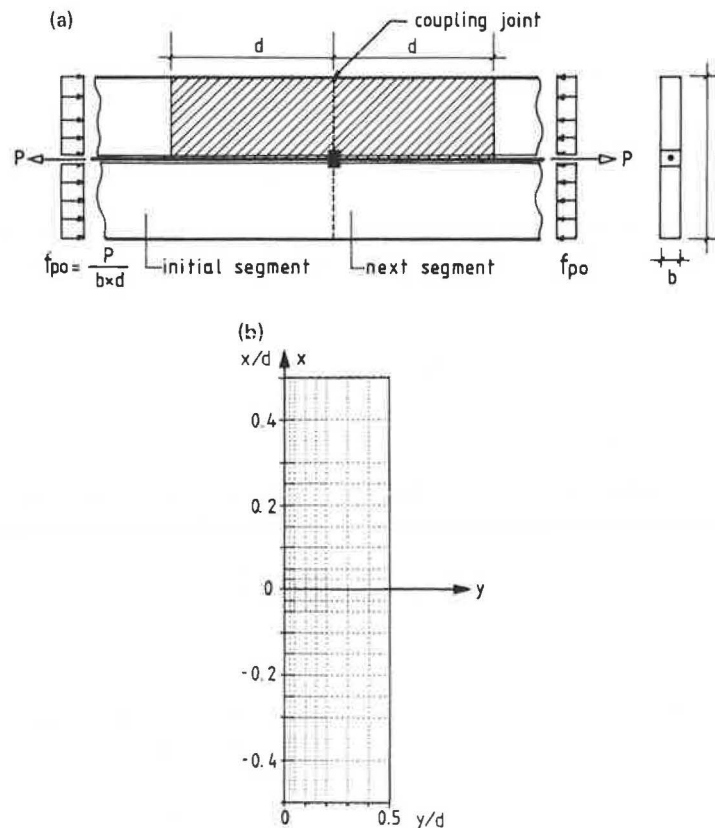


FIGURE 3 Investigated examples: (a) Thin-walled concrete member with single tendon; (b) Analytical model.

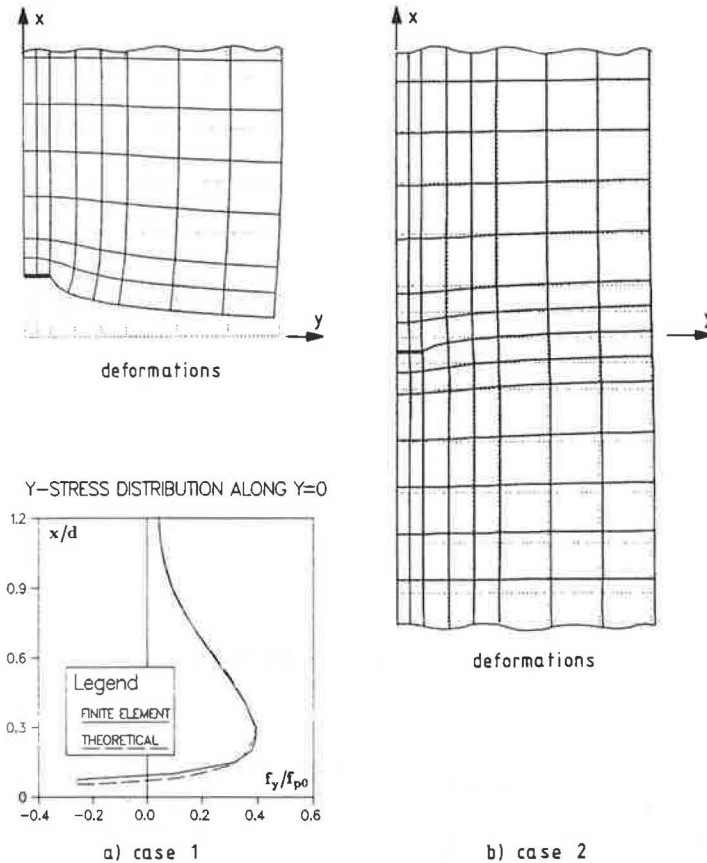


FIGURE 4 Individual construction and posttensioning stages: (a) Deformations and splitting stresses (Case 1); (b) Deformations (Case 2).

(3.5 MN/m^2) are not uncommon in investigated bridge structures. A summary of the individual load conditions is given in Figure 5.

Initial Individual Stress States

Contour plots, shown in Figure 6 for the longitudinal and Figure 7 for the transverse stresses in the coupling joint vicinity, are presented for all four individual load conditions (the construction and posttensioning of the initial segment, the construction and posttensioning of the subsequent segment, the prestress loss in the coupler, and the additional flexural stress state) denoted as Cases 1 through 4, respectively.

Although Case 1 shows the typical stress contour lines for the in-plane distribution of a concentrated edge load and Case 4 shows the trivial pattern for a uniform state of bending, the stress contour lines for Cases 2 and 3 are not so frequently encountered. Of particular interest is the longitudinal stress distribution for the posttensioning of the subsequent segment (Figure 6, Case 2) in which stress levels of $0.5 f_{p0}$ dominate along the construction joint. This can be attributed to half the posttensioning force for the subsequent segment at the coupling joint being absorbed by the initial segment in the form of a relief stress before direction is reversed in order to satisfy the self-equilibrating applied force state (Figure 6, Case 2).

COMBINATION OF STRESS STATES

The prototype bridge structure experiences a combination of the previously discussed individual

stress states. The construction and posttensioning sequence will leave inherent stress states, which deviate substantially from assumed theoretical linear stress distributions of the prestressed concrete structure, in the construction and coupling joint area. Any additional stresses that result from the use of the structure and time or environmentally dependent effects have to be combined with this inherent construction stress state. Because the entire member is subjected to substantial compressive stresses due to prestressing, and because initial cracking during construction can be assumed to be minimized by providing minimum reinforcement for shrinkage, it can be assumed that at low additional load levels the concrete will behave linear elastically, which justifies simple superposition of the previously discussed load and stress patterns.

Inherent Stress State After Segmental Construction

Following the actual construction process of casting, curing, posttensioning (Case 1) and grouting of the initial segment and subsequent casting, curing, and posttensioning (Case 2) of the next segment, the built-in stresses due to the construction sequence are obtained by combining the individual stresses from Cases 1 and 2. The combined stress contour lines (Cases 1 + 2) in the longitudinal and transverse directions are shown in Figure 8.

The longitudinal stress contour plot (x-stress) shows the uniform state of prestress of $f_x/f_{p0} = 1.0$ over most of the investigated area, and deviations occur only in the immediate vicinity ($x/d = \pm 0.4$) of the coupling joint. Large compressive stress con-

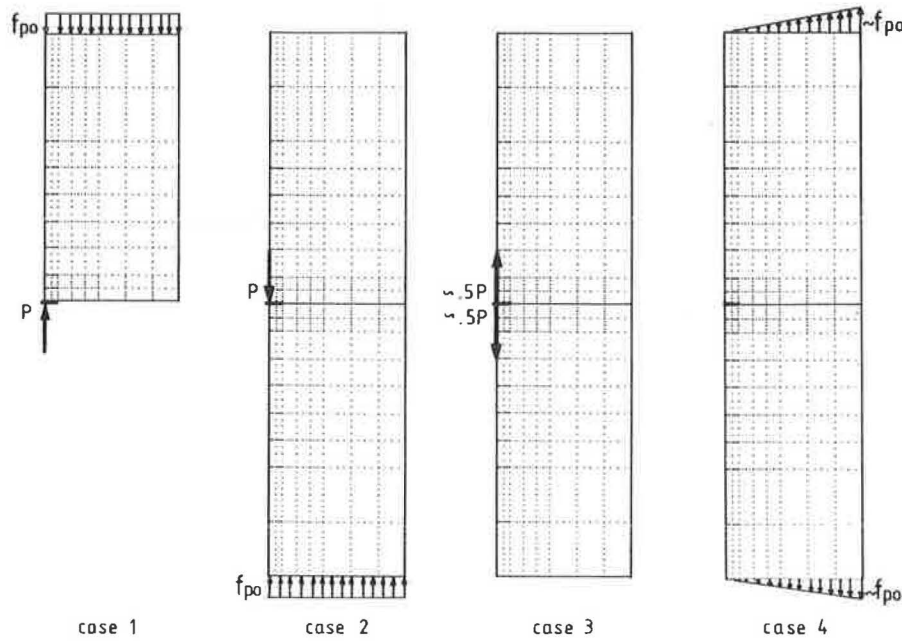


FIGURE 5 Individual load conditions.

centrations are found close to the tendon anchorage or coupler, and a reduced stress state of $f_x/f_{p0} = 0.5$ prevails over the remaining portion of the construction joint. Of particular interest is a zone at $x/d = 0.2$ above the construction joint where at the edge of the member a quite localized reduced stress state of $f_x/f_{p0} = 0.3$ is encountered. If the thin-walled, posttensioned concrete member were prestressed to a uniform 500 psi compressive stress level, Figure 8 indicates that at $x/d = 0.2$, $y/d = 0.5$, a compressive stress reserve of only 150 psi would be available immediately after the segmental construction of the member.

To emphasize the longitudinal stress variation in

the coupling joint vicinity, Figure 9 shows the x-stresses along selected transverse sections of the thin-walled member. Uniform compressive stress states a distance ($x/d = \pm 0.5$) away from the construction joint end, the nonlinear behavior in the direct vicinity of the coupling joint, and the minimum compressive stress reserve at $x/d = 0.2$, $y/d = 0.5$ can be clearly identified in Figure 9.

The contour plot of the combined transverse inherent construction stress state (Figure 8, y-stress) shows clearly the critical regions for splitting stresses both in the initial and the subsequent construction segment. It should be noted, however, that the critical splitting stresses in the initial seg-

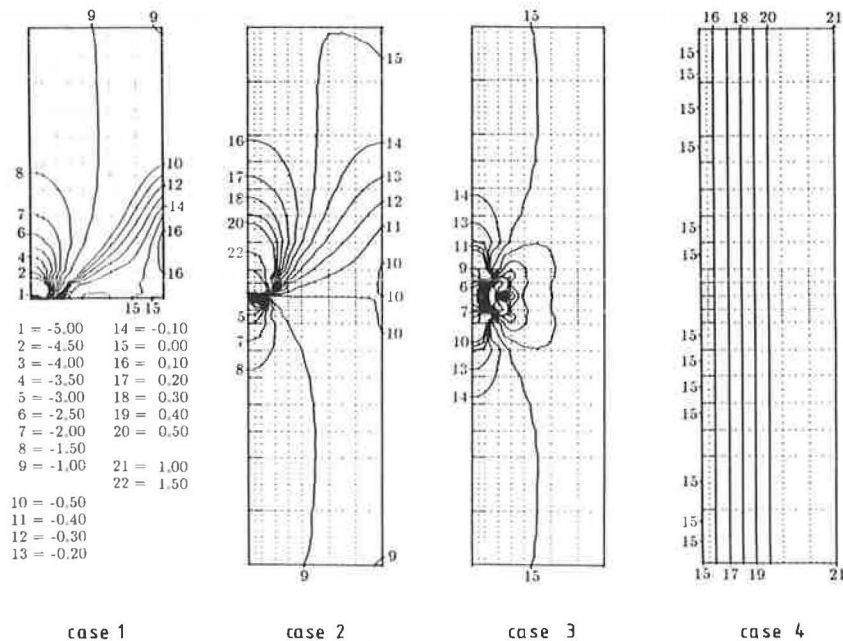


FIGURE 6 Individual longitudinal stress contour lines in coupling joint vicinity.

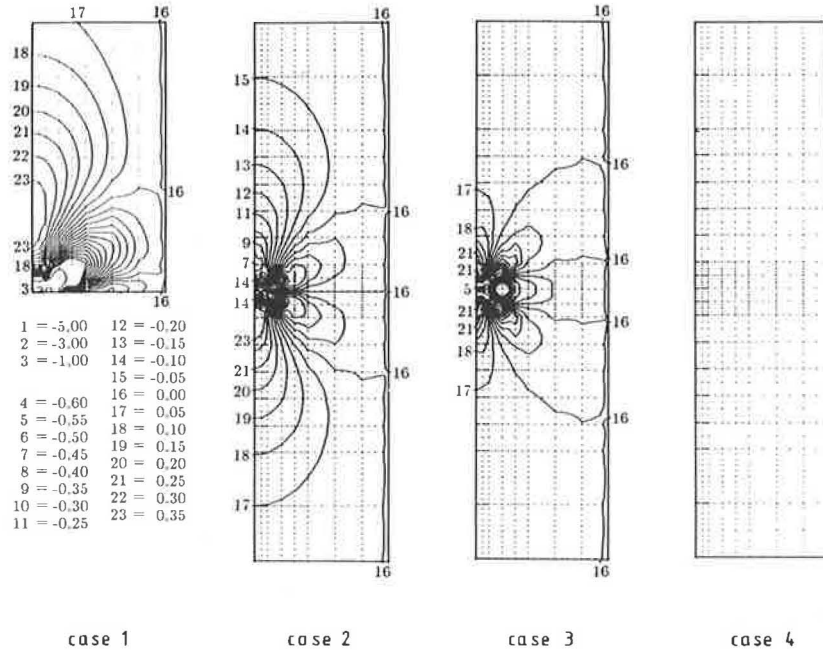


FIGURE 7 Individual transverse stress contour lines in coupling joint vicinity.

ment occur during the posttensioning operation of that segment and are already slightly reduced in Figure 8 by compressive y-stresses from Load Case 2.

Coupled Segments with Possible Losses and Temperature Effects

The longitudinal stress states in the direct coupling joint vicinity for combinations of the in-

herent construction stress (Cases 1 + 2) with additional stresses resulting from prestress losses in the coupler (Case 3), or additional moments due to temperature differences, or time-dependent shifts in the location of the point of inflection (Case 4) are plotted in Figure 10.

The nonlinear compressive stress reserves from the construction stages (Cases 1 + 2) can be easily exceeded by high local tensile stresses directly adjacent to the tendon coupler (Cases 1 + 2 + 3) and for a wider range at the edge of the member by additional flexural tensile stresses (Cases 1 + 2 + 4). Given these tension zones, the construction joint region can no longer be considered fully prestressed and, depending on the intensity of the superimposed loads, cracks can develop. These cracks in turn will significantly reduce the stiffness of the section in the coupling joint region and thus increase potentially dangerous (9) cyclic stress levels.

CRACK DEVELOPMENT

Crack development in the coupling joint region was traced analytically for the additional Load Cases 3 and 4 starting from the initial inherent construction stress state.

The assumed concrete crack limit was equal in magnitude but opposite in sign to the initial level of prestress f_{p0} (e.g., for the assumed 500-psi compressive state of prestress, the tensile crack limit was also set to 500 psi). The principal stresses were evaluated for each of the element integration points as a combination of the inherent construction stresses and superimposed stresses due to the incremental additional loads. Simplified element stiffness deterioration and crack orientation were determined by a weighted averaging procedure over all element integration points. The direction of crack propagation was found based on the error accumulation method outlined in Pfeiffer et al. (10). In this method the crack is assumed to advance to the one element, of all the elements that have exceeded the cracking stress level, that introduces the least amount of accumulated error as defined by

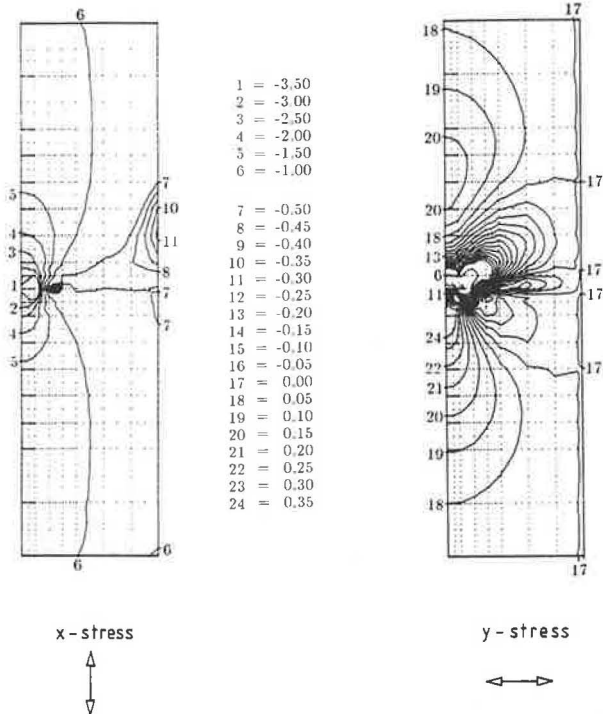


FIGURE 8 Inherent stress contour lines due to construction and posttensioning sequence (Case 1 and 2).

$$\theta_{error} = \sum_{i=1}^N (\theta_{L_i} - \theta_{PA_i}) \quad (1)$$

$$\theta_{PA_i} = 1/3 (\theta_{P_{i-1}} + \theta_{P_i} + \theta_{P_{i+1}}) \quad (2)$$

where

- i = counter of elements along the crack path,
- N = number of cracked elements,
- θ_{L_i} = angle of the line connecting the i th element with the i th-plus-one element,
- θ_{PA_i} = average minimum principal stress direction of three adjacent elements at the i th element, and

θ_{P_i} = direction of minimum principal stress of the i th element.

It should be noted that no stress redistribution of the initial inherent construction stresses was performed because only the crack origination and starting direction, not the complete failure, were investigated.

The two crack patterns for Cases 3 and 4 are shown in Figures 11a and 11b, respectively. Integers from 1 through 4 indicate the order in which elements exceeded the cracking stress limit at three or more integration points, and the weighted minimum principal stress directions for these elements are indicated. The final crack patterns, as determined by the pro-

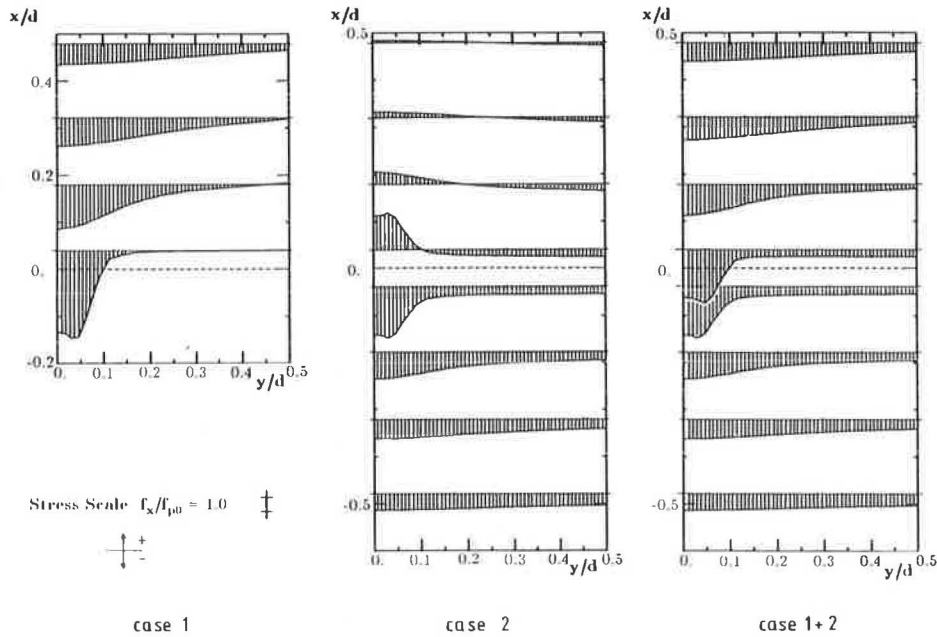


FIGURE 9 Longitudinal stress variations due to construction and posttensioning sequence.

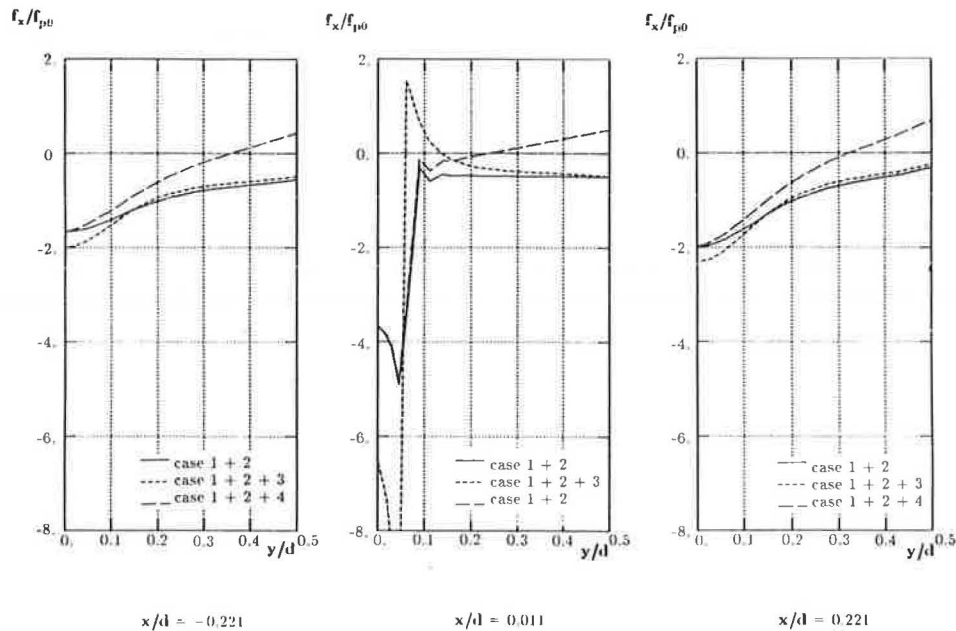


FIGURE 10 Possible longitudinal stress combinations in the construction joint vicinity.

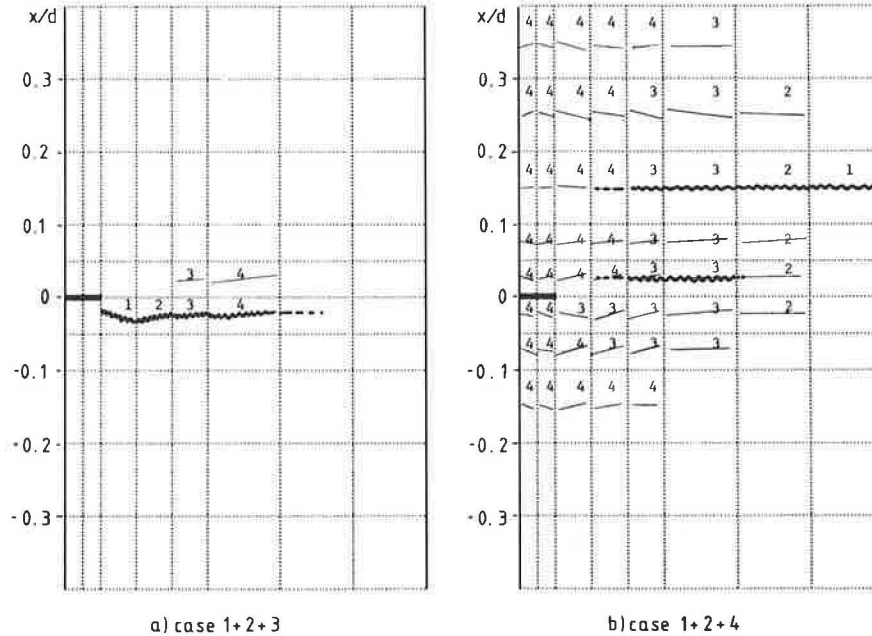


FIGURE 11 Theoretical crack initiation and development.

cedure outlined previously, are shown with bold lines through the cracked elements.

The simplified theoretical crack pattern developments shown in Figure 11 correspond to actual crack patterns encountered in coupling joints of prototype bridge structures with cracks parallel to the construction joint (see Figure 1) and are a direct result of the reduced compressive stress reserves and the nonlinear stress states in the coupling joint region.

CONCLUSIONS AND DESIGN RECOMMENDATIONS

To properly design or evaluate coupling joints of posttensioned concrete members and the direct construction joint vicinity, the following findings from the present investigation should be considered:

- Seemingly uniform compressive stress states of concentrically posttensioned concrete members can be reduced by 50 percent or more in the direct vicinity of the coupling joint as a result of sequential construction and prestressing.

- The same phenomenon applies to eccentrically posttensioned concrete members with one or more coupled tendons with deviations in the expected stress state from the initially assumed linear stress distribution.

- Nonlinear, even though mostly self-equilibrating, local stress states due to increased prestress losses in the coupler or the nonlinear portion of a temperature gradient can quickly exhaust reduced compressive stress capacity and reach cracking levels of the concrete.

- Additional linear stress distribution from linear temperature gradients of unaccounted moments due to creep redistributions or dead load inaccuracies, or both, can also exceed the compressive stress reserves and reduce the section from full to partial prestressing.

General design recommendations, given elsewhere (1), for coupling joints of posttensioned concrete bridges can be formulated more explicitly on the basis of the present findings:

- A simple plane stress investigation of the coupling joint region covering approximately $1d$ (d = depth of structure) from the construction joint can yield detailed information about the actual compressive stress reserves after segmental construction and posttensioning.

- Additional posttensioning should be provided in this region to reach the minimum design compressive stress levels. If detailed plane stress analysis is not performed, a reduced compressive stress state of $1/2 f_{p0}$ can be assumed in the coupling joint region.

- Where additional posttensioning of the coupling joint region is not feasible, sufficient regular reinforcement should be provided to cover potential tensile stress regions.

- This additional reinforcement through the construction joint should be provided in the form of closely spaced small-diameter bars to prevent single large cracks from opening and thus preserve structural stiffness and corrosion protection characteristics.

The consequences of cracks in the coupling joint vicinity must be explicitly investigated in the design process to determine cyclic stress levels with respect to reduced fatigue life for built-in anchorage-coupler-tendon assemblies.

REFERENCES

1. F. Seible. Coupling Joints of Prestressing Tendons in Continuous Post-Tensioned Concrete Bridges. In Transportation Research Record 1044, TRB, National Research Council, Washington, D.C., 1985, pp. 43-49.
2. Abteilung Strassenbau, der Bundesminister für Verkehr. Schäden an Brücken und anderen Ingenieurbauwerken. Verkehrsblattverlag Borgmann, Dortmund, Federal Republic of Germany, 1982, 462 pp.
3. Risse in Spannbetonbrücken, insbesondere in Koppelfugenbereichen, Ergebnisse der Risserfassung. B 3.2-3590, Standard vom 31.12.80. Bundesanstalt für Strassenwesen, Bonn, Federal Republic of Germany, June 1981.

4. Y. Guyon. Contraintes dans les pièces prismatiques soumises à des forces appliquées sur leur bases, au voisinage de ces bases. Publications, International Association for Bridges and Structural Engineering, Vol. II, 1951, pp. 165-226.
5. K.T. Sundara Raja Iyengar. Two-Dimensional Theories of Anchorage Zone Stresses in Post-Tensioned Prestressed Beams. Journal of the American Concrete Institute, Proceedings, Vol. 59, No. 10, 1962, pp. 1443-1465.
6. R.A. Imbsen and D.E. Vandershaf. Thermal Effects in Concrete Bridge Superstructures. In Transportation Research Record 950, TRB, National Research Council, Washington, D.C., Vol. 2, 1984, pp. 101-113.
7. G. Koenig and T. Zichner. Berücksichtigung der Temperaturdifferenz ΔT , der Streuung des Eigengewichts und der erhöhten Spannkraftverluste an Spanngliedkopplungen bei der Bemessung Massiver Brücken. Presented at the 8th International Conference of the Fédération Internationale de la Précontrainte, London, England, 1978.
8. W. Rossner. Konstruktion und Bewehrungsführung im Fugenbereich von Brücken bei Abschnittsweiser Herstellung. Beton- und Stahlbetonbau, No. 4, 1981, pp. 89-95.
9. A. Naaman. Prestressed Concrete Analysis and Design, Fundamentals. McGraw-Hill Book Co., New York, 1982, 670 pp.
10. P.A. Pfeiffer, A.H. Marchertas, and Z.P. Bazant. Blunt Crack Band Propagation in Finite Element Analysis for Concrete Structures. 7th International Conference on Structural Mechanics in Reactor Technology, Chicago, Ill., Vol. 5, No. 2, 1983, pp. 227-234.

Publication of this paper sponsored by Committee on General Structures.

Umbrella Loads for Bridge Design

HEINZ P. KORETZKY, KANTILAL R. PATEL,
RICHARD M. McCLURE, and DAVID A. VanHORN

ABSTRACT

Recent legislation allowing heavier vehicles on the highway system in Pennsylvania has been assessed for its impact on bridge design. The effect that permit traffic loads and heavy industrial or construction equipment have on bridges has also been assessed. Bending moments for various highway vehicles are illustrated graphically for easy visual comparison. As a result of these studies, Pennsylvania has adopted new umbrella loads for bridge design. The umbrella loads consist of two loads for design purposes (AASHTO HS 25 and 125 percent military) and one load for permit purposes (204,000-lb eight-axle superload).

Described in this paper is the engineering effort that led to replacement of the current AASHTO HS 20 design loading (1) for bridge designs in Pennsylvania with larger loads. Recent legislation allowing heavier vehicles on the state highway system has been assessed for its impact on the umbrella bridge design loads. Various engineering considerations are also outlined including the effect that permit traffic loads and heavy industrial equipment would have on the new design loads. The effect of bending moment

for various highway vehicles is illustrated graphically for easy visual comparison.

PREVIOUS DESIGN LOADINGS

Since 1941 Pennsylvania has used the most conservative AASHTO HS 20 bridge design loading exclusively in the design of every type of state-owned bridge for all classes of highways. This design loading is routinely used by many other states, but some states use the lower class HS 15 loading.

The hypothetical HS loadings are defined in the AASHTO Standard Specifications for Highway Bridges (1). The HS 20 loading is comprised of a single tractor and trailer weighing 36 tons, or an equivalent uniform load with a concentrated load (to simulate a truck train), whichever produces the maximum

H.P. Koretzky and K.R. Patel, Pennsylvania Department of Transportation, 1009 Transportation Safety Building, Harrisburg, Pa. 17120. R.M. McClure, Department of Civil Engineering, The Pennsylvania State University, University Park, Pa. 16802. D.A. VanHorn, Department of Civil Engineering, Lehigh University, Bethlehem, Pa. 18015.

stresses. For bridges carrying the Interstate highway system, an alternate military loading of two axles 4 ft apart with each axle weighing 24 kips is also considered.

In 1982 Pennsylvania bridge engineers changed the live load design criteria for all state-owned bridges to the governing AASHTO HS 20 or alternate military loading. This design loading was previously used only on the Federal-Aid system. Bridges on the local system can be designed using the minimum loadings stated in the AASHTO Standard Specifications for Highway Bridges (1).

For the last several years, AASHTO bridge engineers have debated the need to increase the AASHTO bridge design loads to fit actual conditions. Recently, several states have adopted the HS 25 design loading, and Ontario adopted the Ontario Code (2), and California adopted a new concept of "P-load" design (3).

have increased to a level that now demands the attention of bridge engineers.

In 1970 the Pennsylvania Legislature legalized a four-axle truck with a maximum gross weight of 72,000 lb. In 1980 the Legislature with Senate Bill 10 and House Bill 34 (4) further increased the maximum gross weight of the four-axle vehicle to 73,280 lb. The axle weight distribution of the four-axle truck was also revised from 18,000 lb each to 20,000 lb each for the three rear axles. In the 1980 legislation, 80,000-lb combinations were also made legal with weight distributions complying to the National Bridge Formula (5). The weight and size limits for trucks and combinations in Pennsylvania since 1980 are shown in Figure 1.









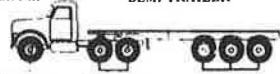


Legal loads vary somewhat from state to state in total weight, weight control on internal axles, and overall truck dimensions. However, in most states they are quite similar to those shown in Figure 1, which satisfy the requirements of the Federal Highway Administration for travel on the Interstate highway system. Federal-Aid Amendments of 1974 increased the permissible weight of vehicles operating on Interstates to 20,000 lb for a single axle, 34,000 lb for tandem axles, and 80,000 lb total gross weight (5). The National Bridge Formula (5) which requires longer axle spacing and lower axle loads for combination vehicles in the 72,000 to 80,000 lb range, was also

LEGAL LOADS

Legal loads are those maximum weights and dimensions of motor vehicles that can operate on highways without special approval from authorities. Legal vehicles are of different types that can be separated into trucks and combinations. Over the years, legal loads

M-946 (8-8-80)
Highway Services



TRUCKS V.C. 4943 (a) GROSS WEIGHT NOT EXCEEDING 73,280 LBS.	COMBINATION 3 AND 4 AXLES V.C. 4941(b) GROSS WEIGHT NOT EXCEEDING 73,280 LBS.	COMBINATION 5 OR MORE AXLES V.C. 4943(b) GROSS WEIGHT EXCEEDING 73,280 LBS.
 <p>TRUCK 2-0 See Note 22,400 LBS MAXIMUM GROSS WEIGHT 44,800 LBS.</p>	 <p>TRUCK-TRACTOR SEMI-TRAILER 2-1 See Note 22,400 LBS 22,400 LBS MAXIMUM GROSS WEIGHT 50,000 LBS. WITH SPECIAL HAULING PERMIT - 69,000 LBS.</p>	 <p>TRUCK-TRACTOR SEMI-TRAILER 2-3 See Note 20,000 LBS. TABLE B MAXIMUM GROSS WEIGHT LEGAL - 80,000 LBS. WITH SPECIAL HAULING PERMIT - 95,000 LBS.</p>
 <p>TRUCK 3-0 See Note 18,000 LBS EACH MAXIMUM GROSS WEIGHT 58,400 LBS.</p>	 <p>TRUCK-TRACTOR SEMI-TRAILER 2-2 See Note 22,400 LBS 18,000 LBS EACH MAXIMUM GROSS WEIGHT 60,000 LBS. WITH SPECIAL HAULING PERMIT - 80,000 LBS.</p>	 <p>TRUCK-TRACTOR SEMI-TRAILER 3-2 See Note TABLE B TABLE B MAXIMUM GROSS WEIGHT LEGAL - 80,000 LBS. WITH SPECIAL HAULING PERMIT - 123,000 LBS.</p>
 <p>TRUCK 4-0 See Note 18,000 LBS EACH MAXIMUM GROSS WEIGHT 73,280 LBS.</p>	 <p>TRUCK-TRACTOR SEMI-TRAILER 3-1 See Note 18,000 LBS EACH 22,400 LBS MAXIMUM GROSS WEIGHT 60,000 LBS. WITH SPECIAL HAULING PERMIT - 80,000 LBS.</p>	 <p>TRUCK-TRACTOR SEMI-TRAILER 3-3 See Note TABLE B TABLE B MAXIMUM GROSS WEIGHT LEGAL - 80,000 LBS. WITH SPECIAL HAULING PERMIT - 150,000 LBS.</p>
	 <p>TRUCK TRAILER 2-2T See Note TABLE A MAXIMUM GROSS WEIGHT 62,000 LBS.</p>	 <p>TRUCK-TRACTOR 3-4 See Note TABLE B TABLE B MAXIMUM GROSS WEIGHT LEGAL - 80,000 LBS. WITH SPECIAL HAULING PERMIT - 177,000 LBS.</p>

LEGAL SIZE RESTRICTIONS - INCLUDING LOAD

Total Length: (including bumpers)	40 ft.
Motor Vehicle	60 ft.
Combination	70 ft.
Any LOAD nondivisible as to length hauled on a combination of vehicles	
Total Width: (excluding mirrors and sunshades)	8 ft.
Nondivisible LOAD on highways having a roadway width of twenty feet or more, except for Interstate highways	
Total Height:	13 1/2 ft.

NOTE:
No motor vehicle or combination shall, when operated upon a highway, have a weight upon any one wheel in excess of 800 pounds for each nominal inch of width of tire on the wheel.

LOAD OVERHANG RESTRICTIONS

Maximum extension of load beyond extremities of vehicles, provided no legal size restrictions are exceeded:

Front	3 ft.
Rear	6 ft.
Left Side	None
Right Side	1 ft.

FIGURE 1 Weight and size limits for trucks and combinations in Pennsylvania.

TABLE A AXLE WEIGHT LIMIT WHEN GROSS WEIGHT DOES NOT EXCEED 73,280 POUNDS		
Maximum axle weights are as shown provided all other requirements are met as outlined in the Vehicle Code such as manufacturer's rated axle capacity, tire size, etc.		
If the Center-to-Center Distance Between the nearest Adjacent Axle is:	Maximum Axle Weight in Pounds Upon:	
	One of Two Adjacent Axles	Other of Two Adjacent Axles
Under 6 feet	18,000	18,000
6 to 8 feet	18,000	22,400
Over 8 feet	22,400	22,400

TABLE B AXLE WEIGHT LIMIT WHEN GROSS WEIGHT EXCEEDS 73,280 POUNDS						
Center-to-center distance in feet between the first and last axles of any group of 2 or more consecutive axles	Maximum load in pounds carried in any group of 2 or more consecutive axles					
	2 axles	3 axles	4 axles	5 axles	6 axles	7 axles
NOTES:	4	34,000				
	5	35,000				
A) Use this TABLE only when both of following conditions apply:	6	36,000				
	7	37,000				
	8	38,000	42,000			
	9	39,000	43,000			
1) Combination Gross Weight must exceed 73,280 lbs.	10	40,000	43,500			
	11		44,500			
	12	45,000	50,000			
2) Combination must have at least five (5) axles.	13	46,000	50,500			
	14	46,500	51,500			
	15	47,500	52,000			
	16	48,000	52,500	58,000		
	17	49,000	53,500	58,500		
B) No axle weight shall exceed the lesser of the manufacturer's rated axle capacity or 20,000 Lbs.	18	49,500	54,000	59,500		
	19	50,500	54,500	60,000		
	20	51,000	55,500	60,500	66,000	
	21	52,000	56,000	61,000	66,500	
	22	52,500	56,500	62,000	67,000	
C) All lengths shall be measured longitudinally to the nearest foot.	23	53,500	57,500	62,500	68,000	
	24	54,000	58,000	63,000	68,500	74,000
	25	55,000	58,500	63,500	69,000	74,500
	26	55,500	59,500	64,500	69,500	75,000
	27	56,500	60,000	65,000	70,000	76,000
	28	57,000	60,500	65,500	71,000	76,500
	29	58,000	61,500	66,000	71,500	77,000
	30	58,500	62,000	67,000	72,000	77,500
	31	59,500	62,500	67,500	72,500	78,000
	32	60,000	63,500	68,000	73,000	78,500
	33		64,000	68,500	74,000	79,500
	34		64,500	69,500	74,500	80,000
	35		65,500	70,000	75,000	
	36		68,000	70,500	75,500	
	37		68,000	71,000	76,000	
	38		68,000	72,000	77,000	
	39		68,000	72,500	77,500	
	40		68,500	73,000	78,000	
	41		69,500	73,500	78,500	
	42		70,000	74,500	79,000	
	43		70,500	75,000	80,000	
	44		71,500	75,500		
	45		72,000	76,000		
	46			77,000		
	47			77,500		
	48			78,000		
	49			78,500		
	50			79,500		
	51 and over			80,000	80,000	80,000

AXLE WEIGHT LIMIT WITH SPECIAL HAULING PERMIT	
1. Unloaded Motor Vehicles must be hauled on a combination when any axle weight exceeds 50,000 pounds.	
2. Combinations hauling a nondivisible load may not exceed 27,000 pounds on any axle.	
3. No vehicle or combination shall have a weight upon any axle in excess of the manufacturer's rated axle capacity.	

FIGURE 1 (continued)

introduced. It is a simple engineering fact that if loads are distributed over a larger area, they have a smaller effect on bridges.

Figure 2 shows a comparison of bending moments for simply supported spans between AASHTO HS 20 design loading and the critical maximum legal loads. The HS 20 design load is used as a base for ease of comparison and is represented by the 100 percent line. All moment curves falling below the 100 percent baseline are not overstressing bridges designed after 1949 when the HS 20 loading was adopted. Load Con-

figuration G representing AASHTO alternate military loading is also shown in Figure 2. From the plot it is apparent that this load governs HS 20 loading in the span range of from 11 to 37 ft and peaks at about 127 percent of HS 20. All moment curves falling below the combined 100 percent baseline and alternate military curve G are not overstressing bridges designed after 1982. Single vehicles rather than the equivalent uniform load with a concentrated load will govern for simply supported spans of up to approximately 145 ft.

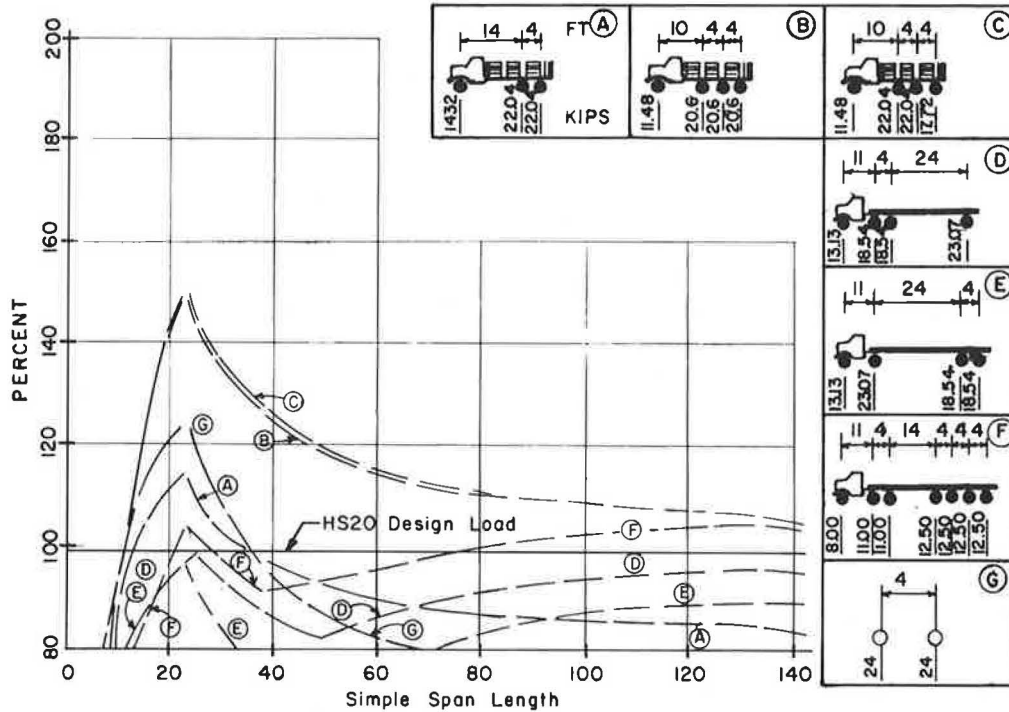


FIGURE 2 Bending moment expressed as percentage of HS 20 for maximum legal loads (1980).

For many years AASHTO HS 20 bridge design loading has been considered conservative by bridge engineers. This is no longer true because of periodic increases in legal load limits. From Figure 2 it can be seen that the most critical maximum legal load is the four-axle truck that is represented by Curves B and C. These curves peak at about 151 percent of HS 20. Such trucks could be coal, gravel, and ready-mixed concrete trucks frequently used in Pennsylvania. It can also be seen from Figure 2 that maximum legal loads represented by Curves B, C, and F are overstressing bridges designed after 1982. Furthermore, maximum legal loads represented by Curves B, C, and F are overstressing bridges not on the Interstate system designed before 1982. Figure 2 also demonstrates that the maximum legal combinations of 72,000 lb generated moment curves (D and E) less than the design load before 1982. In accordance with federal regulations, a bridge must be posted if it cannot handle the maximum legal load at the operating stress level.

The reader must keep in mind that the curves shown in Figure 2 represent only one parameter of many that severely influence the strength of a bridge. In this case, the live load bending moment was used as a basis for comparison. The effect of impact loads, multiple loaded traffic lanes, shear, dead load-to-live load ratios, and frequency of loadings have not been included in this comparison.

PERMIT LOADS

Permit loads are loads that exceed legal limits but are allowed to operate on the highway under a permit issued by a regulatory agency. These loads are quite heavy--often between 2 to 3 times the design live loads. Permit loads, because of their large gross weights or extremely heavy axle weight or axle group weight, produce stresses much higher than the stresses used for the design of bridges.

The weight and size limits for trucks and combinations that can operate with special permits in Pennsylvania are also shown in Figure 1. These limits went into effect in 1980 along with the increase to 80,000 lb for the maximum gross legal weight for combinations.

There has been a significant increase in the number of vehicles that exceed legal loads. The frequency and magnitude of various permits issued in Pennsylvania during 1 recent calendar year are given in Table 1. It can be safely assumed that the numbers given in Table 1 reflect combinations because weight permits are not regularly issued for trucks and construction load permits are rather infrequent. The

TABLE 1 Frequency and Magnitude of Various Permits Issued During 1 Calendar Year

Category	Weight Range (lb)	No. of Permits
1 ^a	0-73,281	108,704
2	73,281-95,000	24,547
3	95,001-123,000	18,989
4	123,001-150,000	7,557
5	150,001-177,000	435
6	177,001-204,000	179
7	More than 204,000	39
Total		160,450

^aCategory 1 consists of over-width permits.

data in Table 1 indicate that approximately 8,210 permits were issued yearly for vehicles in excess of 123,000 lb, 653 permits yearly for vehicles in excess of 150,000 lb, and 39 permits yearly for vehicles in excess of 204,000 lb. The 204,000-lb load is designated as a "Superload" in Pennsylvania and is subject to various other permit limitations.

The results of a study of 1980 permit loads are shown in Figure 3. This figure shows a comparison of bending moments for simply supported spans. Again, the HS 20 design load is used as the base and is represented by the 100 percent line. Load Configuration 5 representing AASHTO alternate military loading is also shown in Figure 3. The sketches on the right side of Figure 3 depict five-axle combinations (123,000 lb), six-axle combinations (135,000 lb) and seven-axle combinations (172,000 lb). These vehicles are based on the maximum axle loads of 27,000 lb permitted by regulations put in force in 1980. It was the thinking before 1983 that moment curves produced by legal loads should not exceed the HS 20 design moment curve to any large degree, because legal loads are frequent loads. However, permit loads are considered rather infrequent loads; therefore, 160 percent of the design moment, which is equivalent to an HS 32 design moment, would be tolerable. If these limits are exceeded for a given bridge, the structure must be individually investigated by a bridge engineer.

From the study depicted in Figure 3, it can be seen that permit loads for which permits were routinely issued after 1980 cause stresses much larger than the 160 percent design moment values. Stresses substantially higher than design stresses will reduce the service life of the bridge, may cause an increase in maintenance costs, and could lead to fatigue failures in frequently loaded steel elements. From these curves it is apparent that the practice of indiscriminately issuing permits for 27-kip axle vehicles is detrimental to bridges.

A contact with permit offices in Pennsylvania revealed that trucks would not be given overload permits, but combinations and construction vehicles subject to a maximum axle load limitation would.

In 1984 the weight and size limits for trucks and combinations with special hauling permits changed (6). The policy of permitting maximum axle loads of 27,000 lb was revised, and maximum axle loads were determined using the National Bridge Formula (4).

Figure 4 shows a comparison of bending moments for simply supported spans for 1984 permit vehicles

with up to seven axles and a maximum gross weight of 136,000 lb. It should be noted in this figure that the moments do not exceed approximately 160 percent of the design moment (HS 32). This led to the department's requirement that bridge engineers must review permit loads of 135,000 lb or larger for combinations with a maximum of seven axles. Figure 5 shows the results of a similar study using two-axle recommended construction loads. Even though the loads peaked in the short span range of approximately 30 ft, they did not exceed the effect of approximately 160 percent of the design moment (HS 32).

Pennsylvania's heavy haulers and heavy industry wanted assurances that the department would promptly issue permits for heavy industrial loads without the lengthy delay that may result if bridge engineers review the many permit applications for loads of 135,000 lb or larger. This request led the department to initiate a study of the feasibility of developing an automated permit routing system.

PRESENT DESIGN LOADINGS

In 1983 the Pennsylvania Department of Transportation made the decision to change from working stress design to load factor design (7). At the same time, it was decided to change the design loading for state-owned bridges.

A study comparing design live load moments for various vehicle configurations was made and the results are shown in Figure 6. The HS 20 design load is used as a base and is represented by the 100 percent line. The alternate military loading and the four-axle truck (ML 80 loading), which is the critical maximum legal load that can use the highways today without special approval from authorities, are also shown in Figure 6. Truck axle loads and dimensions are shown on the right side of the figure. From the lower portion of the figure it can be seen that the moments from the HS 25 design loading (125 percent line) and increased military design loading (125 percent times military load) almost completely envelop the moments caused by the ML 80 critical legal

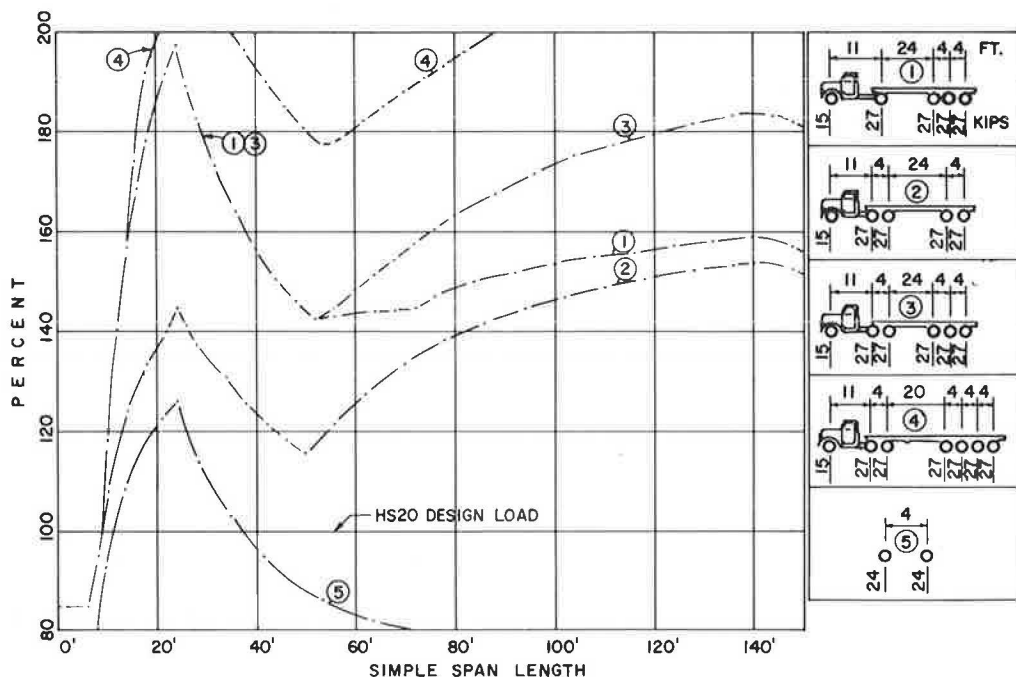


FIGURE 3 Bending moment expressed as percentage of HS 20 for permit loads (1980).

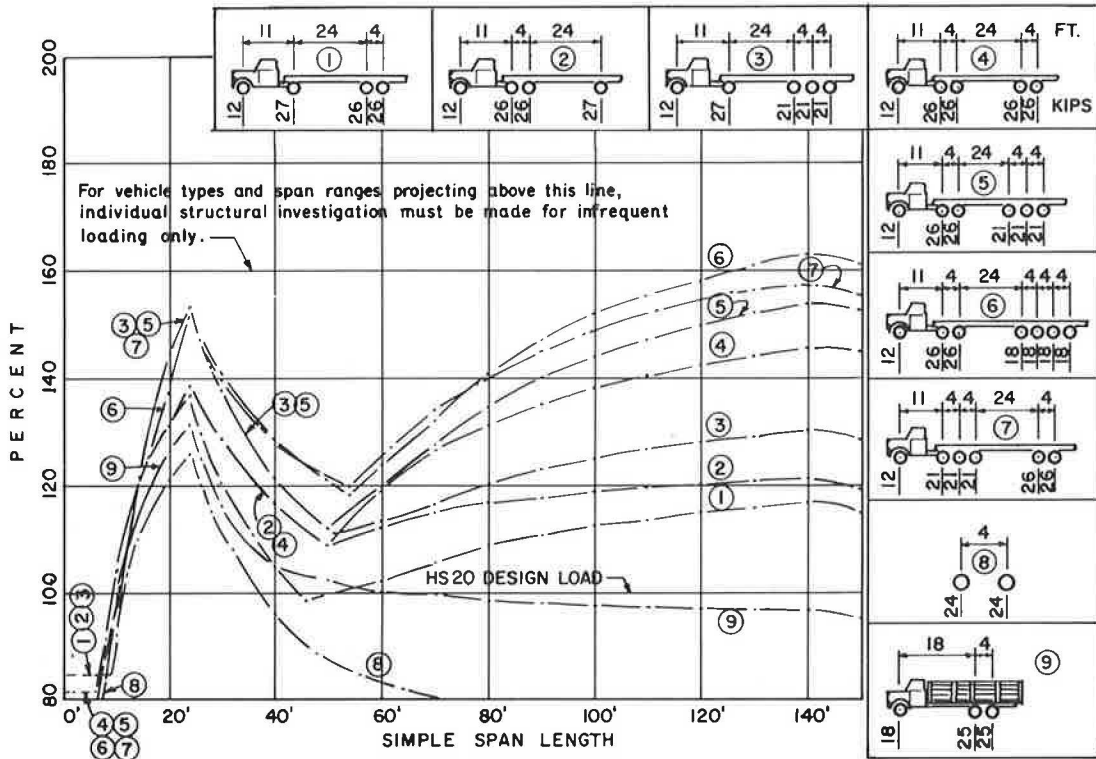


FIGURE 4 Bending moment expressed as percentage of HS 20 for permit loads (1984).

loading. From the lower portion of Figure 6 it can also be seen that the increased military load governs for simple spans of from 11 to 37 ft. For the remainder of the simple span lengths, the HS 25 truck loading governs. It should also be mentioned that HS 25 equivalent lane load, which is 125 percent of AASHTO HS 20 lane loading, should be considered for simple spans longer than approximately 140 ft. All truck and lane loadings will have a width of 10 ft.

The only way to correlate design practice directly with permit policy is to check or design the structure for the permit load that is expected to be applied to it. In other words, attaining the desired permit load capacity becomes one of the performance conditions in the design procedure. Using the load factor design method, which includes a permit load check, should produce structures with a more uniform overload capacity. Being able to use every structure

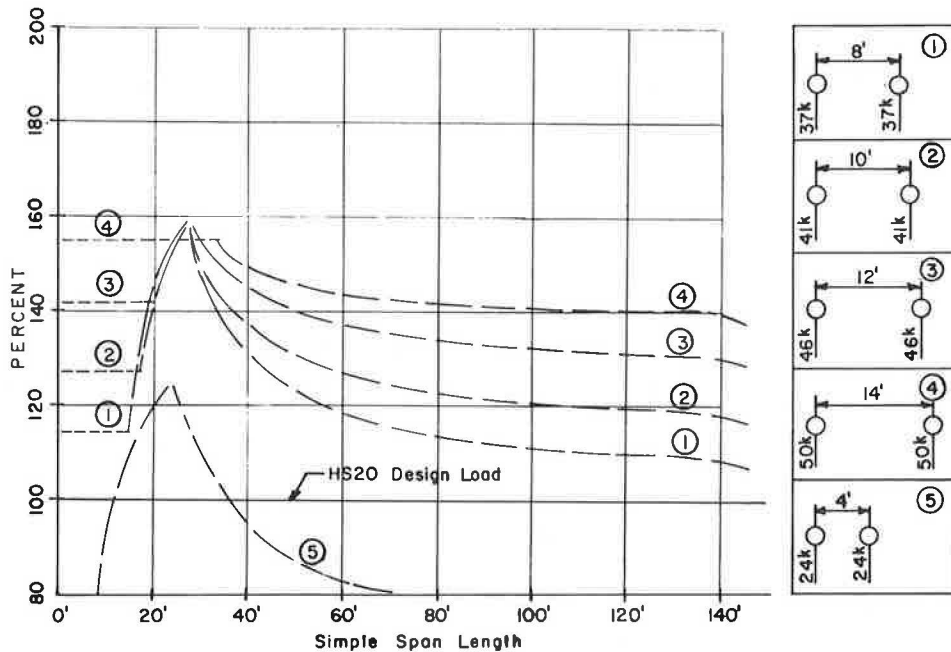


FIGURE 5 Bending moment expressed as percentage of HS 20 for recommended two-axle permit vehicle.

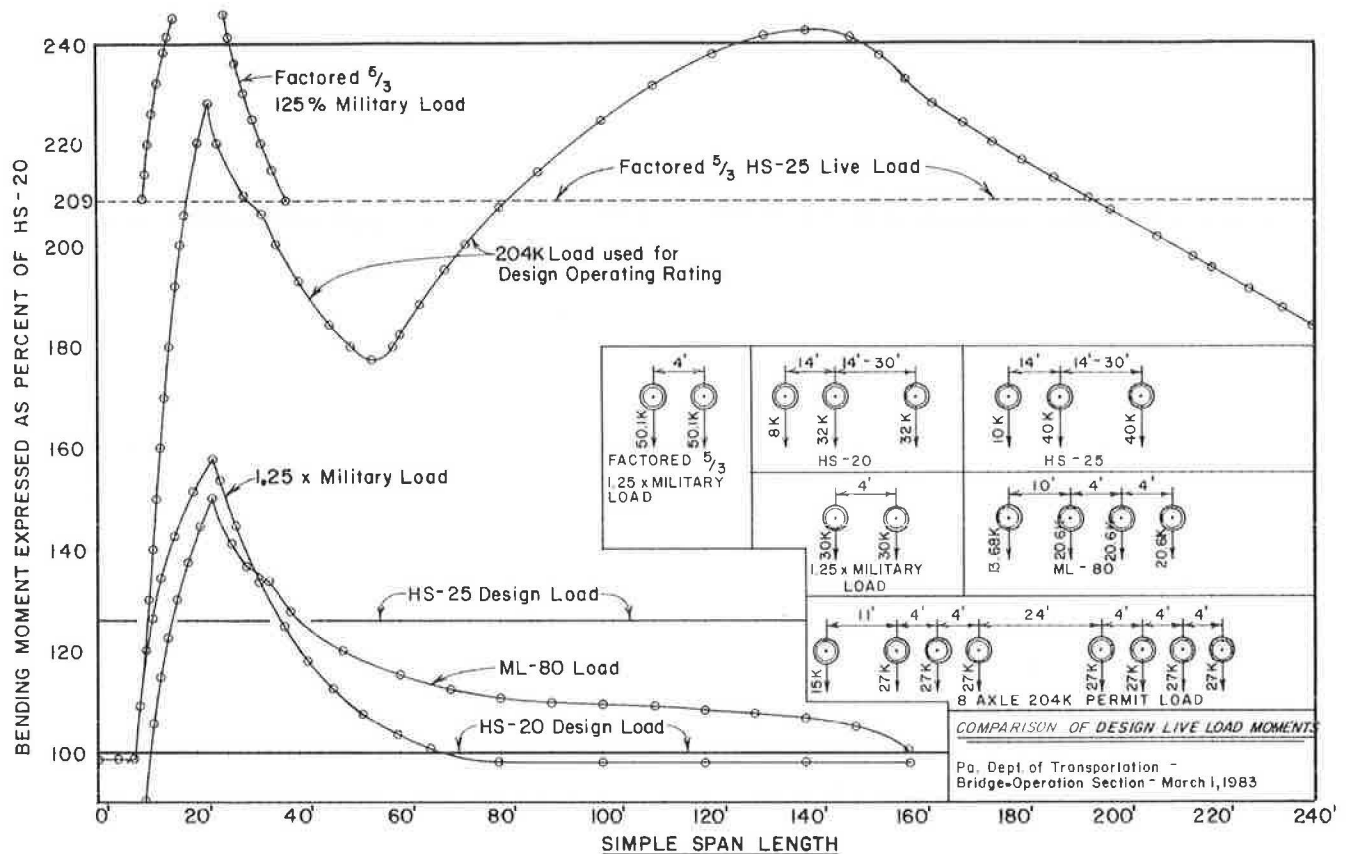


FIGURE 6 Comparison of design live load moments for various vehicle configurations.

along a route to its fullest provides maximum usability at minimum cost (3).

Concurrent with the adoption of load factor design and the heavier design loads, all structures will be checked to see if they can carry a 204,000-lb eight-axle permit load at operating rating in accordance with the 1983 AASHTO Manual for Maintenance Inspection of Bridges (8). This check is equivalent to designing for the 204,000-lb permit vehicles as Group IB loading in accordance with Article 3.22 of the AASHTO Standard Specifications (1). The axle loads and dimensions, as well as the relationship of live load bending moments for various span lengths, for the 204,000-lb permit load are also shown in Figure 6. Because the $5/3$ B factor applies to the design loads and not the permit loads, the upper portion of the diagram in Figure 6 shows that the 204,000-lb permit load will govern for simple span lengths of from 85 to 195 ft. The check for the 204,000-lb superload applies to the superstructure only. Substructure and foundation need not be checked, except for pier caps under superstructures that exceed a 65-ft span length. Dead, live, impact, and centrifugal forces should be included in the check. Deflection and fatigue criteria are not applicable.

The 204,000-lb permit vehicle is assumed to have the same width as the 10-ft-wide standard AASHTO truck. When checking the bridge or its components, one 204,000-lb permit vehicle is placed in the worst position in one traffic lane and HS 25 design loading is placed in the remaining traffic lanes. Article 3.23 of the AASHTO Specifications can be used for the distribution of the wheel loads to stringers, longitudinal beams, and floor beams (1). Using these conservative methods would be equivalent to placing the permit loads in all lanes. Distribution based on

established theoretical analysis can be used instead of AASHTO empirical formulas when it allows greater economy.

The 204,000-lb eight-axle permit load was developed by the permit regulatory office to facilitate the issuance of permits. This 204,000-lb superload is more critical than the 135,000-lb six-axle vehicle because the 27,000-lb maximum axle loads for permit vehicles have now been reduced in accordance with the National Bridge Formula (5). Permits will be issued routinely for new structures if the loads applied are smaller than the 204,000-lb superload. Permits may also be approved for heavier loads, but this will require a special analysis of each structure on the planned route for the specific loads and vehicle under consideration.

CONCLUSIONS

Pennsylvania has confirmed that a true umbrella load could be represented by two design loads for design purposes (HS 25 and 125 percent military) and one design load for permit load purposes (204,000-lb superload). By staying with the vehicle configurations previously used by AASHTO (HS and military), the designs have been kept simple.

REFERENCES

1. Standard Specifications for Highway Bridges. 13th ed. AASHTO, Washington, D.C., 1983.
2. Ontario Highway Bridge Design Code. Ontario Ministry of Transportation and Communications, Downsview, Ontario, Canada, 1983.

3. R.C. Cassano and R.J. LeBeau. Correlating Bridge Design Practice with Overload Permit Policy. In Transportation Research Record 664, TRB, National Research Council, Washington, D.C., 1978, pp. 230-238.
4. Laws of the General Assembly of the Commonwealth of Pennsylvania, Senate Bill 10, House Bill 34. Commonwealth of Pennsylvania, Harrisburg, Vol., 1, 1980.
5. Bridge Gross Weight Formula. FHWA, U.S. Department of Transportation, Washington, D.C., April 1984.
6. Pennsylvania Consolidated Statutes--Title 75--Ve-

- hicles. Legislative Reference Bureau, Commonwealth of Pennsylvania, Harrisburg, 1982.
7. R.M. McClure and H.H. West. Load Factor Design for Highway Bridges. Pennsylvania Transportation Institute, University Park, Pa., July and August 1983.
8. Manual for Maintenance Inspection of Bridges. AASHTO, Washington, D.C., 1983.

Publication of this paper sponsored by Committee on General Structures.

Application of Expert Systems in the Design of Bridges

JAMES G. WELCH and MRINMAY BISWAS

ABSTRACT

The principles of artificial intelligence have been used to develop an expert system for the design of bridge superstructures. The expert system developed, a Bridge Design Expert System (BDES), applies the ideas of artificial intelligence to the bridge design process. The result is a practical system capable of aiding any bridge designer. BDES at its preliminary stage considers superstructures of short- to medium-span bridges. It designs for structural steel and prestressed concrete girders. The developed BDES is a valuable design tool, but, more important, it has shown the potential applications of expert systems in bridge design.

The application of computers in engineering has aided in the solution of numerous problems. This is especially true for problems of analysis for which programs have been constructed to assist the engineer in determining stresses, strains, and strengths of structures. Computer systems are also available to aid in detailed drafting. However, computer applications for decision making in design problems have been limited. Programs to aid the designer proceed through different phases of the design process have been developed, but programs to carry out the entire design decision-making process are scarce. The designer is required to make various decisions throughout the design process (1, pp.3-6). Design decisions may include selecting feasible structure types, making appropriate approximations and assumptions, and sizing individual members to satisfy the design criteria. Such problems are "ill-structured" and are not well suited for conventional programming procedures (2).

However, a program capable of proceeding through the entire design process has been developed by applying a relatively new technology called expert systems. Expert systems, also called knowledge- or rule-based expert systems, are intelligent computer

programs that are capable of solving practical problems that have heretofore been considered difficult enough to require human intelligence for their solution (3). The developed expert system, Bridge Design Expert System (BDES), was constructed to explore the applications of expert systems to the design of bridge superstructures.

EMERGENCE OF EXPERT SYSTEMS

Interest in developing expert systems has greatly increased in recent years because of their advantages over more conventional computer programming procedures. The following table gives some expert systems and the problem domain that they attempt to address (3,4).

<u>Expert System</u>	<u>Domain</u>
MYCIN	Medical diagnosis
DENDRAL	Organic chemistry
MACSYMA	Symbolic mathematics
HEARSAY II	Speech understanding
PROSPECTOR	Exploratory geology
GENESIS	Genetic engineering

However, because the idea of expert systems is quite new, their potential use in many areas has not yet been investigated. This is certainly true for civil engineering applications, and especially in the area

of transportation engineering. The following table gives some engineering expert systems along with their problem domain.

Expert System	Domain
HI-RISE	Building design
FAX	Failure analysis
SAGE	Structural analysis
BDES	Structural design

EXPERT SYSTEMS

Expert systems attempt to model the problem-solving expertise of a human expert within a particular field. This requires representing specific knowledge or expertise of an expert as well as general problem-solving strategies. In knowledge-based expert systems, the expert's knowledge is stored in the system's knowledge base. This is analogous to a data base in a conventional program. The problem-solving strategy involves drawing inferences and controlling the reasoning process (3). These strategies comprise the inference procedure of an expert system. The inference procedure is included in what has been termed the expert system's "inference engine" (3,4).

The knowledge base includes two different types of knowledge: factual and heuristic (3,4). Factual knowledge can usually be found in textbooks and other references and hence is common knowledge (3,4). For example, in BDES factual knowledge may include AASHTO requirements, material properties, and potential superstructure designs typically used. Factual knowledge is referred to as simply the "facts."

Heuristic knowledge is mostly private knowledge that experts have gained through experience (3). This knowledge is characterized by rules of good judgment, rules of good guessing, rules of plausible reasoning, and rules of thumb. These rules model the decision expertise the expert uses to solve the problem. This heuristic knowledge is represented in the form of rules and is thus referred to as the "rules." Rules in BDES may be used to select the superstructure type, determine the girder spacing, or decide between a simple or continuous span design.

KNOWLEDGE-BASED EXPERT SYSTEM

Figure 1 shows a schematic representation of a knowledge-based expert system. The figure illustrates that a user of an expert system may be an expert or a nonexpert. The analogy in BDES is the experienced bridge designer as the expert and the novice engineer as the user.

Whether the user is an expert or not, the system must require input from the user to begin. The input,

represented here by the problem statement, consists of all engineering data required to state the problem for the expert system to solve. The problem statement basically symbolizes the memory that stores the problem data.

The expert system now combines the data of the problem statement with the facts and rules contained in the knowledge base. The rules in the knowledge base use the problem data and the facts of the knowledge base to draw inferences and solve intermediate steps leading to the final design decision.

The inference engine uses control procedures to draw appropriate inferences. Drawing inferences in an expert system simulates the expert's reasoning process. Reasoning requires processing the problem and the problem expertise to make decisions.

Inference procedures typically use if-then rules to model the decision making of the expert. If-then rules state that if a certain condition or set of conditions is true, then a particular conclusion becomes true. The knowledge base may contain many if-then rules and thus require the inference engine to provide a suitable strategy to control the selection of appropriate rules.

Ideally the inference engine should trigger rules that generate decisions comparable to those that the expert would make at any point in the solution process. The control procedures must therefore find a way to systematically proceed from the initial problem state to the final goal. The solution or goal in many problems, including design, requires searching many possible outcomes until one satisfying the goal is found. The inference engine continues using rules to search for a solution until the solution has been found.

Figure 1 shows three outputs to the expert/user. These include solution, explanation, and knowledge update. The solution output is obviously the desired solution to the problem. However, the user may wish to know more than just the final solution. The user may want to know how or why a certain conclusion was reached. The explanation output represents this feature. All expert systems do not give explanations of why or how they reached a certain conclusion. However, this feature is obviously quite desirable.

The knowledge update output represents an ideal feature by means of which the expert system can learn from its experience and thus suggest ways to the user (expert) for updating the knowledge in the knowledge base. The expert user can then update that knowledge. Of course the expert user may still update the knowledge base or enter new knowledge without this feature.

ARTIFICIAL INTELLIGENCE SEARCH STRATEGIES

Artificial intelligence has developed efficient strategies for solving search problems. Most notable are "breadth-first" and "depth-first" search processes using forward and backward chaining strategies (5,6). Breadth-first and depth-first differ in the way they proceed through a search space. A search space includes all possible outcomes at each stage of the solution process. This can be viewed as a treelike structure that contains at the top the initial state and at the bottom many goal or solution states. Levels in the middle of the structure correspond to intermediate solution states along some path to the goal state. A breadth-first search proceeds down the structure one level at a time examining each intermediate state of the next level to decide what is the best path. A depth-first search assumes one path and proceeds down it until it either determines that that path will not lead to a solution or reaches the final goal state.

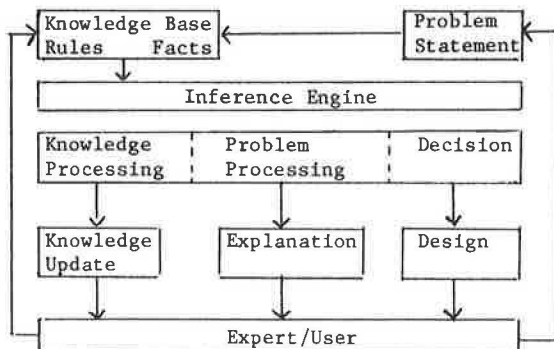


FIGURE 1 Knowledge-based expert systems.

Forward chaining starts at an initial state and infers intermediate subgoals in an orderly fashion until the final goal is found. Backward chaining assumes a goal and attempts to verify the assumed goal by attempting to proceed backwards to the initial state. Forward chaining is useful when many goal states are possible and backward chaining is useful when a few goal states are possible.

IMPLEMENTING AN EXPERT SYSTEM IN BRIDGE DESIGN

Implementing an expert system in bridge design first requires identifying the knowledge of the bridge design process to use to build and develop a knowledge base. Steps in the bridge design process (design procedure) are shown in Figure 2. Knowledge used in each step of the process is also displayed.

The second task is to develop suitable inference procedures to process the knowledge. Different procedures could be used. However, a strategy that best simulates the reasoning process of the bridge designer should be identified.

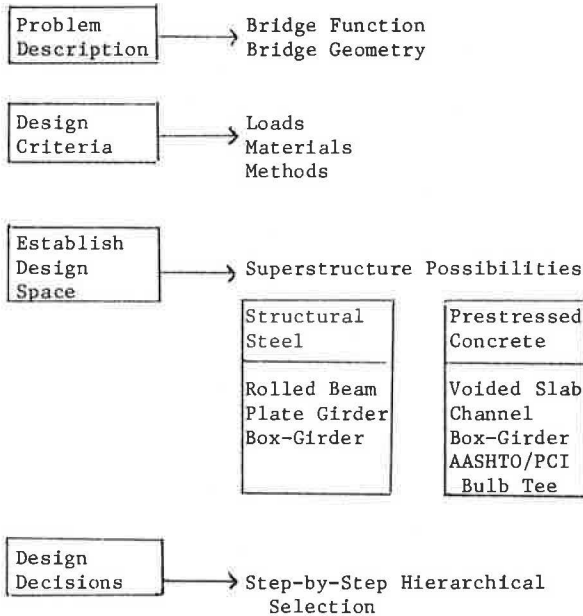


FIGURE 2 Design procedure.

KNOWLEDGE OF THE BRIDGE DESIGN PROCESS

Establishing the information or data needed to adequately describe the problem is the first step. Bridge geometry and bridge function give this information. Bridge geometry includes bridge length, width, height, and skew. The number of lanes, the number of spans, and the lengths of the spans are also part of the geometry input. Bridge function describes the reason for constructing the bridge (e.g., to cross over another roadway, to cross over a stream). Information describing the problem is design specific and is therefore required input by the user. This information is thus not part of the expert system's knowledge base.

The next step in the design process represents factual knowledge stating the constraints and criteria to which the design must adhere. The loading, material properties, and method of design to be used must be established. For example, the method of

design could consist of either load factor or working stress.

The next step shown in Figure 2 refers to the establishment of the design space. The design space represents all possible bridge superstructure designs. Examples of structural steel and prestressed concrete superstructures included in the design space of BDES are shown in Figure 2 (6-9). Figure 3 illustrates further the design space for structural steel. The figure shows a treelike structure in which levels of the tree correspond to different design characteristics.

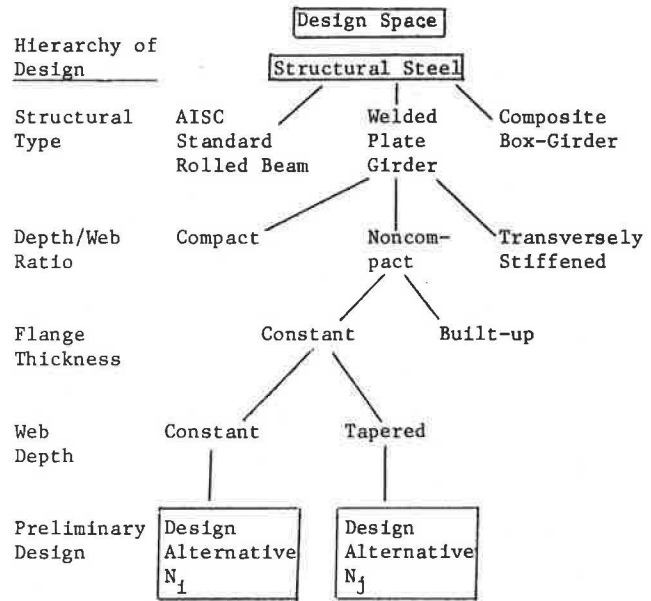


FIGURE 3 Design space.

The many characteristics allow for a great multitude of potential designs. Establishing the design space provides the designer with all the possible solutions to the design problem. It should be pointed out that this step does not represent an input, action, or decision in the design process. However, this step is shown to stress that the designer must be aware of all of the possible superstructure designs. It should be noted that the design space represents factual knowledge in the knowledge base. This is true because the different designs in the design space are typically used standard designs.

The design process must now begin making decisions that will ultimately lead to a final design. The design decisions in themselves constitute a series of steps. Each step requires drawing inferences to make appropriate selections given some discrete set of choices. These steps are normally performed in a generally fixed sequence thus creating a hierarchy of selections. Figure 4 shows the steps contained in the design decisions. These include selecting a set of promising and feasible design alternatives, sizing the members in the alternatives, and comparing the alternatives to select a preliminary design. A structural analysis step is shown to emphasize that analysis may play a role in the design decisions.

Selecting a set of promising and feasible design alternatives requires heuristic knowledge. Rules of thumb, rules of good judgment, and rules of plausible reasoning govern decisions about appropriate selections. Typical rules include decisions to choose between steel or prestressed concrete; among a compact,

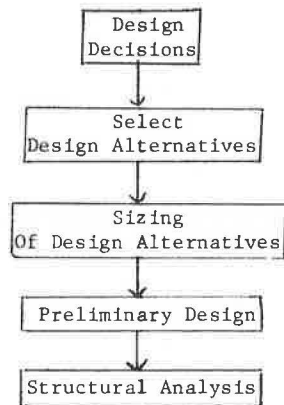


FIGURE 4 Design decisions.

noncompact, or stiffened web; or between a constant or built-up flange section. Some rules may be documented and practically universally used. However, many rules comprise the knowledge that the bridge designer has gained with experience.

Sizing the members of the design alternatives is another step that requires heuristic knowledge. In this step rules of good guessing are used to design members of the design. Typical rules include rules for selecting girder depths and spacings, web and flange dimensions, and slab thickness.

Comparing the design alternatives to select a preliminary design is also governed by rules. It should be clear that one rule used in this step is to select the "best design." However, the best design selected by one designer may not be the best design selected by another. The reason is that designers use many different rules to quantitate the affects of aesthetics, environmental concerns, and local economics.

The next step in the design process is to structurally analyze the selected design alternatives. The analysis uses mostly factual knowledge regarding common and documented procedures to find the stresses, deflections, and so forth.

INFERENCE AND CONTROL IN BRIDGE DESIGN

Heuristic knowledge is easily cast into a form of if-then rules that implies a modus ponens inference strategy (3,5). This strategy uses logical if-then rules to draw inferences and hence make decisions. For example, in BDES a typical inference can be made to select a potential superstructure type using the following rule:

If: Span length is less than 80 ft,
Then: Consider a rolled beam.

Note that the rule only infers considering a rolled beam, it does not use a rolled beam. This example illustrates a few key points. First, many conditions may have to be true in order for a certain decision to be reached. For example, conditions other than the fact that the span length is less than 80 ft will have to occur before a rolled beam becomes the selected design. Second, a rule drawing an inference does not have to dictate a decisive action; it may instead prompt a tentative decision. Eventually, with enough rules, a final decision can be reached. Although not evident in this example, it should be pointed out that the decisions reached by rules may themselves be conditions for new rules.

The control strategy must now be selected to process the rules in such a fashion as to eventually produce a final design. A breadth-first search using forward chaining appears to be most appropriate for a design problem. The large number of possible outcomes (final designs) favors the forward chaining process. The selection of the design types, characteristics, and sizes proceeds in a systematic order thus prompting the need for a breadth-first strategy.

Figure 3 shows the advantages of using a breadth-first search. Breaking a design into a hierarchy of design characteristics allows rules pertaining to each characteristic to be grouped. A group of rules can then be examined to select a particular design characteristic at each level in the hierarchy. After all characteristics have been examined, a design alternative has been found.

BRIDGE DESIGN EXPERT SYSTEM

BDES designs superstructures of short to medium span. The potential designs comprise practically all designs normally used today. Possibilities may include structural steel or prestressed concrete with either simple or continuous spans.

BDES is highly user interactive with graphic capabilities to aid in input and output. The system requires the bridge geometry as minimal input. However, the user may intervene at each step of the design process to alter assumed facts. Graphic displays guide the user in inputting geometry. Graphic output displays various cross sections to illustrate clearly the designs generated by BDES.

BDES requires the bridge geometry as discussed previously. Figure 5 shows a graphic output of the bridge geometry. The geometry input is flexible in that it allows the user a choice between entering the width or the number of lanes. The system will suggest a width using assumed values of shoulder, median, railing, and lane widths.

The reason for constructing the bridge, bridge function, is another input to the system. Bridge function dictates vertical clearance requirements. For example, in North Carolina the clearance must be from 16 ft 6 in. to 17 ft 0 in. for bridges crossing over Interstate highways (10).

The environment may affect the selection of materials. For example, North Carolina suggests using ASTM A588 unpainted steel except in highly corrosive environments (11). Thus BDES requires information regarding the environment.

Assumptions regarding materials, loading, design method, and other constraints and criteria are incorporated in BDES. However, assumptions may be changed by the user to allow for maximum flexibility. A typical assumption might include an AASHTO HS 20-44 loading. Only one method of design, load factor, is used in BDES.

BDES now begins making design decisions using the rules. A set of design alternatives is generated first. More than one alternative is usually generated because not enough knowledge is known at this point in the design process. For example, it may not be clear whether a rolled beam or an AASHTO-PCI prestressed concrete girder is the best design for a simple span length of 60 ft. Alternatives may be similar except for one particular characteristic, such as a plate girder with and without transverse stiffeners. In BDES each is considered a separate alternative. However, there is enough knowledge to guarantee that only a small number of alternatives will be generated.

The next step in BDES is to size the members for each alternative in the set just created. The main structural members are sized along with the slab

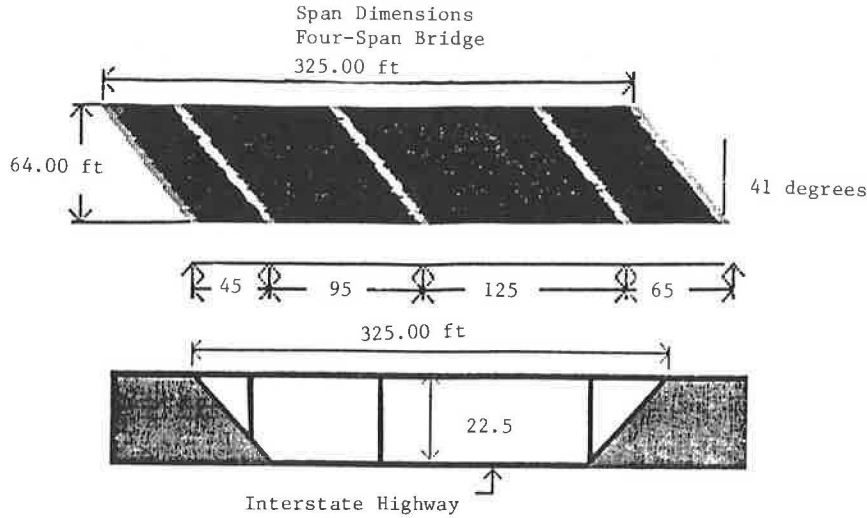


FIGURE 5 Bridge geometry.

thickness (all designs assumed a reinforced concrete deck). The spacing of the members is also generated. Rules are used to make good guesses of the member dimensions. This process proceeds in a systematic order using breadth-first search strategy similar to the process for determining the set of design alternatives. The hierarchical design is required because sizing some dimensions depends on other dimensions. For example, the web depth is found first with a rule that uses the span length. Then the web thickness is found with a rule using the web depth as a condition. Specifically, in the design of a compact plate girder the web thickness will be limited by AASHTO code requirement 10.48.1(b) (12). This requirement specifies the maximum depth-to-thickness ratio allowed for a compact section.

BDES must now select one of the design alternatives. The selected design alternative is governed

by the "least weight" design. The "weight" of a design alternative includes the material weight plus "equivalent weights" to account for the differences in fabrication or construction costs, or both. Material weights are obviously easily calculated. Equivalent weights are found by equating x number of pounds of material to unit values of different design parameters. For example, BDES assumes 700 lb of steel for each field splice (13). The user may input several different equivalent weight conversions: the user might equate x number of pounds of steel per linear foot of weld.

BDES now selects the least weight design and verifies its adequacy by structural analysis. The analysis checks for all AASHTO code requirements. Included in BDES are also requirements dictated by North Carolina (11).

Figure 6 shows the design recommendation generated

Superstructure Characteristics						
Material Type	Girder Type	Span Type	Length	Web	Flange	Depth
Structural Steel	Plate Girder	Simple Span 2	125 ft	Compact	Built-Up	Constant

Preliminary Design Data							
Girder Spacing	No. of Girders	Top Flange Plate		Web Plate		Bottom Flange Plate	
		Width	Thickness	Depth	Thickness	Width	Thickness
12.50 ft	5	11 3/4 in.	1 1/8 in.	60 in.	1 1/16 in.	16 3/16 in.	1 1/8 in.

Flange Build-Up					
Width	Bottom Flange Thickness	Length	Width	Top Flange Thickness	Length
11 3/4 in.	1/2 in.	56.3 ft	11 3/4 in.	1/2 in.	56.3 ft

FIGURE 6 Preliminary design alternative.

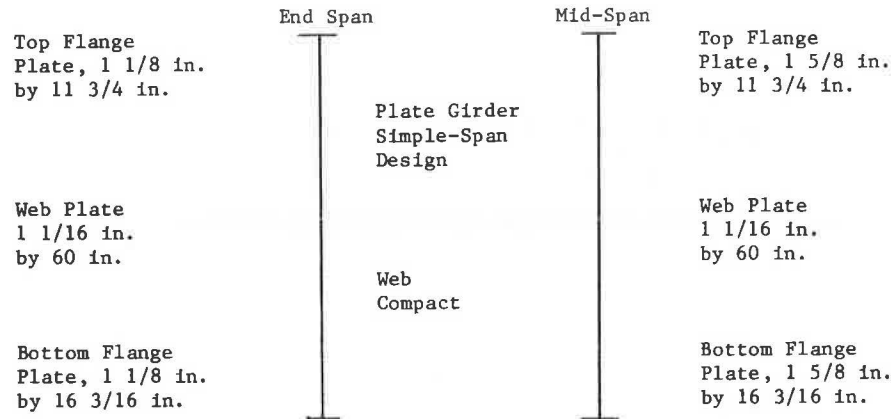


FIGURE 7 Girder cross section.

by BDES corresponding to the geometry displayed in Figure 5. Figure 7 shows a typical graphic output of the girder cross sections for this design.

If the recommended design satisfies all requirements, BDES will advise the user that the design is usable. If the design does not meet required specifications, BDES will let the user know why the design was not acceptable. However, at this time BDES does not redesign. The next phase in developing BDES would thus be to incorporate redesign rules.

CONCLUSION

Great potential exists for the use of expert systems in design problems. The bridge design expert system developed, BDES, has certainly shown this potential. BDES has demonstrated that expert systems are well suited for "ill-structured" problems. Capturing the knowledge of the bridge designer and integrating it with a workable inference procedure has resulted in a system capable of making intelligent design decisions.

REFERENCES

1. D.J. Fraser. *Conceptual Design and Preliminary Analysis of Structures*. Pitman Publishing Corp., New York, 1981.
2. S.J. Fenves, M.L. Maher, and D. Sriram. Knowledge-Based Expert Systems in Civil Engineering. *In Computing in Civil Engineering, Proc., Third Conference, American Society of Civil Engineers, 1984*, pp. 248-255.
3. P. Harmon and D. King. *Expert Systems Artificial Intelligence in Business*. John Wiley & Sons, Inc., New York, 1985.
4. F. Hayes-Roth, D. Waterman, and D. Lenat. *Building Expert Systems*. Addison-Wesley Publishing Co., Inc., Reading, Mass., 1983.
5. N.J. Nilsson. *Principles of Artificial Intelligence*. SRI International, Tioga Publishing Co., Palo Alto, Calif., 1980.
6. *Manual of Steel Construction*. 8th ed. American Institute of Steel Construction, Inc., New York, 1980.
7. C.P. Heins and D.A. Firmage. *Design of Modern Steel Highway Bridges*. Wiley-Interscience, New York, 1979.
8. *Precast Prestressed Concrete Short Span Bridges*. 2nd ed. Prestressed Concrete Institute, Chicago, Ill., 1980.
9. J.R. Libby and N.D. Perkins. *Modern Prestressed Concrete Highway Bridge Superstructures*. Grantville Publications, Los Angeles, Calif., 1976.
10. *Bridge Policy*. Division of Highways, North Carolina Department of Transportation, Raleigh, Aug. 1981.
11. *Bridge Design Manual*. Highway Design Branch, North Carolina Department of Transportation, Raleigh, March 1984.
12. *Standard Specifications for Highway Bridges*. 13th ed. AASHTO, Washington, D.C., 1983.
13. R.P. Knight. *Economical Steel Plate Girder Bridges*. *In Bridge to the Future, National Bridge Conference, Pittsburgh, Pa., 1983*, pp. 110-115.

Publication of this paper sponsored by Committee on General Structures.

Evaluation of Steel Bridges Using In-Service Testing

MICHEL GHOSN, FRED MOSES, and JOHN GOBIESKI

ABSTRACT

Highway bridges often exhibit higher strengths than indicated by AASHTO rating procedures. This is because the code is inherently conservative and is intended to be applied to general situations. A more appropriate approach is to incorporate field observations in the rating process. A field measurements (weigh-in-motion) system is capable of providing all pertinent data on the loading and response of highway bridges. The data collected include measured stresses and girder distribution factors in addition to truck weights and volumes. The data are then incorporated in a working stress design rating or in a reliability-based safety evaluation of bridge members. Results from an example site indicate high safety levels despite the large numbers of permit vehicles allowed.

More than 100,000 bridges in the United States are reported to be structurally deficient (1). Many of these bridges, however, were designed and constructed in a manner that achieved greater strength than is recognized in conventional code rating provisions. Current evaluation and rating investigations emphasize bridge condition and member dimensions. Inspection methods rarely determine bridge loads or member performance under loading. Developments in weigh-in-motion technology, however, make it feasible to investigate existing bridges and provide more accurate site-specific load and response data for the evaluation process.

Bridge rating is a continuous and vital activity for most bridge bureaus. Safety and economic decisions must be made about each bridge: repair, rehabilitate, post, allow permits, close, or replace. Existing regulations prescribe inspection techniques and guidelines for evaluation. Field inspection establishes member properties, deterioration, and dimensions of load-carrying members and connections. Evaluation calculations generally follow AASHTO procedures (2). These are similar to the bridge design guidelines and specify loads, analysis (girder distribution), impact (dynamic amplification), and allowable stresses (3). The factors in the AASHTO design manual are necessarily conservative because they must apply to a variety of situations. Obviously, a specific bridge will have performance factors that are different from the ones cited in the code. For new construction, the additional cost associated with using conservative performance predictions is usually slight because adding capacity for new bridges will increase the overall construction cost by only a small amount. For in-service bridges, however, the cost of either adding capacity to the existing bridge or penalizing users with low posting or permit levels can be high.

The AASHTO bridge inspection manual, however, does permit wide latitude in selecting checking parameters if more data are available. There has been limited use of this flexibility in modifying evaluation parameters because the guidelines for incorporating any new data into the evaluation calculations are vague.

The objective of this paper is to provide a procedure that uses field measurements in connection with weigh-in-motion technology to assist in bridge evaluation and rating. Data were recorded on truck loads, dynamic impacts, girder distributions, and member stresses. These data are incorporated in an improved deterministic rating analysis and a proposed probabilistic approach for the evaluation of existing steel bridges.

EVALUATION PROCEDURES

Most states and bridge bureaus use rating procedures that generally follow AASHTO's guidelines. For example, the method followed by the Ohio Department of Transportation calculates the maximum moment at various points on the bridge due to a number of typical heavy trucks. This moment is multiplied by the impact factor for the location under consideration and the girder distribution factor, which depends on the bridge type and the girder spacings.

Usually, the available capacity for live load (member capacity minus dead load effect) is obtained by using the higher permitted operating stresses to reflect the uncertainties in strength and load associated with the rating period (usually 2 years) that are smaller than those associated with the design period.

Absent from the rating evaluation is any use of site-specific load and response information although it is obtainable by observing performance of an existing bridge. It should be noted that the AASHTO Maintenance and Inspection Manual (2) does allow considerable flexibility. For example, it states: "A higher safety factor for a bridge carrying a large volume of traffic may be desirable." Further, "impact may depend on deck roughness or approach." The manual also mentions consideration of the probability of closely spaced heavy trucks. These guidelines, however, are rarely used because the acquisition of relevant load data has, until recently, been difficult. Instead, most rating is done with prescribed factors that govern all bridges equally. For example, the same allowable stresses and nominal loading are used for heavily traveled Interstates and for rural roads with little traffic.

The following considerations, compared with the parameters in the AASHTO manual, may govern the true loading and response situation.

1. The girder distribution factor in AASHTO is

M. Ghosn, Department of Civil Engineering, The City College of New York, New York, N.Y. 10031. F. Moses and J. Gobieski, Department of Civil Engineering, Case Western Reserve University, Cleveland, Ohio 44106.

generally conservative although the margin on the safe side can vary considerably. It may depend on lane position relative to girder and curb locations and relative lateral, torsional, and longitudinal stiffnesses. Much research on predicting wheel load distributions is under way, but the scatter in analysis is always greater than what could be obtained for an existing bridge by direct measurements.

2. The impact allowance specified in AASHTO is usually higher than that obtained by testing. Moreover, the observed value is often a function of maintenance (bump or roughness) rather than span length as given in AASHTO.

3. Truck traffic and weight distribution will vary considerably from site to site. These parameters affect the likelihood of occurrence of extreme combinations of truck overloads. For example, the probability of occurrence of very heavy and closely spaced vehicles is affected by the truck weight distribution, volume, percentage of side-by-side occurrences, and inspection interval.

The most direct way to consider these observations in the rating process is by using field strain measurements to determine girder distribution and impact factors. The values that are presented by AASHTO are by nature conservative and intended to fit a variety of situations. For a specific bridge the field data will obviously give more exact values.

The approach proposed in this section is simply to modify the AASHTO design girder distribution and impact factors and substitute the field-measured values. In general, this approach will change the live load stresses by about 30 percent for the distributions and about 15 percent for the impact. (Examples will be given later.)

According to the maintenance manual, the safety factors should be increased if the site contains a large volume of vehicles or many heavily loaded trucks. These traffic-related variables are addressed in the subsequent section in which structural reliability techniques are used in assessing the safety of bridge members.

SAFETY ANALYSIS

Bridge safety compares loading demand on the component and strength capacity. Safety factors are needed to account for the possibility of overloads; inaccuracies in calculation of load effects; and variability of material properties, fabrication, and other tolerances. Modern safety theory has as a goal the quantification of uncertainties and the application of design factors that produce structures with uniformly consistent reliabilities. For new bridges, the safety factors reflect the long-term distributions of maximum load and deterioration of member strengths. For rating bridges, the safety factor can be lower because the exposure period is shorter, knowledge of loading is more precise, and member deterioration can be revealed by inspection and corrected.

The basic reliability model is used to examine the safety margin (4):

$$g = R - S \quad (1)$$

where

g = safety margin;
 R = member strength capacity; and
 S = load effect on the member; S includes the dead (D) and live (truck) loads (L):

$$S = D + L \quad (2)$$

The component is safe as long as the safety margin (g) is positive. A convenient measure of safety is the reliability or safety index (β). This includes the mean value of g and its uncertainty as expressed by its standard deviation (σ_g):

$$\beta = \bar{g} / \sigma_g \quad (3)$$

The standard deviation of g for a simple case is obtained from the expression for a sum:

$$\sigma_g^2 = \sigma_R^2 + \sigma_D^2 + \sigma_L^2 \quad (4)$$

where σ_R , σ_D , and σ_L are the respective standard deviations of R , D , and L . In the bridge rating example, σ_R will depend on the variability of material properties as well as the estimation of scatter in material deterioration. σ_D depends on the dead weight including estimations of overlays; and σ_L depends on truck weight parameters, volume, girder distribution, and dynamic amplifications.

A model presented previously for calculating safety indices is briefly reviewed here (5). The maximum live load effect (L) at a position along a bridge is expressed as

$$L = a m W^* H g I \quad (5)$$

where

a = constant based on span length and configuration of design vehicle;
 m = variable that reflects the randomness in the axle configurations of representative random truck traffic;
 W^* = variable that corresponds to the weight of the upper 5 percent of the gross weight histogram; this magnitude, which is typically in the 60- to 80-kip range, was found to adequately represent the severity of truck weights at a site;
 H = multiple presence or headway variable to reflect the ratio of maximum moment to a load caused by a design weight equal to W^* ;
 L = live load effect including all loaded lanes; L includes the likelihood of side-by-side occurrences or multiple presence on the bridge and the extreme tail of the weight histogram;
 g = girder distribution factor; and
 I = impact factor.

The values of the means and standard deviations of all the random variables listed can be obtained from observations of the capacity of the bridge members and the traffic crossing the bridge as will be illustrated in a later section.

WEIGH-IN-MOTION SYSTEM

The data needed for the examples in this paper were obtained using the weigh-in-motion (WIM) system developed at Case Western Reserve University under the sponsorship of the Ohio Department of Transportation and the Federal Highway Administration (6,7). The system uses existing bridges as equivalent static scales to obtain unbiased truck gross and axle weights, classification, dimensions, and speed. For the purpose of this study, the WIM system provided the following information on the vehicle traffic on the instrumented bridge:

1. A total count of the vehicles that cross the bridge;
2. The lane traveled by each vehicle;

3. The time of arrival of each vehicle on the bridge;
4. The speed of each vehicle;
5. The truck type, found from the axle configuration of vehicles heavier than 10 kips;
6. The spacings between the axles of each truck;
7. The weights of the trucks' axles; and
8. The trucks' gross weights.

In a second step, information on the behavior of the bridge members is obtained by observing

1. The stresses at the gauge locations,
2. The girder distribution factors, and
3. The dynamic amplifications of the strain records.

This information is assembled in histograms and the means and standard deviations of the variables are calculated and used as illustrated in the examples given in the next sections.

RATING EXAMPLE

Five sites were instrumented to illustrate this study. All five bridges had parallel steel girders and gave fairly typical representation of bridges in Ohio in terms of design (both composite and noncomposite bridges were instrumented) and truck traffic composition (posted bridges and bridges with high permit loads were evaluated). In this section, the results for one site are presented; the results for the other sites are given elsewhere (8). This bridge on I-475 in Lucas County was chosen because of the large number of heavy special vehicles that crosses it. The layout of the six-girder 176-ft bridge is shown in Figure 1. The bridge was overdesigned according to AASHTO specifications and was allowed high levels of permit trucks.

Truck Traffic

More than 600 trucks were observed during the 4 hr of continuous data acquisition. Seventy-six percent

of these trucks were in the right lane. The number of side-by-side occurrences is an important factor in determining the maximum expected load on a site. For the purposes of this study, all trucks that run over the bridge within 0.5 sec of each other in the two lanes are considered to constitute one side-by-side occurrence. It was observed that 0.7 percent of the trucks were in the left lane following, within 0.5 sec, a leading truck in the right lane. Also, 0.3 percent of the trucks were in the right lane within 0.5 sec of a leading truck in the left lane. This indicates that about 1 percent of all truck occurrences are side-by-side events. This value is consistent with measurements at other sites (8). The truck gross weight histogram for this site is shown in Figure 2. The mean of the loaded semitrailer trucks (heavier than 20 kips) is 45 kips. The 95th percentile weight (W*) is 78 kips, which indicates a relatively high loading distribution compared with other sites in Ohio. The 95th percentile weight excluding permit trucks is 74 kips.

Measured Stresses

Part of the WIM operation consists of a "calibration" phase during which the strain record of a "test" truck of known weight is recorded. The 29-kip truck used on this bridge produced a maximum stress of 1.12 ksi on the third girder when the truck traveled in the right lane. The stresses were measured on the first span at a location corresponding to the lowest rating value as determined by the standard AASHTO procedures. The stresses on each girder from several other truck crossings in different lateral positions are given in Table 1. Table 2 gives the measured stresses due to the heaviest trucks recorded at this site. It can be observed that the maximum single girder stress is 3.40 ksi, which was caused by a 136.7-kip truck with five axles.

Girder Distribution

Random traffic with a minimum gross weight of 20 kips was used to determine girder distributions for each lane (Table 3). The distribution factors for side-

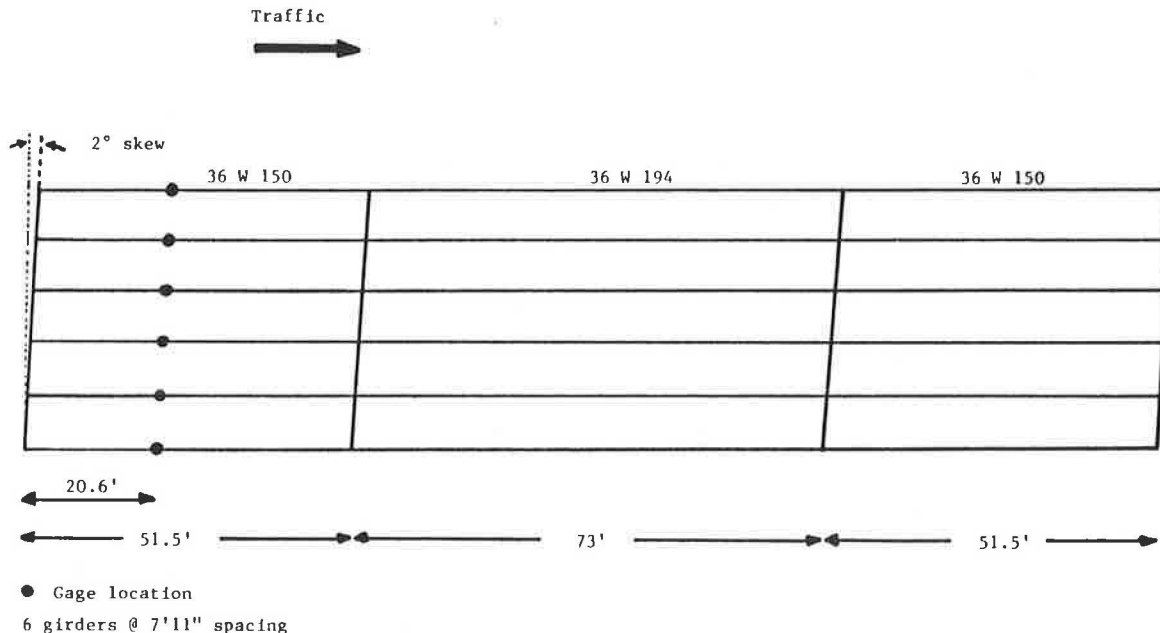


FIGURE 1 Layout of I-475 site.

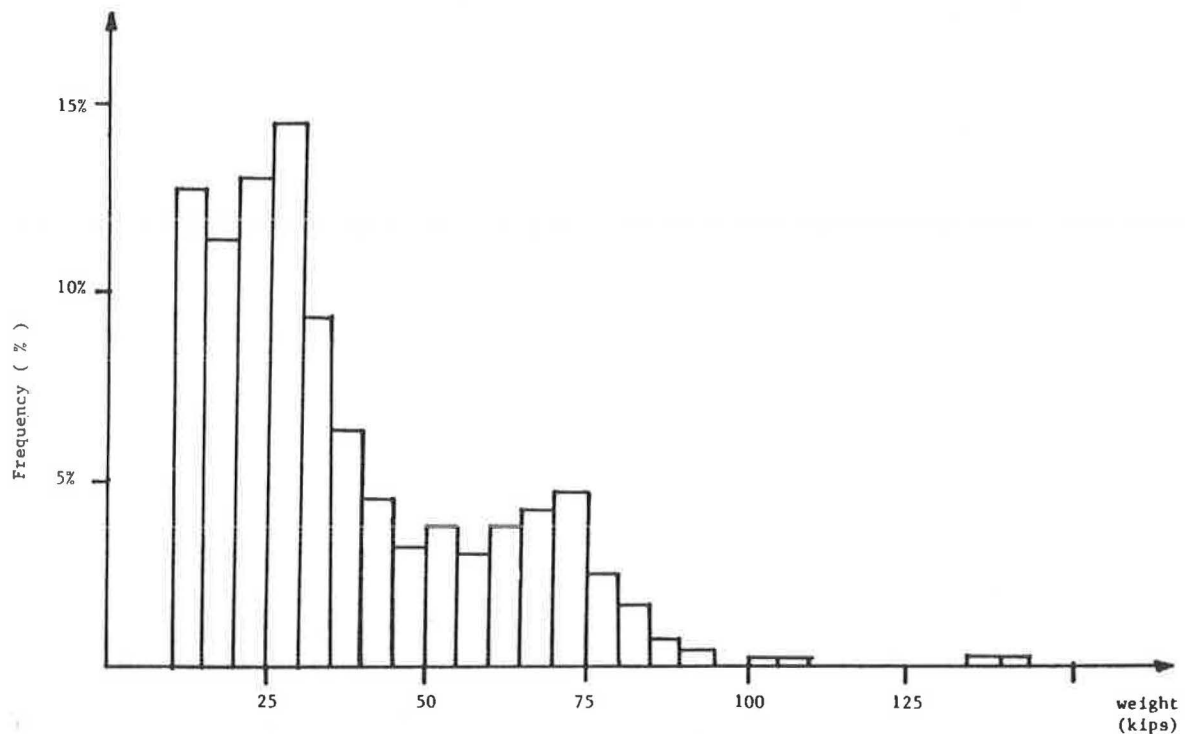


FIGURE 2 Truck weight histogram.

TABLE 1 Test Truck Stresses

Record	Location	Stress (ksi) at Girder					
		1	2	3	4	5	6
2	Right lane	0.30	0.78	1.10	0.69	0.54	0.13
11	Right lane	0.21	0.75	1.12	0.70	0.47	0.10
12	Right lane	0.22	0.71	1.03	0.68	0.49	0.21
13	Left lane	0.07	0.27	0.44	0.82	0.93	0.57
14	Left lane	0.02	0.20	0.37	0.75	0.93	0.57
15	Left lane	0.12	0.33	0.50	0.87	0.98	0.57

Note: Test truck weight = 29 kips.

by-side occurrences are found by summing the average distributions (plus one standard deviation) from each girder for both lanes. The most heavily loaded girder was determined to be the fourth girder with a distribution factor of 54 percent of a single lane load. The calculation is executed as follows:

21 percent (distribution of Lane 1) + 3 percent
(standard deviation Lane 1) + 28 percent
(distribution of Lane 2) + 2 percent
(standard deviation Lane 2).

TABLE 2 Random Heavy Truck Stresses

Weight (kips)	Moment (kip-ft)	Axles	Stresses (ksi)			
			Measured	Composite ^a	Noncomposite ^a	Noncomposite ^b
136.7	707	5	3.40	12.14	7.70	3.32
141.4	568	11	2.17	9.75	6.19	2.66
141.9	623	11	2.39	10.69	6.78	2.92
138.3	513	11	2.40	8.82	5.59	2.41
106.1	496	6	2.17	8.51	5.40	2.32
103.8	562	6	2.07	9.65	6.12	2.63

^aUsing AASHTO distribution factor.

^bUsing average measured distribution factor (31 percent).

TABLE 3 Girder Distributions (%)

	Girder					
	1	2	3	4	5	6
Lane 1						
Average ^a	7	23	31	21	14	4
COV	3	3	4	3	3	3
Lane 2						
Average ^a	2	7	11	28	33	19
COV	2	2	3	2	3	3
Total	14	35	49	54 ^b	53	29

Note: COV = coefficient of variation.

^aAverage of random vehicles with weights greater than 20 kips.

^bMaximum distribution factor.

The 49 percent distribution and the 54 percent distribution used herein compare favorably with the applicable AASHTO value of 72 percent $[7.92/(2 \times 5.5)]$.

The standard deviation is added to the average distribution of each lane to account for possible situations in which the girder under consideration supports a higher than average percentage of the total load. The 54 percent distribution factor is an extrapolated value that would exist if two identical vehicles were exactly side by side.

Dynamic Impact

The dynamic responses for the test truck and heaviest vehicles were estimated from the response strain record. These are generally under 10 percent and are significantly less than the 28 percent prescribed by AASHTO (Figure 3). The one exception noted to the 10 percent value is a 106.2-kip vehicle with six axles that had a dynamic response of 15.4 percent. The dynamic response for the I-475 bridge was taken as 10 percent for the rating calculations.

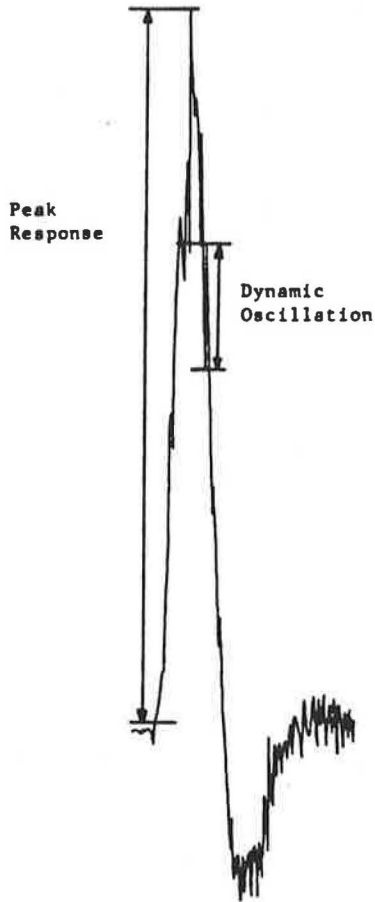


FIGURE 3 Example strain record.

Computed Stresses

The maximum measured stresses were compared with calculated stresses from the influence curve for selected heavy trucks (Table 2). The results confirm that the bridge provided a large composite action even though it was designed as a noncomposite bridge. For example, the 136.7-kip, five-axle truck produced a measured maximum single girder stress of 3.40 ksi. This value compares with a calculated stress of 12.14 ksi assuming noncomposite action and 7.70 ksi assuming composite action and using AASHTO's girder distribution factor. If the average measured girder distribution factor (31 percent) for Lane 1 is used, the girder stress assuming composite action is 3.32 ksi. Similar differences between maximum measured stresses and computed stresses have appeared in all the noncomposite design sites surveyed. It should be noted that, in all cases observed, the top flanges of the steel girders were partly encased in the deck, which provides shear transfer.

CONCLUSIONS--SITE 4

1. Measured stresses for the test truck and selected heavy trucks are lower than calculated stresses because of composite action, lower impact, and lower girder distribution factors than prescribed in AASHTO's specifications.

2. Using the measured values for impact and girder distribution increases the rating factors in comparison with those in ODOT's rating report. For example, using operating stresses of 27 ksi and

looking at the middle point of the center span, a rating factor of 1.94 is calculated using field measurements. This value compares with 1.28 calculated using AASHTO's impact and girder factors. In both of these calculations noncomposite sections are assumed. Table 4 gives a comparison of the rating factors as given in ODOT's report and the rating factors obtained when field measurements are used.

TABLE 4 Comparison of Rating Factors for Five Sites

Site	Rating Factor	
	AASHTO	Field Measurements
1	1.42	1.75
2	1.59	1.50
3	1.57	2.06
4	1.28	1.94
5	2.34	3.46

Note: Noncomposite action assumed except for Site 5.

3. It should be noted that Site 4 had extremely heavy vehicle traffic compared with other sites observed in Ohio. Thus consideration should be given to raising the load factor to account for additional uncertainty in maximum loading. This factor and reliability-based procedures to account for load uncertainty are discussed in the next section.

SAFETY LEVEL FOR RATING

Measured data are available for calculating the uncertainties of the random variables discussed earlier. As an illustration of the procedure that can be used to evaluate the safety of an existing bridge (rating), the information collected at the Lucas I-475 bridge is used in the following example.

First, a deterioration factor is introduced as a random variable to reflect uncertainty about losses of girder section over the years. The deterioration factor (Det) expresses the percentage of the original section still capable of carrying load; a factor of 1.0 implies that no section loss was detected for the bridge's girders. This Det factor is also expressed with some uncertainty. Because the rating report for the I-475 structure did not indicate any deterioration in the steel members, a Det factor of 1.0 is used for the mean of this variable, and a standard deviation equal to 5 percent of the mean [coefficient of variation (COV) = 5 percent] is associated with Det to model the uncertainty in the evaluation procedure. The term R in Equation 1 is then replaced by Det x R where R is the original resistance of a member as provided by the plans. The nominal value of R as calculated from the site plans for a girder in the middle span is equal to 1,990.5 kip-ft. Coupon tests on rolled beam members, however, show that the average stress capacity of A36 steel is closer to 40 ksi not 36 ksi, which suggests that the mean member capacity of a girder at the midspan of the bridge is really 2,212 kip-ft, the value used in this example. A COV of 8 percent is associated with R to reflect uncertainty in the steel yield stress, section dimension, and so forth.

The dead load (D) in Equation 2 was estimated by the bridge engineers to be 316.9 kip-ft. A COV of 5 percent is herein associated with D to reflect the level of confidence of this estimate. In reality, this COV should be based on the level of effort made to estimate the existing dead loads acting within the structure.

The I-475 site is a "special" route for extremely heavy permit vehicles; three different cases of maximum expected live loads are considered:

1. Random vehicle occurrences,
2. Combinations of random vehicles and permit trucks, and
3. Combinations of permit trucks only.

Random Vehicle Occurrences

The expression of Equation 5 is used to predict the maximum expected load due to random vehicles:

"a" is a factor that gives the moment effect of the design vehicle at the point being analyzed. For the midspan, the semitrailer vehicle or Rating Vehicle b (Figure 4) controls the design and is used to calculate "a." This "a" factor is known precisely and has no uncertainties associated with it. "a" is calculated for a truck of one unit load and thus is a reflection of the axle spacings and axle weight distributions of Truck b rather than of its total weight.

"m" represents the variation between the effect of random trucks and the effect of the rating vehicles specified in the analysis. From the truck data collected at this site, it was found that "m" at the midpoint of the middle span has a mean of 0.94 and a COV of 14 percent. This means that, on the average, the rating vehicle overestimates the effect of the random vehicles that crossed the bridge by 6 percent.

W* is a characteristic weight calculated from the gross weight histogram of the semitrailers collected at this site. W* is calculated so that it gives the upper weight limit of 95 percent of the trucks counted. A value of 74 kips was measured when the permit loads were excluded and it is associated with

a COV of 5 percent. The latter uncertainty is based on comparison with similar sites and also reflects the limited test period (4 hr of data).

H reflects the effect of multiple occurrences and is calculated using simulation techniques (8). The H-value calculated for this site is 3.14 with a modeling uncertainty or COV of 10 percent. This value of H corresponds to an expected maximum occurrence of 232 kips (3.14 x 74) on the bridge at one time during the 2-year period. The 10 percent uncertainty implies that there is a 5 percent chance that this weight might actually exceed 279 kips.

For the girder distribution factor (g) for this site, the fourth girder counting from the extreme girder of the main lane is the most critical member. From the field measurements, it was found that, on the average, this member carries 24 percent of the total load (49 percent of one lane load) on the bridge with a COV of 7.5 percent.

From the strain traces of random heavy vehicles it was found that the maximum total effect (static + dynamic) of the impact factor (I) for this site is on the average 1.06 times the static effect with a COV of 8 percent.

The means and standard deviations of the random variables used in this example are given in Table 5. The safety index (Equation 3) calculated for this site under random vehicle crossings is 6.96, which indicates an extremely high safety level. The failure function used in these calculations is

$$g = \text{Det } R - D - a m W^* H g I \tag{6}$$

Typically, new design codes such as those of Ontario (9) or the American Institute of Steel Construction are calibrated to achieve lifetime safety indices on the order of from 3.0 to 3.5. The high safety factor calculated in this example is not surprising considering that the bridge has a rating

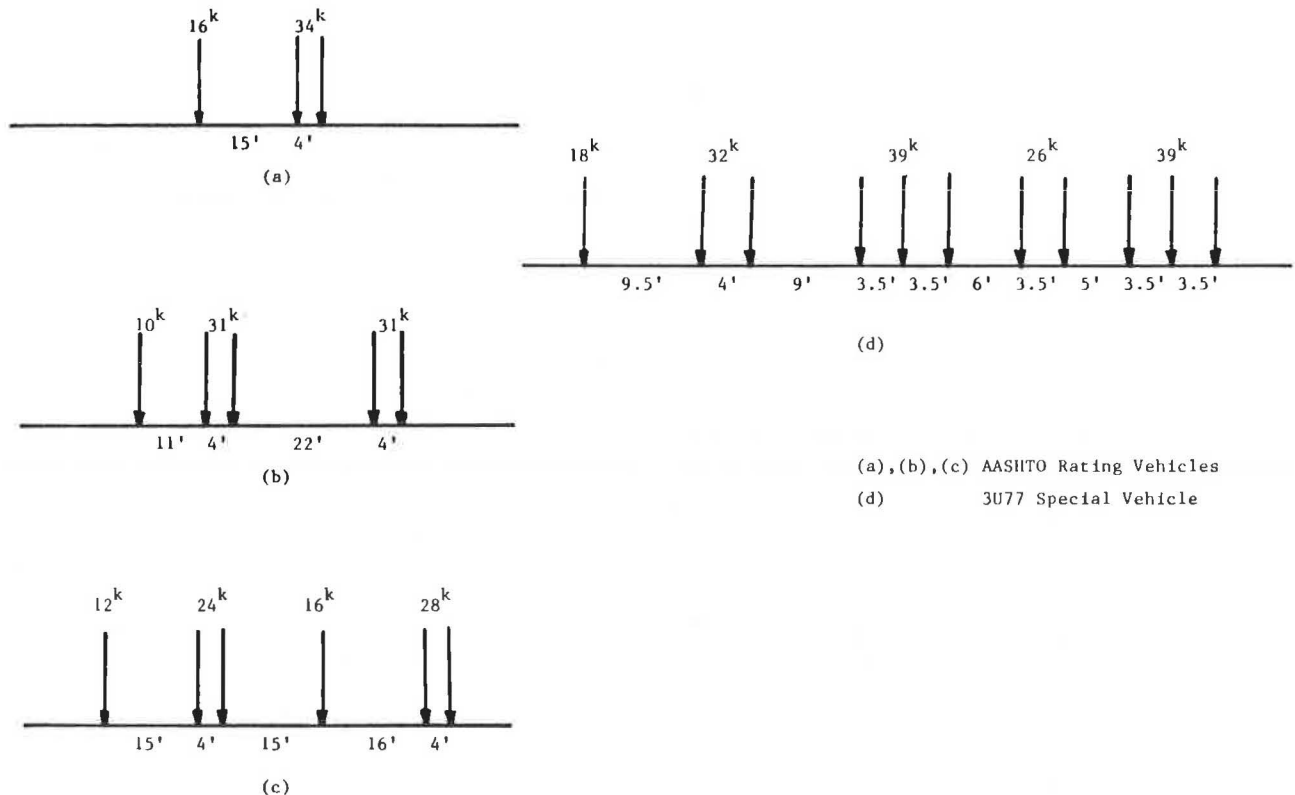


FIGURE 4 Examples of special vehicle configurations.

TABLE 5 Summary of Input Data for the Safety Evaluation

Variable	Mean	COV (%)
R	2,210 kip-ft	8
Det	1.0	5
D	316.9 kip-ft	5
W*	74 kips	5
H	3.14	10
m	0.94	14
g	0.24	7.5
I	1.06	8
α	1.21	10
C _h	1.03	5
P	1,020 kips	5

factor of 1.28 based on AASHTO's working stress design method.

Combinations of Random Vehicles and Permit Trucks

Because of the large number of permit vehicles at this site, the possibility of a permit vehicle alongside a heavy random truck is likely to control safety. The method by which this possible combination is considered in the safety analysis is detailed elsewhere (8). Det, R, D, W*, g, I, m, and a factors are calculated as previously described. Because in this situation one of the side-by-side vehicles is known, H is replaced by an α factor that describes the overload due to a random vehicle in only one lane.

For this site, assuming 10,000 permit vehicles in 2 years, α was found to be equal to 1.21 and is associated with a COV of 10 percent to reflect uncertainties in the modeling of the live load and limitations in available site data. The failure equation or safety margin (g) now takes the following form:

$$g = \text{Det } R - D - (\alpha m W^* \alpha + P) C_h g I \quad (7)$$

where

- α = lane overload factor,
- P = weight effect of a permit vehicle, and
- C_h = headway correction factor for vehicles ahead of and behind the permit truck in the random vehicle combination.

The other factors are as defined earlier. The values of the means and standard deviations used in the safety index calculations are given in Table 5.

P at this site is due to the effect at the middle point of the midspan of a 150-kip permit vehicle with the axle configuration shown in Figure 4. It is associated with a COV of 5 percent to model the possibility that some of the permit vehicles may have slightly different axle weight distributions or axle configurations. A C_h of 1.03 with a COV of 5 percent is obtained from Moses and Ghosn (5). The safety index calculated using the information for this site is 8.42. This is even higher than the 6.96 calculated for random vehicle occurrences because some of the random vehicles showed gross weights as high as the permit weight and axle configurations that produced higher moment effects.

Combinations of Permit Trucks

Because of the large number of permit vehicles at this site, this possible combination should be considered in the safety evaluation of this bridge. The

method used here first calculates the safety index of a bridge member, given the occurrence of this combination, then modifies this safety index to include the probability of such an occurrence. The latter probability depends on the number of permits issued, which is assumed to be 10,000 a year for this example (8). The safety index for the fourth member at the middle point of the middle span of this bridge is calculated using the safety margin equation:

$$g = \text{Det } R - D - 2 P C_h g I \quad (8)$$

Equation 8 is similar to previous safety margin models (Equations 6 and 7) with the exception that the live load is due to the effect of two permit loads represented here by the term 2 P. A safety index of 7.26 is calculated for this condition. The safety index is conditional on an actual occurrence of two permit loads side by side. Given that 10,000 permit crossings are expected in 2 years, with 1 percent of these crossings occurring side by side, and that 2.9 million crossings (4,000 per day) of random trucks are expected in the 2-year rating period, the probability of having two permit vehicles side by side is calculated to be 30 percent. Combining this probability with the conditional safety index of 7.26 yields a final safety index of 7.42.

Combining the safety indices for the random-random, random-permit, and permit-permit combinations yields an overall safety index of 6.95. This safety index, which is much higher than the acceptable range of from 3.0 to 3.5, indicates high safety levels. This is due to several circumstances including the overdesign of the bridge by some 30 percent at some locations and the apparent good maintenance (there was no member deterioration detected). The well-kept pavement preceding the bridge produced low dynamic impacts on the bridge members. All of these factors combined increase the level of confidence that a bridge rating engineer should have in the safety of this bridge. It should be noted, however, that no fatigue evaluation is being undertaken here and that consideration of fatigue failures might decrease the safety level.

CONCLUSION

The field data demonstrated the following conclusions for the five sites surveyed:

1. The maximum stresses were significantly below values predicted by conventional procedures. The major reasons for this observation are (a) all sites behaved with composite action, though only one had been constructed in this manner; (b) additional contributions to section modulus may result from over-lays, parapets, curbs, steel in the concrete deck, and the like, which are not normally considered in analysis; (c) girder distributions are more conservative than predicted by AASHTO values; only in the case of closely spaced girders (5.5 ft) were the AASHTO values exceeded; (d) measured impact values are lower than AASHTO's, presumably because the sites had relatively smooth surfaces although this was not a factor in site selection; and (e) the occurrence of extremely heavy trucks in both lanes simultaneously is rare.

2. The rating factor computed after incorporating the measured data usually exceeded the values obtained by conventional rating procedures.

3. Numerous cases in which truck weights exceeded legal loads were observed; however, these did not impair overall bridge safety.

4. Predicted reliability levels for the sites studied were high, though only strength, not fatigue, was modeled.

5. All the bridges studied were redundant multi-girder systems; for this type of bridge a safety index of from 3.0 to 3.5 provides an acceptable level. For nonredundant bridges, the target safety index should be much higher.

ACKNOWLEDGMENT

This work is part of a study carried out at Case Western Reserve University entitled "Weigh-in-Motion Applied to Bridge Evaluation." Support for the project came from the Ohio Department of Transportation and the Federal Highway Administration.

REFERENCES

1. Better Targeting of Federal Funds Needed to Eliminate Unsafe Bridges. GAO-CED-81-126. Government Accounting Office, Aug. 1981.
2. Manual for Maintenance Inspection of Bridges. AASHTO, Washington, D.C., 1982.
3. Standard Specifications for Highway Bridges. AASHTO, Washington, D.C., 1983.
4. P. Thoft-Christensen and M.J. Baker. Structural Reliability Theory and Its Application. Springer-Verlag, New York, 1982.
5. F. Moses and M. Ghosn. A Comprehensive Study of Bridge Loads and Reliability. Final Report FHWA/OH-85/005. FHWA, U.S. Department of Transportation, Jan. 1985.
6. F. Moses and M. Ghosn. Weighing-Trucks-In-Motion Using Instrumented Highway Bridges. Final Report FHWA/OH-81/008. FHWA, U.S. Department of Transportation, Dec. 1981.
7. F. Moses and M. Ghosn. Instrumentation for Weighing-Trucks-In-Motion for Highway Bridge Loads. Final Report FHWA/OH-83/001. FHWA, U.S. Department of Transportation, Aug. 1983.
8. F. Moses, M. Ghosn, and J. Gobieski. Weigh-In-Motion Applied to Bridge Evaluation. Final Report FHWA/OH-85/012. FHWA, U.S. Department of Transportation, Sept. 1985.
9. Ontario Highway Bridge Design Code. Ontario Ministry of Transportation and Communications, Downsview, Ontario, Canada, 1979.

Publication of this paper sponsored by Committee on Dynamics and Field Testing of Bridges.